Analyses of Foil Configurations of IMOCA Open 60s with Towing Tank Test Results

Teksen AYGOR

Master Thesis

presented in partial fulfillment
of the requirements for the double degree:
“Advanced Master in Naval Architecture” conferred by University of Liege
"Master of Sciences in Applied Mechanics, specialization in Hydrodynamics, Energetics and Propulsion” conferred by Ecole Centrale de Nantes

developed at West Pomeranian University of Technology, Szczecin
in the framework of the

“EMSHIP”
Erasmus Mundus Master Course
in “Integrated Advanced Ship Design”

Ref. 159652-1-2009-1-BE-ERA MUNDUS-EMMC

Supervisor:	Dr. Monika Bortnowska, West Pomeranian University of Technology, Szczecin
Co-Supervisor:	Jean-Baptiste R. G. Souppez, Southampton Solent University
Reviewers:	Prof. Lionel Gentaz, Ecole Centrale de Nantes Prof. Hage André, University of Liege

Szczecin, February 2017

Declaration of Authorship

I declare that this thesis and the work presented in it are my own and has been generated by me as the result of my own original research.

Where I have consulted the published work of others, this is always clearly attributed.

Where I have quoted from the work of others, the source is always given. With the exception of such quotations, this thesis is entirely my own work.

I have acknowledged all main sources of help.

Where the thesis is based on work done by myself jointly with others, I have made clear exactly what was done by others and what I have contributed myself.

This thesis contains no material that has been submitted previously, in whole or in part, for the award of any other academic degree or diploma.

I cede copyright of the thesis in favour of the West Pomeranian University of Technology, Szczecin.

Date: Signature:

ABSTRACT

The main aim of this master thesis is to evaluate the hydrodynamic effects of two different foil configurations used on a monohull sailboat. This representative vessel is the IMOCA Open 60 which is the most extreme sailing racing monohull in the world, and skippers sail it in races such as the Vendée Globe. According to class rules, the powerful racing sailboats have to be equipped with five appendages which are typically two rudders, a canting keel, and two daggerboards. Nowadays, the teams in this competition prefer one of two different daggerboard configurations which are straight and curved foils.

The primary objective is to compare the straight and curved foil configurations based on effective draft values in some upwind conditions experimentally. For that purpose, the 1/8th scale models of the Open 60 sailboat hull and its appendages were used for getting experimental results in the towing tank facility at Southampton Solent University. Firstly, a test matrix was prepared for the various appendages configurations. The main parameters were measured Side Force, Drag, Heave and Trim in an array of conditions (heel angle, leeway angle and velocity-Froude Number) during the towing tank tests. The viscous and wave resistance values were calculated based on ITTC formulations, and then the resistance and side force values were scaled to full size based on 1/8th scale factor for each condition. Also, some towing tank tests were done with only the bare hull for obtaining the form factor values of the upright and heel states. The uncertainty analysis calculations were applied to determine the uncertainty of these experiments based on the ITTC-Recommended Procedures and Guidelines. The available model sizes of the straight foil configuration, keel, bulb, and hull were employed for the towing tank tests. However, the curved daggerboard dimensions were taken from pictures of the new generation Open 60 sailboats. The representative curved foil was designed in 3D, and it was manufactured in a plastic material (PBC) by the 3D printer and then it was covered with carbon fibre.

The 0° and 40° canting keel conditions were evaluated based on the effective draft and righting arm and the 40° canting keel was employed together with the 1/2- full straight and 1/2 - full curved daggerboard configurations during the tests. The straight and curved daggerboards were compared at certain sailing conditions according to the effective draft and heave values to find the more effective and lifting foil configurations in the upwind conditions. As a result, the full-straight foil configuration is the most efficient daggerboard configuration in the upwind conditions however the curved daggerboards have more lifting force advantage due to their shapes as compared with the straight foils despite being less efficient in the upwind conditions.

ACKNOWLEDGEMENTS

Foremost, I would like to thank my parents for all their motivational and financial supports during the adventure. I am too much grateful for their continuous and unwavering assistance.

Firstly, I would like to thank my supervisor, Jean Baptiste who helped me a lot about every process from the beginning of this adventure. I kept going during the thesis period thanks to his recommendations and supports. I really appreciate him for his time and patience.

I would like to thank Prof. Giles S. Barkley from Southampton Solent University for his shared theoretical and practical knowledge. I have got very useful and significant viewpoints about the behaviours of the foiling sailboats in the sea conditions and towing tank experiments thanks to his supports. I am very grateful for his valuable advice.

I would like to thank Jack Cunningham Burley from Southampton Solent University for his shared composite knowledge and assistance. I learned much information with information exchange obtained from our discussions about the racing sailboats.

I would like to thank my supervisor, Dr. Monika Bortnowska who assisted me with her general recommendations and supports. I am grateful for her advice about vital constituents to finalise the thesis adventure.

NOMENCLATURE

Symbols	Explanations
L	Lift force
D	Drag force
CFD	Computational Fluid Dynamics
ITTC	International Towing Tank Conference
IMOCA	International Monohull Open Class Association
DSS	Dynamic Stability System
DBD	Daggerboard
Ru	Upright Resistance
Ri	Induced Drag
Rh	Heel Resistance
SF	Side Force
Te	Effective Draft
λ	Scale Factor
Ls	Ship Length
Lm	Model Length
P	Pressure
V	Velocity
S	Foil Area
Cl	Lift Coefficient
Cd	Drag Coefficient
ρ	Density
ν	Kinematic Viscosity
μ	Dynamic Viscosity
α	Angle of Attack
Rt	Total Resistance
Rv	Viscous Resistance
Rw	Wave Resistance
Cf	Frictional Resistance Coefficient
C_R	Residual Resistance Coefficient
k	Form Factor
Re	Reynolds Number
Fr	Froude Number
WSA	Wetted Surface Area

CONTENTS

LIST of FIGURES

List of Figures of Appendices

LIST of TABLES

List of Tables of Appendices

1. INTRODUCTION

The hydrofoil technology has been adapted to many maritime vessels such as naval, passenger and sailing vessels for many years in the shipbuilding industry. Several hydrofoil configurations had been tried on crafts since the 1900s by many inventors such as Enrico Forlanini, and Alexander Graham Bell, etc. [1]. The lifting surfaces have been designed in lots of different shapes which could be C-shape, L-shape or T-shape, etc. The principle of a hydrofoil is to lift the hull out of the water using wing-like raising structures that provide reduced wetted surface area, less wave drag and more speed for vessels, unlike the other conventional vessels.

The different foil configuration systems can be fitted on both monohull and multihull types of the sailboats. In general, the multihull (catamaran or trimaran) hydrofoil sailboats have better stability because of their number of the hulls. Some multihulls can use two or three foils on the hulls, and the main lifting foil can be placed on the centre of gravity of the hull. The multihulls use the rudders, daggerboards or centerboards as a foil that provides better control, balance and performance for the sailboat. The hydrofoil catamaran sailboats are also known as foil-cats. The mono-hull sailboats employ two foils to lift the hull out of the water generally, and they use a ladder type foil configuration.

Nowadays, there are many competitions for sailboat races, and the ability of the skippers and crews are very significant to win the races in the well-known competitions. However, the innovations and technologies for vessels have affected the performance of the sailboats as well as the ability of the skippers; therefore, we can see several changes on the sailboats. For instance, the wing sail, canting keel and daggerboards have been fitted on the new class racing sailboats.

There are various foil configurations which are used for racing and performance on monohull and multihull sailboats such as the NACRA 17, AC 72, and IMOCA Open 60. The straight and curved daggerboards are two main foil configurations which are used in the racing sailboat industry. These sailboats can use foils to improve performance due to the competition rules. The competitors and engineers have developed the foil shapes and sections to get a high lift to drag ratios (L/D) at both upwind and downwind conditions. For this purpose, they have done lots of model tests in towing tank facilities and used some CFD (Computational Fluid Dynamics) analysis software to find the optimum foil configuration at sailing conditions.

1.1 Aims and Objectives

The aim of this thesis is to analyse a racing sailboat together with its appendages based on some hydrodynamic parameters (side force, drag, and heave) experimentally. The representative sailboat (the Open 60) has employed five appendages which are two rudders, one canting keel and two dagger boards. These daggerboards have straight or curved foil configurations and the two different foil configurations used by Vendée Globe teams will be analysed at some particular conditions according to hydrodynamic towing tank values. The upwind condition will be the main focus for the analyses. Firstly, the bare hull will be towed to get form factor values at various heel angles and low velocities. After that, the model boat will be tested using appendages which are one 40 ° canting keel and straight or curved daggerboards. The hydrodynamic parameters will be obtained with these different foil configurations at particular sailing conditions (heel angles, leeway angles and velocities). The obtained model values will be extrapolated to full size based on 1/8th scale factor and then the effective draft values will be calculated for each situation. The all effective draft results will be considered in certain states to determine the best configuration in the upwind condition.

- Form Factor values will be determined for some heel angles and uncertainty analysis will be done to get error quantity of the desired experimental tests.
- Effective draft values of 0° and 40° canted keel will be calculated at some particular conditions and the canting keel situations will be evaluated with righting arm and effective draft results.
- Drag, Side Force and Lift values will be obtained from towing tank tests with the two different foil configurations separately and 40° canted keel in various sailing conditions.
- These effective draft, Lift and Drag values will be considered in comparison of both foil configurations and these obtained values will be analysed to get critical results in the upwind condition.

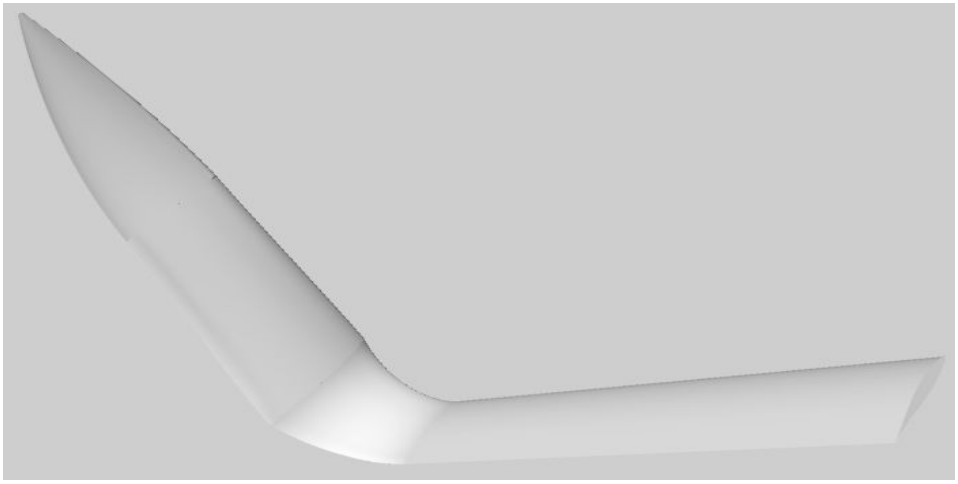

Figure 1-1: A 3D view of the curved daggerboard configuration [23]

1.2 Scope of Study

Basically, the master thesis contains experimental data obtained from the model basin at Southampton Solent University. Model of the Open 60 racing sailboat has been already built by the university facilities and it has been given to get the desired hydrodynamic values. The towing tank tests will be done based on the ITTC (International Towing Tank Conference) [2]. The ITTC formulations and procedures will be applied for computational and experimental processes [3, 4]. Hydrodynamic analyses and uncertainty analyses will be the main focus of this study to get critical results. The hydrofoil configurations will be used as observed and tested appendage based on foil theory. The hydrodynamic model values obtained by model boat will be scaled to full size based on dynamic similarity and 1/8th scale factor. According to full-size results, the effective draft values will be calculated to compare the effectiveness of the two different foil configurations. Eventually, the most effective configuration will be found in the upwind condition, according to the analyses and some remarks and ideas will be presented about the foil configurations.

Figure 1-2 : Towing tank facility of the Southampton Solent University

1.3 Methodology and Approaches

All model experiments are performed based on some assumptions and requirements. The towing tank tests will be performed on ITTC approaches for obtaining the desired analysis results. According to the ITTC method, there should be a similarity in the forces between model and full scale, therefore there are three similarities which are kinematic, dynamic and geometric. The geometric similarity assumes that the model and full ship hulls have similar geometry and the approach is presented as the ratio of the model and full hull lengths using a constant scale factor. Based on this geometric similarity, many hydrodynamic and hydrostatic parameters can be scaled from model size to full size values. [5]

$$\boldsymbol{\lambda = \frac{Ls}{Lm}} \qquad (\mathbf{1})$$

On the other hand, the ratio between inertia and gravity forces should be equal in both model and full scale to have similar flows based on dynamic similarity. It means that Fn (Froude Number) is respected to scale the model to full size so the relation between the model and full sizes occurs because of the respect and velocity values of the model and full ship size can be scaled each other. In addition, it is assumed that the wave motions will be same in the model and full size according to Froude number equality. For that reason, the wave making resistance will be equal for both scales, therefore, the residual resistance coefficient will be affected due to wave making resistance and it will be also same for both scales. This situation is expected to be same for Reynolds number in order to have the proper ratio between inertia and viscosity forces. However, it cannot be accepted like Froude number approach exactly because it is hard to change the viscosity of the fluid of model and full-size conditions in order to respect to Reynolds number, therefore, the Froude number approach is more feasible as compared with Reynolds number. According to this consideration, the experimental model results obtained from the towing tank tests can be scaled to full size based on the ITTC method. [2; 5]

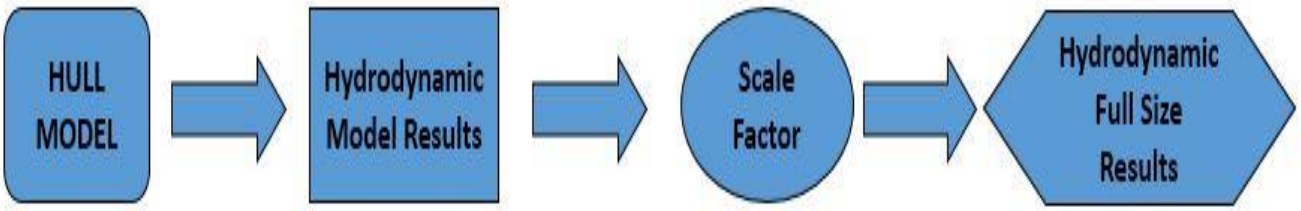

Figure 1-3 : General chart of scaling from model to full size

1.4 Description of Hydrofoils

It is acknowledged that the foil theory section was presented based on the Southampton Solent University Lecture notes [6]. A foil has a solid structure mainly which is placed in an oncoming fluid at a specified angle of attack. The foil generates a lift force in the free stream because of the foil's angle of attack and shape, and the lift force is perpendicular to the free stream. Due to the solid structure of it, there is also a drag force which is parallel to the free flow. The fluid could be gas or water, and if it is a gas, the foil is named as an aerofoil otherwise, it is named as a hydrofoil. There are two kinds of foil theory as 2D and 3D. There are some assumptions for the foil theory. The flow is assumed as incompressible around the foil, and the viscous and boundary layer effects are not taken into account. According to Bernoulli's theory, energy losses are not seen during the free stream. In 2D foil theory, it is assumed that same cross sections seem at each point along the span of an endless long foil; therefore, the foil will have similar flow at any point of its span. It means that the flow will not change around the tip parts of it. However, the flow will be different at the tips of a finite span of any foil according to 3D foil theory. This situation will cause a lift difference between the centre and ends of the foil. There is also a mathematical theory which enables to obtain the lift and drag coefficients of 2D foils, and the theoretical coefficients of 2D foil can be modified for 3D foil calculations. [6]

Normally, if the angle of attack increases for the foil, the lift coefficient will have increase linearly. The foil causes deflection of the oncoming fluid with the angle of attack. The flow separates excessively over one of the foil surfaces with reduction of the lift force when the angle of attack is enhanced too much. This deflection of the flow generates curved streamlines, and these streamlines result in pressure differences on surfaces of the foil therefore while one of the surfaces has low pressure, the other surface has higher pressure. According to Bernoulli's principle, the pressure differences also cause the velocity differences around the foil, so the upper surface has higher average flow speed than the lower surface to catch the incoming flow over the bottom surface at trailing edge section. [6]

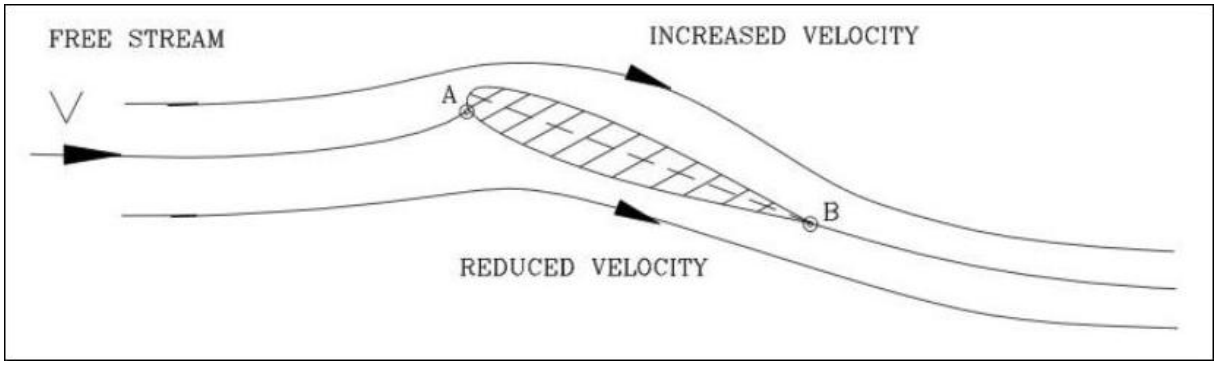

Figure 1-4 : Velocity difference around foil [6]

According to the Bernoulli's equation, there is an equilibrium depending on the pressure and velocity values. These parameters have opposite relation in the Bernoulli's equation to keep it constant. [6]

$$\boldsymbol{P\ (Static) + \frac{1}{2}\ \rho\ V^2 (Dynamic) + \rho g z = Po} \qquad \textbf{(2)}$$

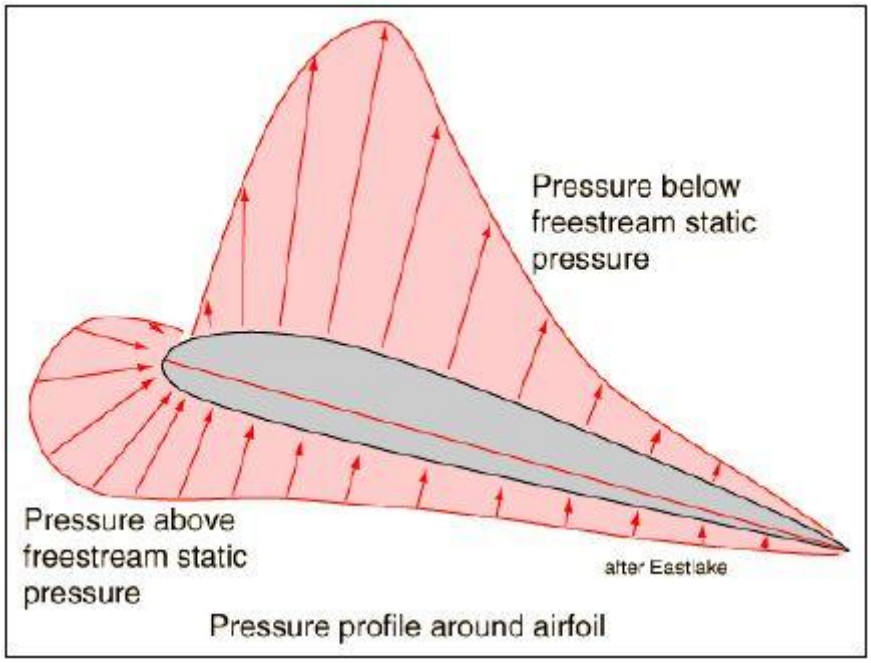

Figure 1-5 : Pressure difference around foil [6]

Deflection effect of the foil on the free stream generates the two forces which are the lift and drag. A 2D foil produces the lift and drag forces with its non-dimensional coefficients as follows:

$$\mathbf{L} = \frac{1}{2}\rho\, V^2 S\, Cl \qquad \textbf{(3)}$$

$$\mathbf{D} = \frac{1}{2}\rho\, V^2 S\, Cd \qquad \textbf{(4)}$$

The primary consideration of a hydrofoil design is to lift a boat's hull and keep it out of the sea water, and it means that there will be less drag. The boats should balance the hull weight with force, and the force is provided by the lifting hydrofoils; therefore, the vessel hull becomes much lighter due to the lift force. The hydrofoils seem as wing-like raising structures which raise the hull out of the water to reduce the wetted surface with having less drag force. Therefore, the lifting hydrofoils enable to increase in speed of the boat at a particular angle of attack. [6]

It is considered that the foils have a finite span and chord length in 3D foil theory as compared to 2D foil theory. For that reason, the flow around tips of the foil is induced because of the pressure differences between the bottom and top surfaces of the foil. Therefore, tip vortex will occur across the chord length of the foil, and the tip vortex streaming will have increase with the flow interaction between the tip and the chord length of the foil at the trailing edge tip. The flow around the tip of the foil begins to act along the span of the foil to generate a span flow above the upper surface, and it also acts to produce the span flow toward the tip at the lower surface. The tip flow due to pressure difference will transform into a vortex sheet from the span streaming at the trailing edge, and the vortex sheet continues until middle span decreasingly. The vortex sheet left from trailing edge combines with the tip vortex to create the trailing vortex. The tip vortex will lose its effect when the trailing vortex is far away from the tip. [6]

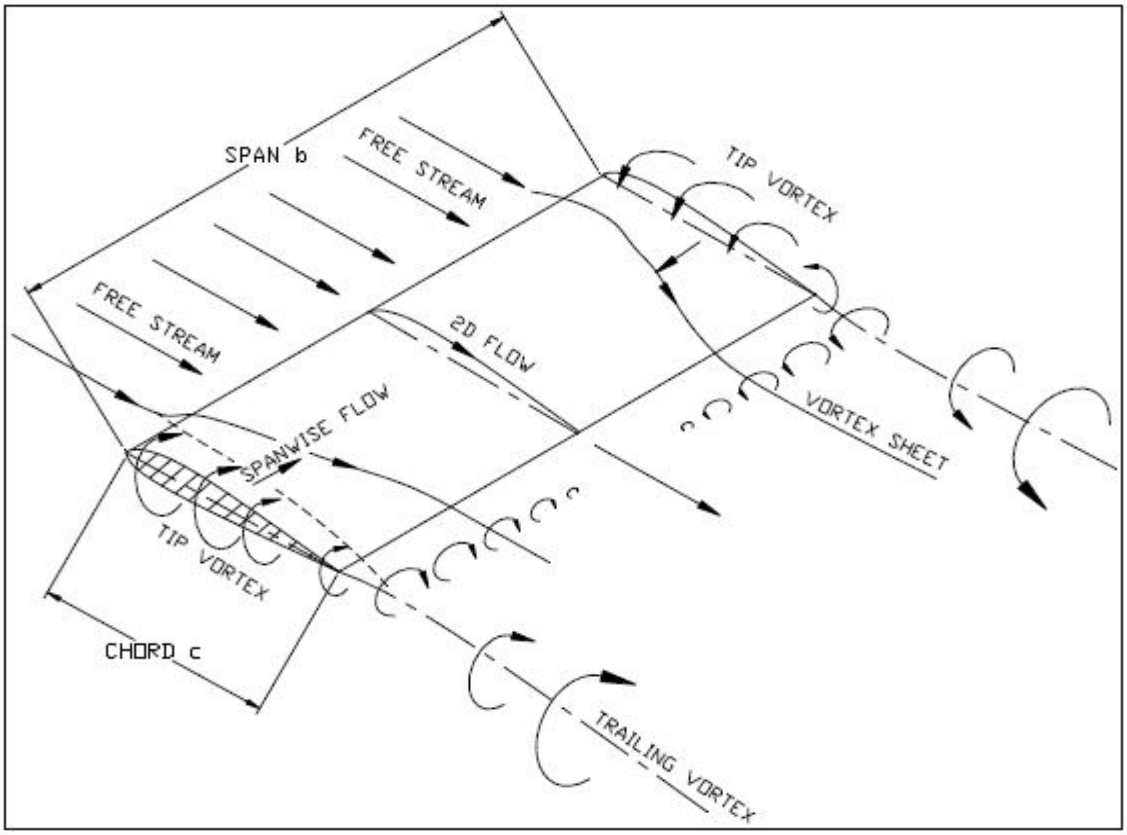

Figure 1-6: The flow vortices around foil in 3D foil theory [6]

This trailing vortex corresponds to lost lift for the foil, and it is called induced drag. The tip vortices emerge around the tips of the foil mainly therefore if the span length is increased with same chord length, the aspect ratio of the foil and the region of the span will have risen therefore this situation will result in fewer tip losses and lift loss. It also means that the foil will generate more lift force with larger aspect ratio. The lift is produced by the centre line of the foil.

The trailing vortices generate a downwash effect at trailing edge of the foil, and this downwash effect change depends on the distance from the tips of the foil. The free stream vector transforms into inflow vector due to the downwash; therefore, the 2D lift vector perpendicular to the free stream also changes its direction based on the inflow vector, and this is indicated by 3D lift vector which is perpendicular to the inflow vector. The rotation of the lift vector causes a drag force which is parallel to free stream vector, and it is called induced drag (Di). The induced drag is produced because of lift that is generated by a 3D foil along it's' the lifting section since the flow is induced by the pressure differences between the top and bottom surfaces of the foil. In other words, the induced drag parameter emerges due to the lift force. There is a formulation to calculate the lift and induced drag coefficients as shown below [6]:

$$\boldsymbol{Cdi = \frac{Cl^2}{\pi . AR}} \qquad (\mathbf{5})$$

According to the above equation, the lift force and induced drag can be obtained by using their coefficients. It also seems that there is an inverse proportion between the aspect ratio and the induced drag. The induced drag decreases with increasing the aspect ratio value in a certain state; therefore, better L/D ratio can be obtained based on chord and span lengths of the same foil. [6]

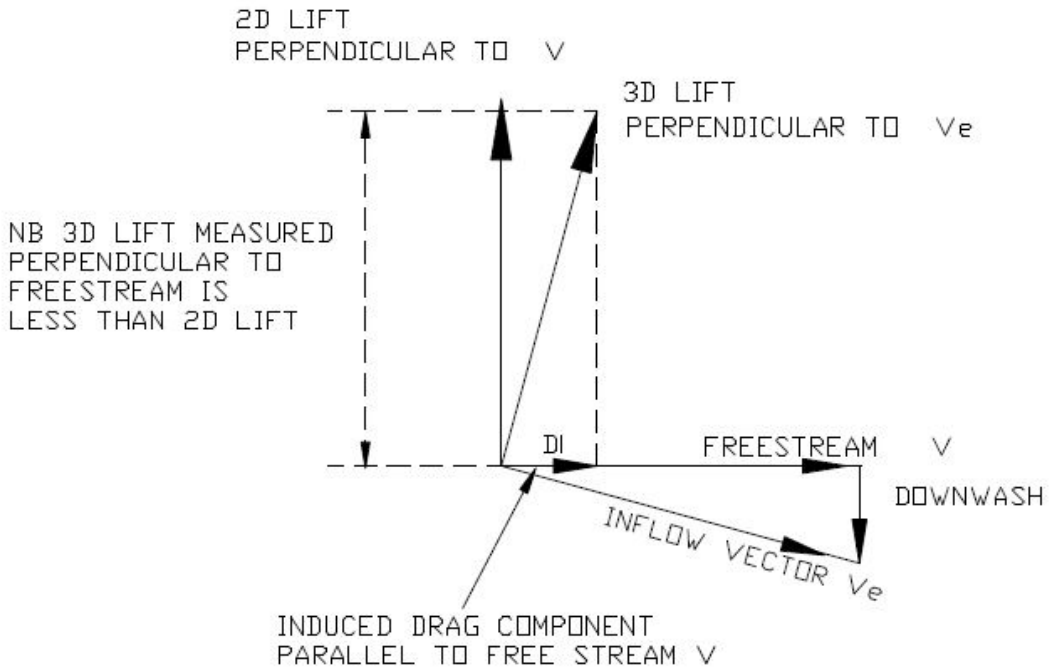

Figure 1-7: Illustration of the 2D and 3D lift vector directions based on the flow vector [6]

1.5 Foil Configurations

Several types of foils are mounted on the sailboats in the small craft industry. The hydrofoil objects might have different foil configurations. In general, there are two main hydrofoil classifications which are surface piercing and fully submerged. These shapes present how the submerged surfaces are adjusted to lift the hull out of the water [1].

The central concept of surface piercing hydrofoil designs is to raise the hull into air-sea interface by using the parts of the foils. The struts provide the connection between the foils and the hull and they support the lifted hull over the water surface with length enough. According to the principle of the surface piercing hydrofoils, the boat's hull rises thanks to the foils, therefore, the speed of the vessel increases because of reduced surface area of the submerged foils instead of the hull. This type of hydrofoils might have U or V shapes.

On the other hand, the fully submerged hydrofoils operate under the water surface. The struts have the same duty as well as surface piercing, therefore, they provide the connection between the hull and foils, but they do not have an effect on the lifting force mostly. The hydrofoil configuration system does not have stabilisation characteristic itself at some sea conditions; therefore, the foils should have the sufficient angle of attack to provide the lifting force efficiently. The hydrofoils with the fully submerged foil configuration enable to minimise the wave effects on the hull at sea conditions and keep it more vibrationless. Therefore, the passengers have more prosperous voyage [7]. The fully submerged hydrofoils might have T or L shape in application areas.

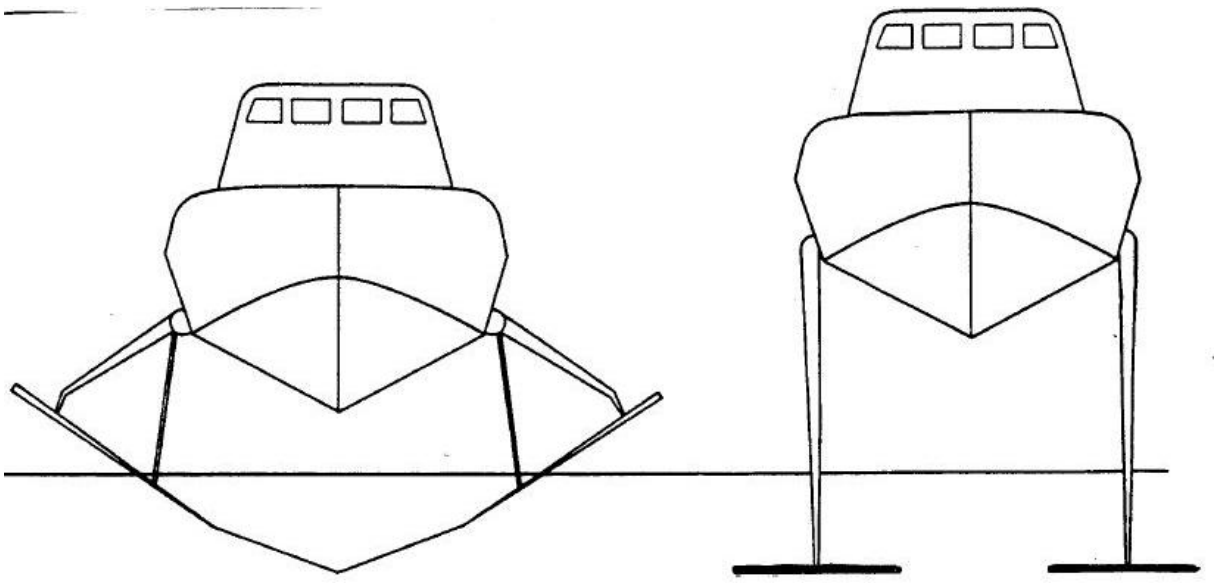

Figure 1-8: Surface-Piercing (Left) and Fully Submerged (Right) hydrofoil types [1]

1.6 Dagger-boards and Centre-boards

The dagger boards and centreboards are used as rigging for stability and lifting on sailboats. They have similar working principle but different retraction system. The universal principle is that these boards enable to sail by a lift in a windward direction efficiently through countering the effect of the sail in a leeward direction while the hull is floating on the water. They enable to convert the sail force because of the wind to forward motion that helps to keep the sailboat more stable. Both of them have a thin plate which is mounted on the bottom of the boat vertically. The dagger boards are usually longer than the centreboards. Therefore, the daggerboards could provide more lift force for the crafts. The dagger board is similar to a real dagger because it also has a case (housing) which is known as dagger board trunk. The dagger board moves only down and up in this trunk vertically. This dagger board trunk has bearing feature for the board, and the trunk prevents to contact between the boat hull and water. On the other hand, the centreboards have different retraction system that pivots up or down through a slot which is known as centreboard trunk. The centreboard trunk has a similar concept with a dagger board trunk however the daggerboard can be removed from its trunk, unlike the centreboard which stays in the same position every time. The centreboard can swing more freely about the slot thanks to the centreboard pin, in contrast to the dagger board which can move only up and down in its trunk. Because of the swing, the balance of the hull can be adjusted by the variance of the centreboard position for different sailing and loading conditions. The slot of the centreboard should be longer than the dagger board's slot, therefore, this slot causes more drag force when the centreboard is used. When the boat sails into shallow water, the dagger board will have more damage accidentally because of its trunk but the centreboard will pivot up to about its trunk with less damage probably. Firstly, the both boards were made of wood; however, the wooden boards tend to float out of the water. This problem can be solved by some locker systems, but they can also be manufactured by using different materials such as aluminium, steel or fibreglass. [8, 9]

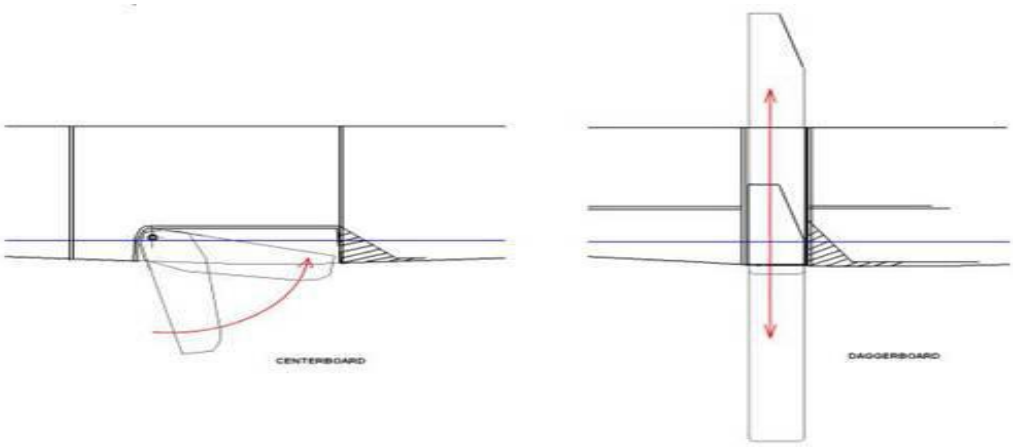

Figure 1-9: Centre board (Left) and Dagger board (Right) Illustrations [9]

2 Vendée Globe

In 1968, the Golden Globe Race was organized as the first non-stop solo round the world race firstly. After this event, the race idea was the initial source of inspiration for the Vendée Globe. Philippe Jeantot is a French yachtsman who sailed in the Velux 5 Oceans Race. He decided to emerge a new and amazing non-stop round the world race in 1989 after his two wins in the Velux 5 Oceans Race which is a solo round the world race with stopovers. This Globe Challenge was called as Vendée Globe in progress of time.

The Vendée Globe is a single-handed race which competitors sail non-stop around the world without any assistance. The Vendée Globe is ultimate experience and test of endurance for sailors. They face many difficulties in ocean conditions by themselves during the world route. Some master sailors have ever achieved to win this extreme challenge. Some of them are Alain Gautier, Christophe Auguin, Vincent Riou, François Gabart and Titouan Lamazou. In 2001 and 2009, Michel Desjoyeaux has won the challenge two times, and François Gabart has set a record with 78 days sailing. It has been arranged every four years enthusiastically.

Open 50 boats were used for the race and nowadays, competitors sail the Open 60 class. The Open boat classes are governed based on a box rule which has parameters such as overall length, draught, appendages and stability, etc. The "Open" class of monohull sailboats is administered by The International Monohull Open Class Association (IMOCA), and the World Sailing (or formerly International Sailing Federation-ISAF) is the main institution for the sailboats. The sailing challenge starts and finishes in Les Sables-d'Olonne. [10]

Figure 2-1: Route of the Vendée Globe Competition [10, 11]

2.1 Sailing Conditions

The route of the Vendée Globe Competition performed around the world has various environmental conditions. It is acknowledged that the all meteorological sea conditions were retrieved from a new Open 60 sailboat project which has been designed for the next Vendée Globe 2020 race [11]. The average values of the probable sailing states were taken from the website of NOAA (National Oceanic and Atmospheric Administration) for certain months according to particular locations of the route. The wind speeds, wave heights and sailing conditions are presented based on the average values and wind directions (Figure 2.2) in the following table.

Table 2-1: Environmental conditions based on the route locations [11]

Location	Wind Speed-[m/s]	Wind Speed-[knots]	Sailing Conditions	Wave Heights-[m]	Beaufort Scale
1	7	14	Running	1,75	4
2	8	16	Broad Reach	2	5
3	10	19	Close Hauled	2,75	5
4	11	21	Close Hauled	3	5
5	6	12	Close Hauled	1,5	4
6	9	18	Running	2,7	5
7	9	18	Running	2,7	5
8	10	19	Running	2,75	5
9	8	16	Running	2	5
10	7	14	Broad Reach	1,75	4
11	9	18	Running	2,7	5
12	4	8	Running	0,7	3
13	5	10	Close Hauled	0,8	3
14	10	19	Close Reach	2,75	5
15	14	27	Running	4	7

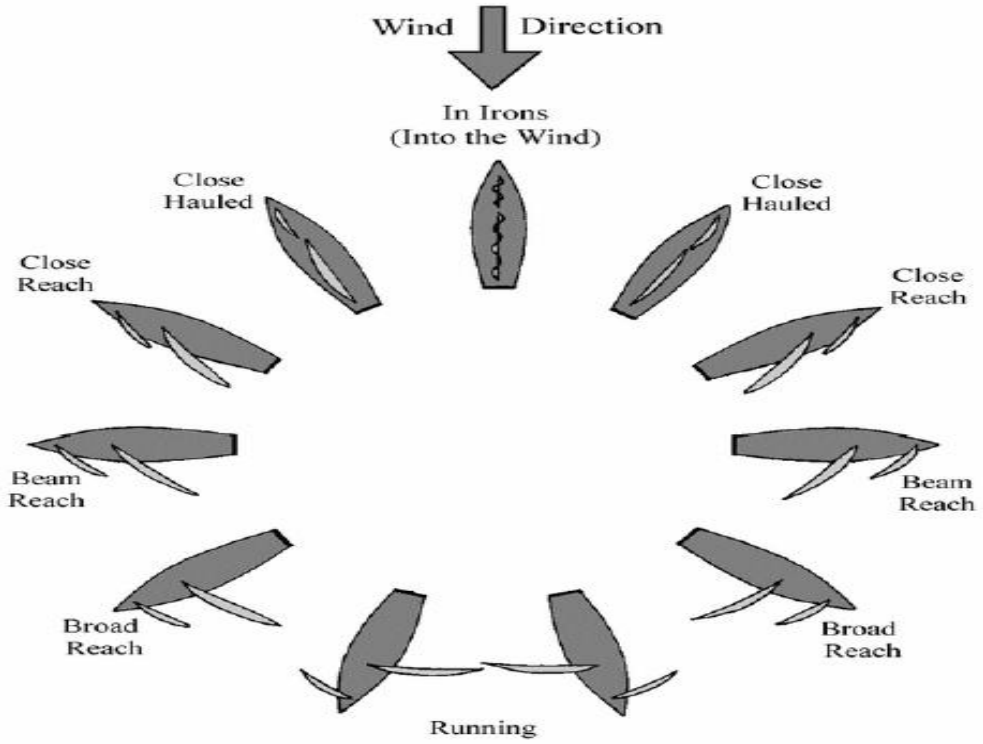

Figure 2-2: The sailing conditions based on the wind directions [11]

The OPEN 60 vessels encounter the some environmental conditions during the race route. The wind speed and wave height are main significant conditions for the competitors and their sailboats. These sailing conditions may have vicious or breeze winds and huge or small waves depends on location of the sailboat. In addition, the wind direction is a critical parameter which affects the sailing and sailboat performance. The wind directions show that the sailboat is sailing under upwind or downwind states basically and the directions are indicated by various names. The names mention sailing direction of the sailboat against the wind. The wind directions are also related to the route. The skippers of the OPEN 60 sailboats try to overcome the hard conditions in order to have good performance. The skippers sail at %80 of the time under downwind condition during the Vendée Globe race route approximately so this is the main wind condition for sailboats to win the extreme competition. They should have good performance at downwind condition but they also need to overcome rest of the wind conditions which take %20-25 of the time during the route. The rest of the wind conditions could be upwind condition which is the hardest situation for the sailboats and skippers. In the Vendée Globe race route, the sailors might encounter with trade winds which have changeable characteristic as wind force and direction. For that reason, the skippers should find sensible strategies or have sailboats equipped by better appendages under these changeable wind conditions. There is one satellite picture which was taken from around the Canary Islands. It is shown that there are stable regions that are blue and green zones and the yellow regions show the oncoming and changeable wind conditions which might cause hard situations to control the sailboat. [12, 13]

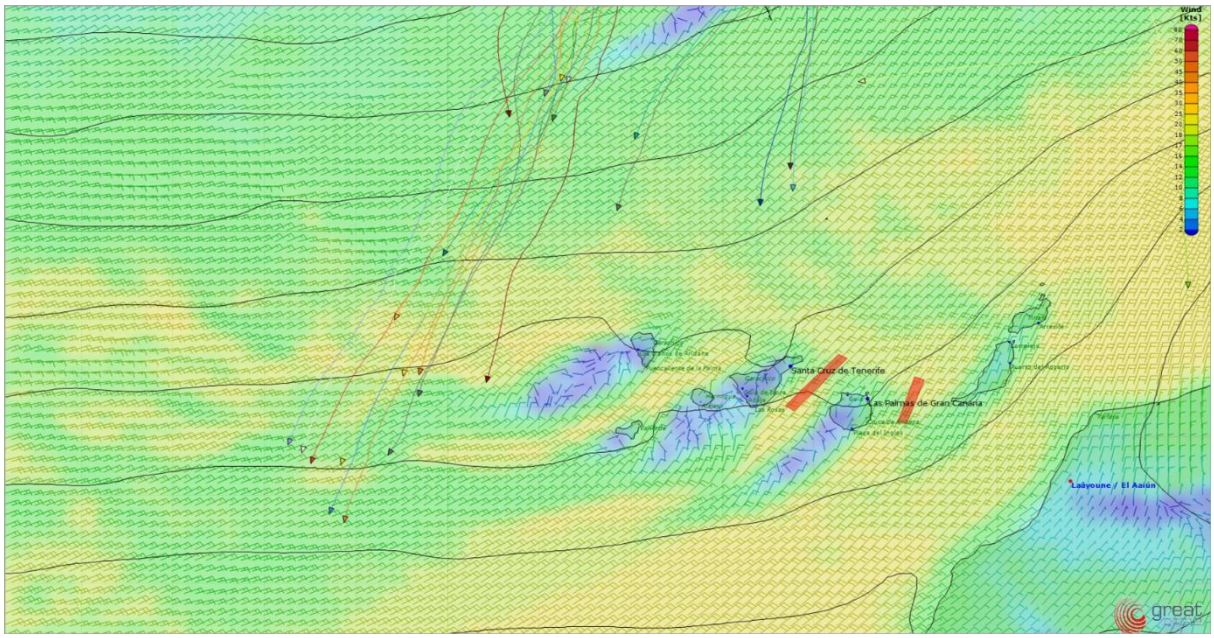

Figure 2-3: Satellite view around Canary Islands from the Vendée Globe race route [12]

2.2 The Open 60 Sailboat

Administrator institution of the Open 60 sailboats is the International Monohull Open Class Association (IMOCA). The Open 60 sailboats are designed based on some restrictions and certain rules however the rules can rarely allow some innovations which the designers can develop them to improve the performance of the sailboat. The Vendée Globe competitors have sailed with the sailboats fitted with five appendages which are two rudders, one canting keel and two dagger boards and the sailboats are equipped with various sail types, one of the different kinds of a mast (traditional or wing) and some technological systems. The skippers sail the most robust and fast racing monohull which can reach 28~30 knots in downwind condition [14]. The Vendée Globe Competition contains lots of sponsors, designers and skippers [15]. However, a representative sailboat of the all competing sailboats [15, 16] was created based on their general specifications to perform the hydrodynamic analysis calculations and it is presented with its' the approximate specifications below.

Table 2-2: General specifications of the representative IMOCA Open 60 Sailboat

Representative Open 60 Sailboat Specifications		Unit
Full-Size Length	18,288	m
Model-Size Length	2,286	m
Full-Size Beam	5,70	m
Model-Size Beam	0,71	m
Full-Size Max. Draught	4,50	m
Full-Size Lightship Displacement	7,6 ~ 8	tonnes
Scale Factor	8,00	-

Figure 2-4: A view of the model boat

2.3 The Straight and Curved Daggerboards

There are two different foil configurations which are used by the IMOCA 60 racing sailboats in the Vendée Globe. The conventional shape is called straight daggerboard which has straight foil configuration and other one is designed with complex shapes which include straight and curved parts, and it is named as curved daggerboard configuration. The main purpose of the configurations is to enhance the stability of the sailboats dynamically to get faster sailboats (VMG-Velocity Made Good) therefore they are created to generate the side force with their various shapes. They are employed as an additional appendage to complete the righting moment effect of the keel and increase the efficiency of total side force generation.

One of them has the conventional foil shape that has been employed by the skippers to increase the sailing performance during the non-stop round the world race. It is called straight daggerboard which has been still preferred by designers for this challenge. Mainly, it is designed to contribute the side force generation (righting moment) horizontally. It also produces the vertical lift force slightly when the boat is heeled. Most of the skippers have won the exciting competition and finished the route in a shorter time thanks to the straight foil and other technologic changes. They believe that the conventional daggerboard configurations are still useful to compete during the extreme sailboat competition.

Nowadays, Dynamic Stability System (DSS) seems an exciting innovation created by designer Hugh Welbourn [17] for sailboats and sailors. The DSS is to lift the hull out of the water thanks to foils to have less displacement; therefore, these sailboats have less wetted surface area and resistance. It provides righting moment dynamically at downwind side of the boat for stability against to the heeling moment which is induced by the wind. The righting moment and lifting features of the retractable foils enable to enhance the performance at some conditions. Some designers and engineers from the Vendée Globe teams wanted to use the new system for their the Open 60 boats, and they have found the new generation curved daggerboard configuration based on the DSS instead of the conventional one for the IMOCA60s. Seven teams had decided to use the sailboats equipped with the curved daggerboards to compete in the Vendée Globe 2016/2017. These seven teams are Safran, Banque Populaire, Edmond de Rothschild, Hugo Boss, No way back (formerly Vento di Sardegna), St Michel-Virbac and Maître Coq [18]. The curved foil configuration of these new generation sailboats and the conventional daggerboard configuration are shown by illustrations in the following Figure 2.5 and 2.6.

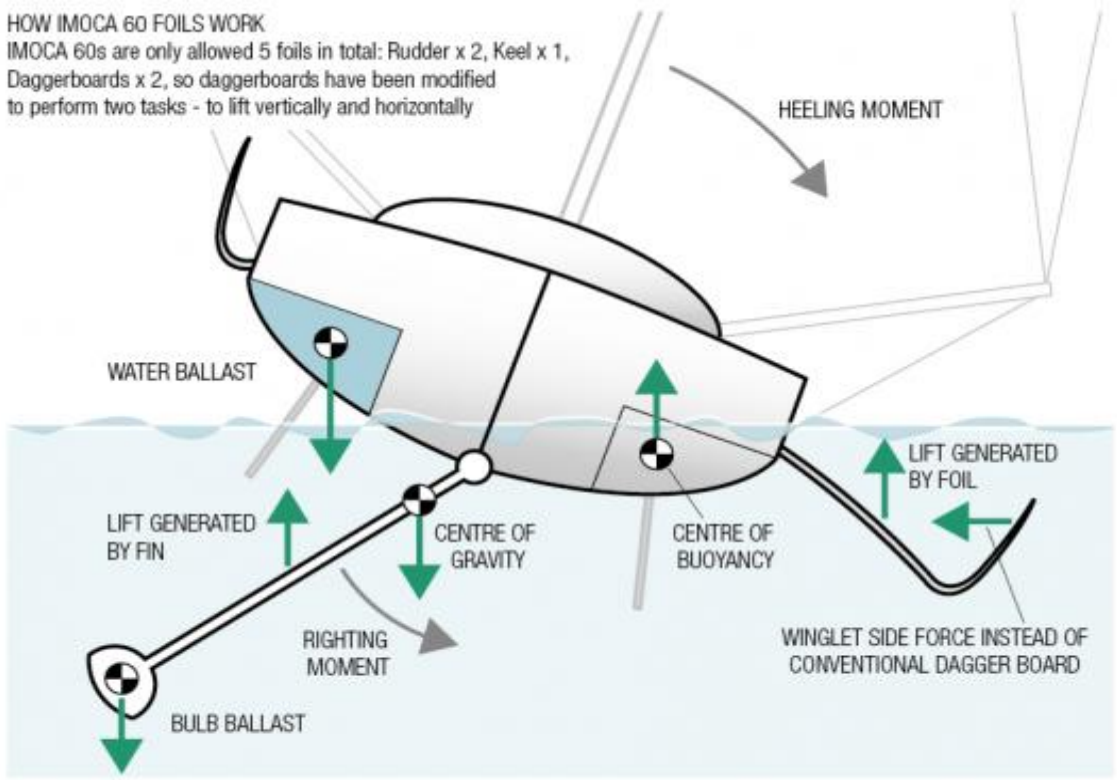

Figure 2-5: Illustration of IMOCA 60 equipped with canting keel & the curved foil configuration [19]

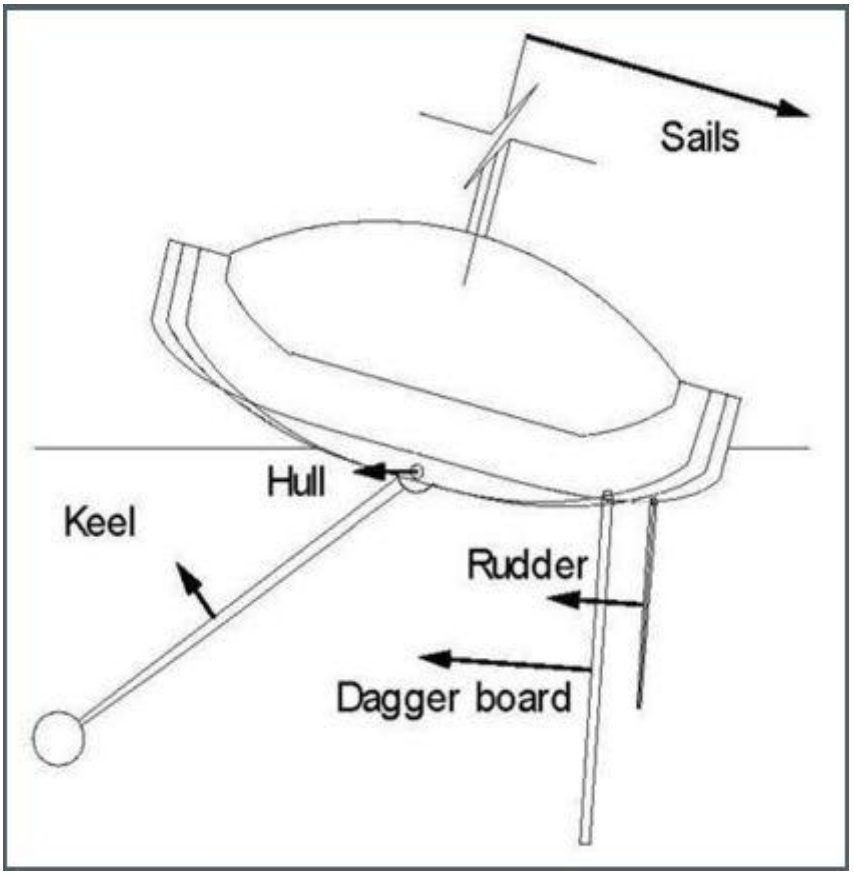

Figure 2-6: Illustration of IMOCA 60 equipped with canting keel & the straight foil configuration [14]

3 ITTC PROCEDURES AND GUIDELINES

In this section, general ITTC resistance and scaling assumptions will be represented with some formulations and approaches. The all towing tank tests used in this master thesis project are performed based on the ITTC regulations and requirements [3]. The chapter will include that the procedures will start with basic scaling rules and assumptions and then the resistance and form factor formulations and processes will be explained step by step generally.

3.1 Scaling Rules and Similarities

There are some requirements and approaches to perform the towing tank tests for all model experiments. According to these requirements, there should be three similarities in forces between the model and full size. The forces between model and full size should have geometric, kinematic and dynamic similarities [5].

Firstly, it is assumed that model and full size of the ship have a similar geometric shape according to geometric similarity. There is a constant scale factor (λ) (Equation 1) for the model and full size. The scale factor shows the ratio between lengths of the model and full size.

According to dynamic similarity, if the ratio between forces is equal, the model and full-size ships will have similar flows. The main forces are inertia, gravity and viscosity for the towing tank test processes. When we take a look at the ratios between these main forces, we can realise the Froude and Reynolds Numbers in the following equations.

$$\frac{Inertia}{Gravity} = \frac{\rho\, U^2\, l^2}{g\, l^3\, \rho} = \frac{U^2}{g \cdot l} = \mathbf{Fr} \quad \& \quad \frac{Inertia}{Viscosity} = \frac{\rho\, U^2\, l^2}{\mu\, U\, l} = \frac{\rho \cdot U \cdot l}{\mu} = \boldsymbol{Re} \quad \textbf{(6)}$$

Firstly, we try to scale the model size according to the Froude Number. In this way, we respect the Fr number [2] to get the proper relation between the model and full size thus we can obtain a correlation between the model speed and ship speed using the scale factor. In addition, the relation shows that if the Froude numbers are same for the model and full scale, the wave resistances will be equal as well. The residual resistance coefficient (C_R) is related to the wave making resistance; therefore, the C_R values will also be equal in the both scales.

$$Fr(m) = \frac{U(m)}{\sqrt{g \cdot l(m)}} = \quad Fr(s) = \frac{U(s)}{\sqrt{g \cdot l(s)}} \quad \rightarrow U(m) = U(s) \cdot \sqrt{\frac{g \cdot l(m)}{g \cdot l(s)}} = \frac{U(s)}{\sqrt{\lambda}} \quad \textbf{(7)}$$

The dynamic similarity assumes that the model and full scales should also have a relation based on the Reynolds number. However, it is not easy like Froude number to respect the Reynolds number because the viscosity of the fluid should be changed to get an accurate correlation between both scales but the situation is not realistically feasible for towing tank tests. Because of that, we just respect to Froude number exactly.

$$\boldsymbol{Re(m) = \frac{U(m) \cdot l(m)}{\nu(m)} = Re(s) = \frac{U(s) \cdot l(s)}{\nu(s)} \rightarrow \nu(m) = \nu(s)\ \frac{U(m) \cdot l(m)}{U(s) \cdot l(s)} = \frac{\nu(s)}{\lambda^{\frac{3}{2}}}} \quad (8)$$

3.2 ITTC 57 and 78 Methods

According to Froude's assumption, there are independent viscous and residuary drag related to the ship hull. The viscous drag is about friction associated with the interaction between the water and hull and the residual resistance consist of wave making drag and other extra rest drags. The non-dimensional resistance coefficient (Ct) is used for resistance tests instead of the total resistance (Rt). There is a general formulation for the model and full-scale resistance calculations [2]:

Where: The total resistance Rt (Newton), ρ (water density)–(kg/m³), V speed (m/s) and S the wetted surface area (m²).

$$\boldsymbol{Ct = \frac{Rt}{\frac{1}{2} \cdot \rho \cdot V^2 \cdot S}} \quad (9)$$

According to ITTC 57, the frictional resistance coefficient can be calculated analytically using an equation, and it is related to Reynolds number. The frictional resistance coefficient can be calculated for appendages as well.

$$\boldsymbol{Cf = \frac{0.075}{(log_{10}Re - 2)^2}} \quad (10)$$

According to ITTC 78, the form factor (1+k) should be determined for the hull to get the corrected frictional resistance exactly. Based on Prohaska's method, the form factor can be obtained at very low speed (Fr ≤ 0.2) [4]. In the following equation, the Prohaska's method is shown below [2]:

$$\boldsymbol{Ct = (1 + k) \cdot Cf + k_1 \cdot\ Fr^4 \rightarrow \frac{Ct}{Cf} = (1 + k) + k_1 \cdot \frac{Fr^4}{Cf}} \quad (11)$$

After these processes, there is a total resistance coefficient formulation which contains all the frictional, wave and additional resistance coefficients. The Cr is the roughness coefficient that is taken as standard racing yacht value (Cr=0.0002) [6] and the air resistance coefficient (Caa= 0.001 x [At-Ship's frontal area/S-Wetted surface area]) [2] is calculated as 0.0002 for the sailboat approximately.

$$\boldsymbol{Cwm(Fr) = Cws(Fr) \rightarrow Ct(Re, Fr) = (1 + k)Cf(Re) + Cw(Fr) + Cr + Caa} \quad (12)$$

3.3 Form Factors

In this section, the form factor values obtained by towing tank tests will be shown at different heel angles. The Open 60 model hull was towed without appendages at the upright condition, 10°, 15°, 20° and 25° heel angles during these form factor tests to get appropriate results. The appendage volumes were measured approximately according to appendage dimensions and the model boat displacement without appendages was calculated by subtracting the appendage volumes (bulb, keel, and dagger board) from half-load model displacement (17,64 kg) and then the necessary ballast weight (6.9 kg) was determined according to the calculations. The model wetted surface areas were scaled from full-scale areas which were obtained using Maxsurf Stability [20] at different heel angles. The Prohaska's method was used for these form factor calculations at very low speeds (Fr≤0.2) according to ITTC procedure [4]. The model total resistance values were obtained at certain Froude numbers, and the frictional resistance coefficient (Cf), and the total resistance coefficient (Ct) values were calculated based on ITTC formulations to apply the Prohaska's method. The 4th power of the Froude number refers to the wave resistance coefficient. The graphs were plotted with the required components according to the Prohaska's formulation [4] to find the form factors. The form factor (1+k) corresponds to the intercept value of the variables (Ct/Cf versus Fr^4/Cf) used in the regression graphs.

$$\boldsymbol{Ct = (1 + k) * Cf + b * Fr^4}$$

$$\boldsymbol{\frac{Ct}{Cf} = (1 + k) + b * \frac{Fr^4}{Cf}} \qquad (13)$$

The model hull was towed at a certain range of Froude numbers (0.1≤Fr≤0.2) to obtain the form factor numbers based on the Prohaska's method for each desired sailing conditions (the upright condition, 10°, 15°, 20° and 25° heel angles). Seven points were used to draw the straight line on the graphs, and when the graphs did not give appropriate results (low R^2) for getting the form factor values, some points were removed to obtain more accurate form factor (1+k) values. Therefore, just 3 or 4 points were used to plot the graphs after some readjustment processes generally. The form factor values were taken into account for resistance calculations in further sections.

After the towing tank tests and readjustment processes, the all final form factor numbers were obtained based on the Prohaska's method for each sailing states. According to the average temperature value (19.5 °C), the environmental specifications were taken into account for the calculations. The all form factor values are shown in the following table, and the detailed form factor tables and graphs are presented for each condition in the Appendix-A section.

Table 3-1: Some general specifications for the form factor calculations

Some General Specifications		
Overall Submerged Length ,LOS	2,286	m
Waterline Length, LWL	2,25	m
Density- ρ - (19.5 °C)	998,31	kg/m³
Viscosity - μ - (19.5 °C)	1,014E-03	(Pa·s)
Gravity	9,81	m/s²

Table 3-2: Form factor values - (1+k) for some sailing states

Form Factor Values - (1+k) For Sailing States	
Upright Condition	1,32
10° Heel Angle	1,26
15° Heel Angle	1,19
20° Heel Angle	1,13
25° Heel Angle	1,12

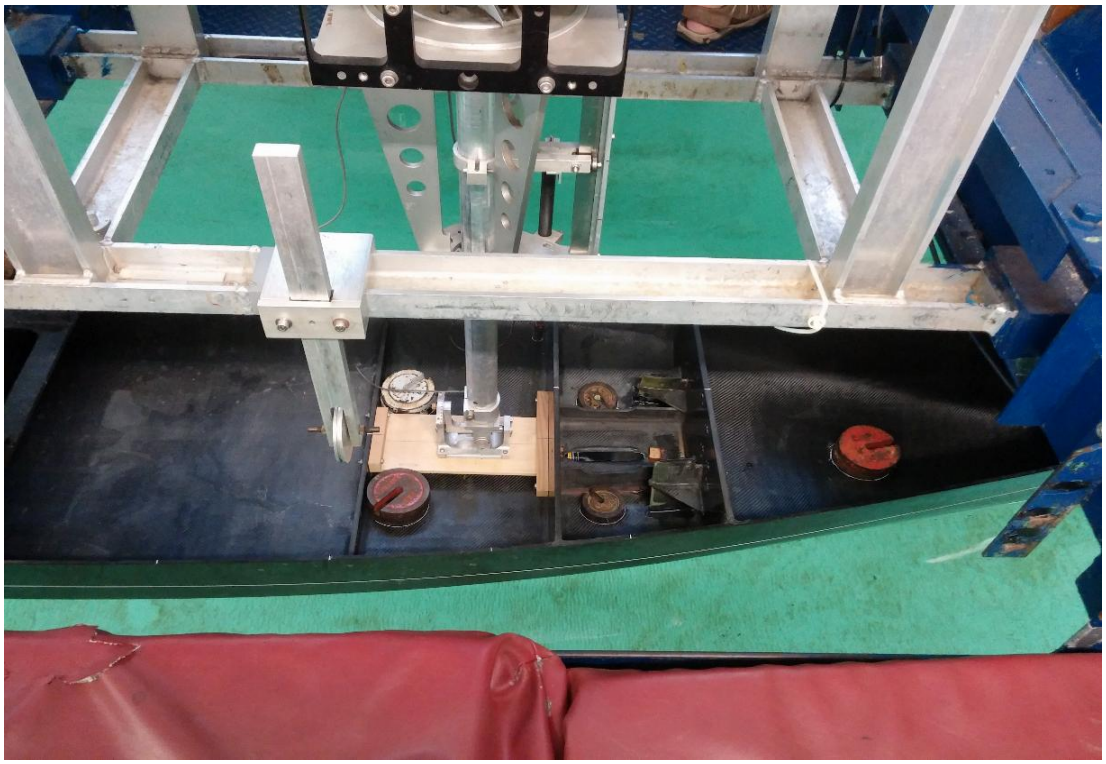

Figure 3-1: A model boat view of the form factor tests

3.4 Uncertainty Analysis

During all the towing tank test processes, there could be little errors or uncertainties about some parameters because of various reasons such as the environmental conditions, user mistakes, geometric roughness, measurement system and so on therefore this situation might modify some hydrodynamic outputs which are obtained by towing the hull model during the experiments. For that reason, the uncertainty analysis can be applied based on the ITTC Recommended Procedures and Guidelines [3, 4] to determine the amount of the uncertainties. According to the ITTC Procedures, there are some requirements and instructions to get the margin of error. The uncertainties of certain main variables are calculated with some formulations and instructions step by step.

In this section, there will be some main parameters such as speed, density, wetted surface area and frictional resistance coefficient (Cf). The fundamental component uncertainties for the towing tank tests are presented based on the ITTC Procedures. The approximate uncertainties will show the probable differences in the analysis results.

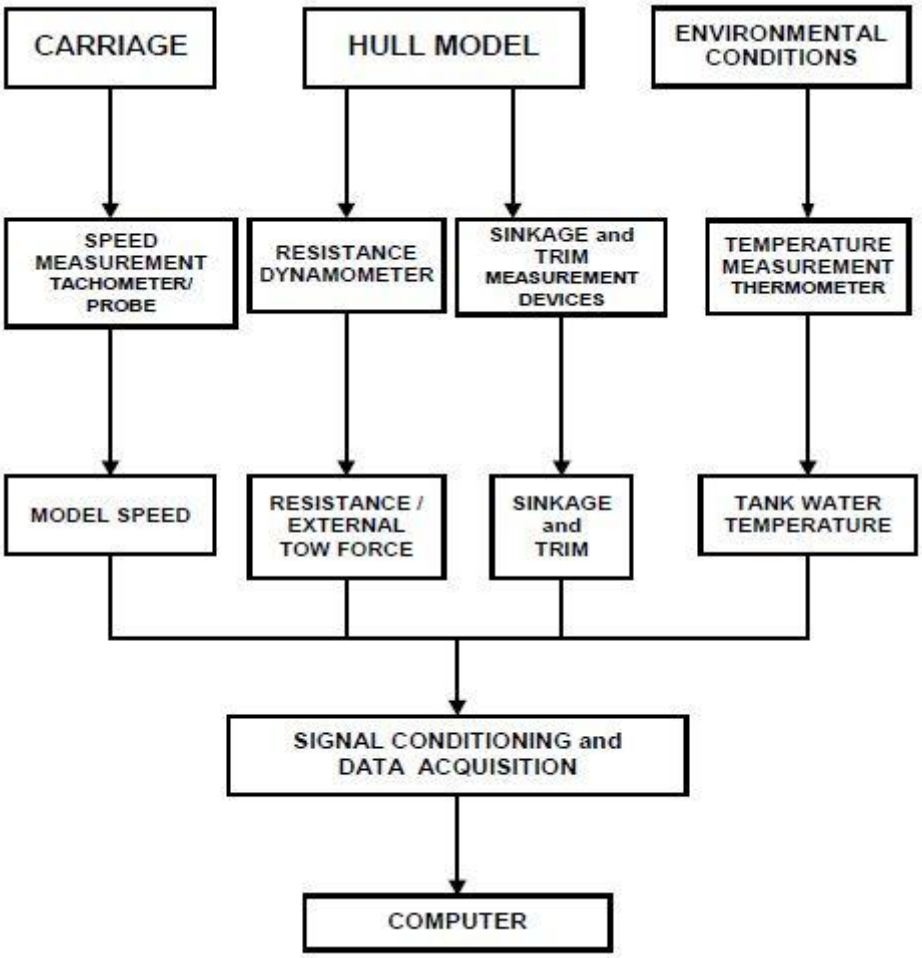

Figure 3-2: General diagram of model towing tank tests [3]

3.4.1 The Main Uncertainty Values

It is acknowledged that the uncertainty calculations were performed based on general sample of an uncertainty excel sheet [29] and a new excel sheet was created based on the latest ITTC Procedures and Guidelines [4]. The analysis was done in a particular upright condition to obtain the general uncertainty values. The error quantities of all these parameters were determined step by step based on formulations and instructions of the uncertainty processes (Type A and type B [4]. The type A procedures include the repeated towing tests to get the precision quantity of some important parameters such as total resistance, velocity, temperature. On the other hand, the type B processes contain some specific equations and variables to find the uncertainty amounts of the main parameters. The detailed tables are shown in the Appendix-B section.

Table 3-3: The main parameter values used in the uncertainty analysis calculations

Main Parameters		
Average Temperature	19,5	°C
Fresh Water Density	998,31	kg/m³
Fresh Water Viscosity-v	1,02E-06	m²/sn
Model Waterline Length-LWL	2,25	m
Model Length Overall Submerged-LOS	2,286	m
Wetted Surface Area	0,88	m²
Speed	1,613	m/s
Froude Number	0,34	-
Reynolds Number	3,63E+06	-
Coefficient of Frictional Resistance-Cf	3,61E-03	-
Total Resistance-Rt	6,18	N
Coefficient of Total Resistance-Ct	5,40E-03	-
Form Factor-(1+k)	1,32	-
Coefficient of Residuary Resistance-CR	6,42E-04	-

Table 3-4: Total uncertainties of the main parameters

Total Uncertainties		
TEMPERATURE	0,5	%
Fresh Water Density	3,02E-03	%
Fresh Water Viscosity	1,1	%
Model Waterline Length-LWL	0,1	%
Model Length Overall Submerged-LOS	0,1	%
Wetted Surface Area	0,1	%
Speed	0,1	%
Froude Number	0,2	%
Reynolds Number	0,3	%
Coefficient of Frictional Resistance-Cf	0,1	%
Total Resistance-Rt	0,3	%
Coefficient of Total Resistance-Ct	0,5	%
Form Factor - k	3	%
Coefficient of Residuary Resistance-CR	4	%

According to the results, there are two examples of the parameter uncertainties to show with a graph. These graphs present that the parameters can change with the margin of the errors in the range of the uncertainty values (plus or minus). Based on the ITTC Procedure and Guidelines, the residual resistance coefficient contains the sum of the uncertainties of the all main parameters in its uncertainty formulation; therefore, it can be seen that the residual resistance coefficient has the maximum uncertainty amount. In the following graphs, the uncertainty percentages are illustrated with some example values below.

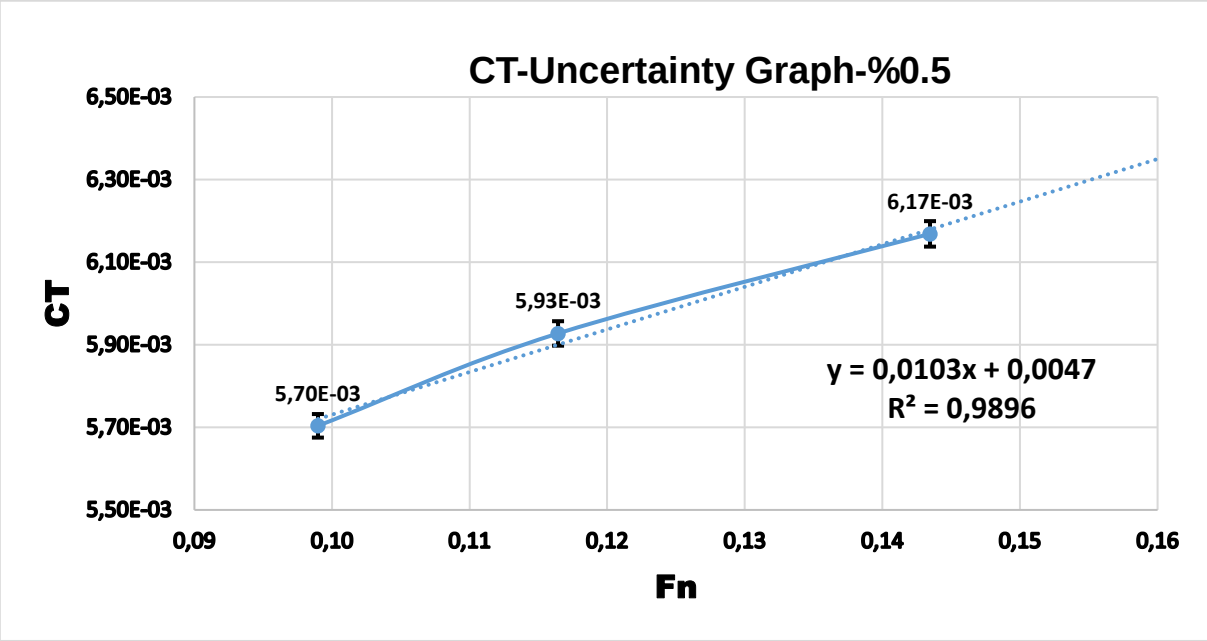

Figure 3-3: Uncertainty analysis graph of the total resistance coefficient

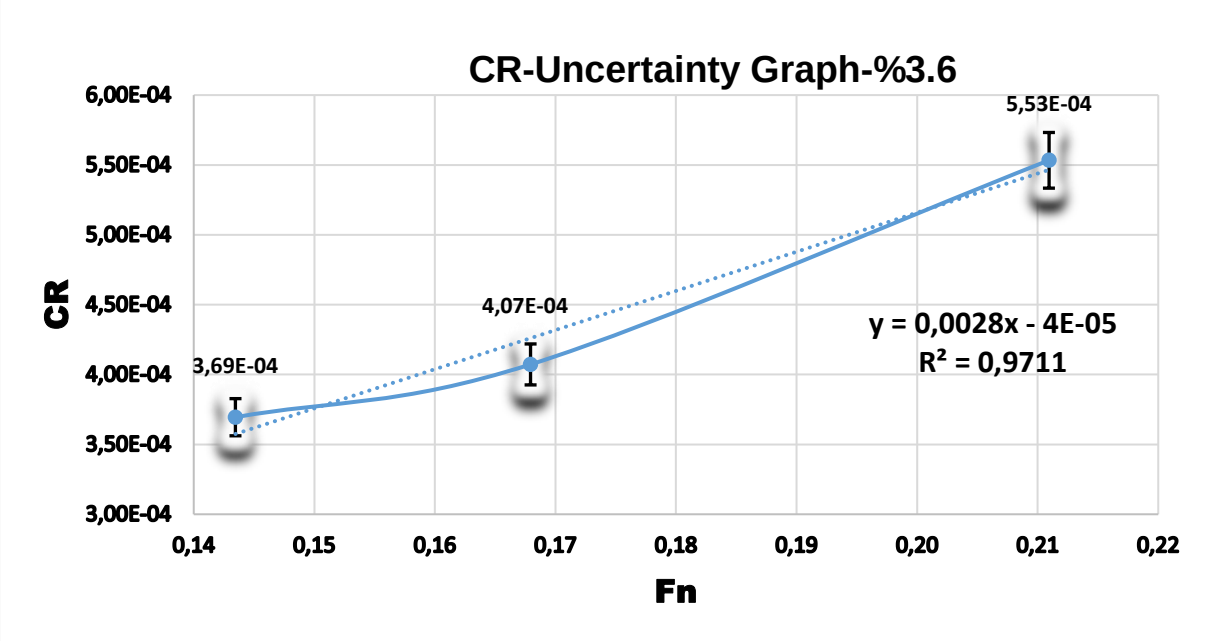

Figure 3-4: Uncertainty analysis graph of the residual resistance coefficient

4 TOWING TANK TESTS

The towing tank experiments were performed to obtain the desired experimental results in Towing Tank Facility of the Southampton Solent University. The first some tests were done together with the Solent staff to verify the test results. The model boat of representative Open 60 sailboat had been already built as made of carbon fibre by the university and it was given for these towing tank tests of the thesis. In addition, the keel, bulb, rudder and straight dagger board models were available for the experiments. The curved daggerboard was designed and produced according to approximate dimensions as one of the objectives of this thesis. The towing tank tests are carried out by towing the model boat via the carriage, and in this way, real ship reactions can be estimated approximately according to model size tests. Firstly, test matrix is created to determine the intended parameters according to particular sailing conditions. These tests were run with appendages or without appendages for various objectives, and they were done based on ITTC procedures. The towing tank carriage has been set up with some measurement devices such as the tachometer, dynamometer to obtain outputs and the hydrodynamic output results are read from records of a specific computer software. The results will be analysed to get some critical assessments about different boat situations. Some specifications of the towing tank facility are shown below.

Figure 4-1 : Specifications of the Towing Tank Facility

4.1 The Model and Full Size Values

Firstly, the displacement value was determined for the towing tank tests. The 3D Maxsurf Hull of this Open 60 sailboat was given by Solent staff to perform some measurements and calculations. As stated previously, the boat was designed about 7.6-8 tonnes according to the un-ballasted situation (lightship) in full size and the sailboat was ballasted to the appropriate waterline value approximately based on the half-load displacement of the sailing condition and the condition is considered as average race position. The model boat displacement was calculated according to scaling the full-size half-load displacement and the bare hull, heel fitting and post weights were measured to obtain the necessary ballast weight during the tests. All model and full-size values are presented in the following tables based on the 1/8th scale factor.

Table 4-1: Some model size measurements

Parameters	Model Size	Unit
Half-Load Displacement	17,64	kg
Bare Hull	9,85	kg
Heel Fitting & Post	1,05	kg
Ballast Weight	6,74	kg
Bulb Volume	0,54	litres
Keel Volume	0,16	litres
Daggerboard Volume	0,09	litres
λ-Scale Factor	8,00	-

Table 4-2: Model hull specifications in the upright condition

Upright - Model Hull Specifications		Unit
Overall Submerged Length ,LOS	2,286	m
Waterline Length, LWL	2,25	m
Wetted Surface Area	0,88	m^2
Density-ρ	998,31	kg/m^3
μ-Dynamic Viscosity	1,14E-03	(Pa·s)
Form Factor-(1+k)	1,32	-
Half-Load Displacement	17,64	kg
λ-Scale Factor	8,00	-

Table 4-3: Full size hull specifications in the upright condition

Upright - Full Size Hull Specifications		Unit
Overall Submerged Length ,LOS	18,288	m
Waterline Length, LWL	18	m
Wetted Surface Area	56,32	m^2
Density-ρ	1025	kg/m^3
μ-Dynamic Viscosity	1,19E-03	(Pa·s)
Form Factor-(1+k)	1,32	-
Half-Load Displacement	9260	kg
λ-Scale Factor	8,00	-

Full Size Hull Specifications

Also, there are the model and full-size dimensions of keel, bulb, rudder and straight dagger board. The model dimensions were measured from the existing model objects, and they were scaled to full size based on 1/8th scale factor. The straight daggerboard has 15° cant angle and 1.5° toe angle. The form factors of these appendages were calculated using a formulation proposed by Hoerner [6] which is shown below:

$$(1+k) = 1 + 2 * \left(\frac{t}{c}\right) + 60 * \left(\frac{t}{c}\right)^4 \qquad \textit{For foil shaped appendages} \qquad (14)$$

$$(1+k) = 1 + 1.5 * \left[\frac{t}{c}\right] \qquad \textit{For bulb shaped appendages} \qquad (15)$$

Table 4-4: Model dimensions of the appendages

Model Dimensions								
Keel		**Rudder**		**Bulb**		**Straight DBD**		**Unit**
Chord	0,082	Chord	0,03	Chord	0,4	Chord	0,063	m
Span	0,46	Span	0,15	Span		Span	0,42	m
WSA	0,075	WSA	0,01	WSA	0,048	WSA	0,053	m²
t/c	0,1	t/c	0,1	t/c	0,152	t/c	0,1	-
(1+k)	1,206	(1+k)	1,206	(1+k)	1,23	(1+k)	1,206	-

Table 4-5: Full size dimensions of the appendages

Full Size Dimensions								
Keel		**Rudder**		**Bulb**		**Straight DBD**		**Unit**
Chord	0,656	Chord	0,24	Chord	3,2	Chord	0,504	m
Span	3,68	Span	1,2	Span	0	Span	3,36	m
WSA	4,83	WSA	0,576	WSA	3,072	WSA	3,39	m²
t/c	0,1	t/c	0,1	t/c	0,152	t/c	0,1	-
(1+k)	1,206	(1+k)	1,206	(1+k)	1,228	(1+k)	1,206	-

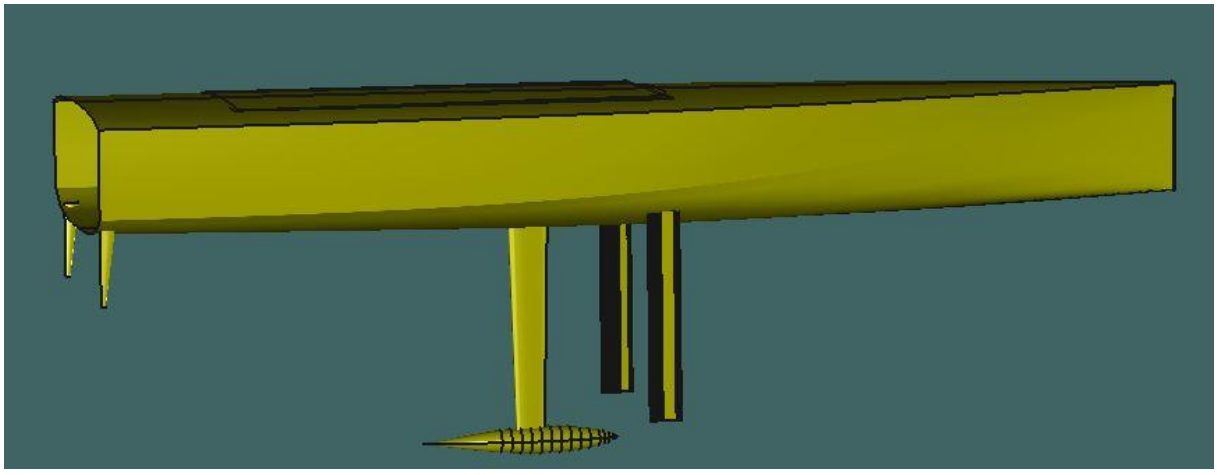

Figure 4-2 : 3D Maxsurf hull view with the appendages [20]

4.2 The Curved Daggerboard Design

Firstly, the curved daggerboard configurations were investigated on the seven Open 60 sailboats which are Safran, Banque Populaire, Edmond de Rothschild, Hugo Boss, No way back (formerly Vento di Sardegna), St Michel-Virbac and Maître Coq [18]. Some dimensions were measured by using scaling method from pictures of these representative sailboats approximately. The foil dimensions were averaged to determine only one representative curved foil and the Naca section of foil was selected as Naca 63-412 [21, 22] which is used for foiling Moth boats generally because there is no a specific foil section which is used by designers for these curved daggerboard designs. After that, the 3D drawing was created according to these average model value in Rhinoceros Software [23]. It was prepared for manufacture processes with various adjustments. These average model dimensions and views of the curved foil are shown in following table and drawings.

Table 4-6: Table of the approximate model size specifications of the representative curved foil shape

Approximate Specifications of Representative Curved Foil				
Model Average Values				
Chord1	**0,047**	**m**	**47**	**mm**
Span1	**0,217**	**m**	**217**	**mm**
Chord2	**0,071**	**m**	**71**	**mm**
Span2	**0,227**	**m**	**227**	**mm**
Radius-R	**0,041**	**m**	**41**	**mm**
Location from aft	**1,12**	**m**	**1119**	**mm**
Naca Section NACA 63-412 was used for the foils				

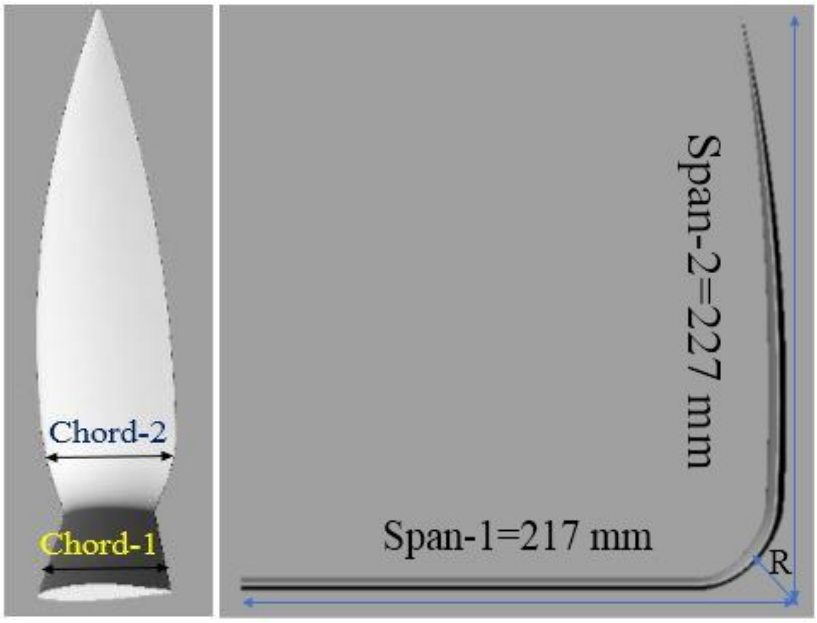

Figure 4-3: Design dimensions of the curved daggerboard [23]

There are two kinds of curved daggerboards which have half and full Span-1 lengths. However, the curved part (Span-2) is same for both dagger board configurations. Firstly, the curved daggerboards were produced by 3D printer, and they were made of plastic material (PBC) and then they were covered with the carbon fibre by using hand lay-up technique. After these processes, they were painted and sanded to have a smooth surface. The cant and toe angles of the curved foil were taken same as the straight foil. Therefore, the foils were placed with 15° cant angle and 1.5 ° toe angles (for both parts) from centre line approximately by using some wooden tools and a wooden object was used to arrange the position of the foil properly, so it was fixed to the appropriate location from aft with nuts. It is informed that the Solent University staff provided the manufacturing and 3D modelling of the curved foils. The manufacture and final views of the curved daggerboards are shown in the following pictures.

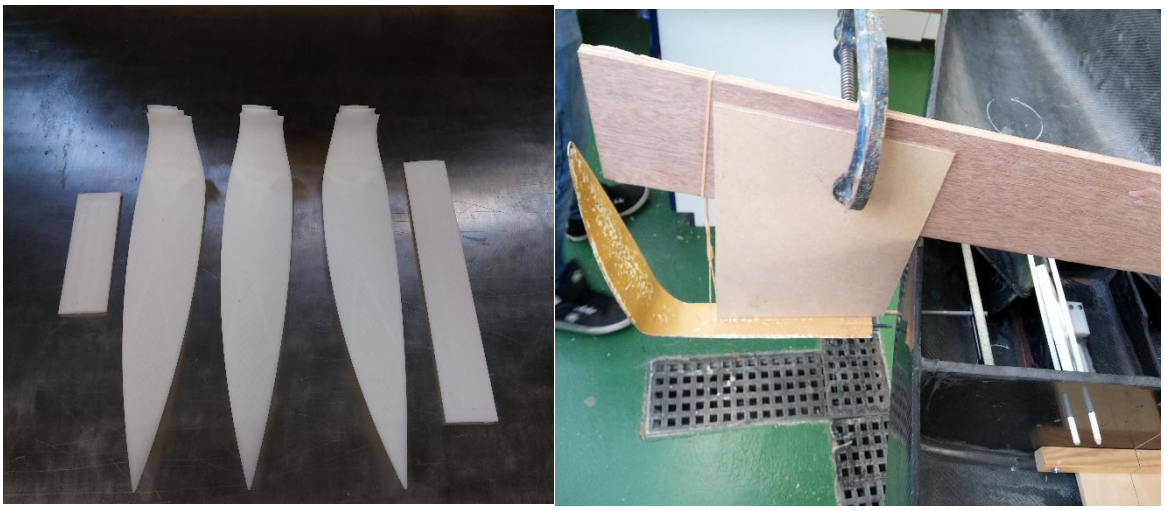

Figure 4-4: Plastic parts manufactured from 3D printer (Left) & the full foil with the wooden fixing tools (Right)

Figure 4-5: Half Curved Dagger Board (Left) & Full Curved Dagger Board (Right)

5 HYDRODYNAMIC ANALYSES

In this chapter, the straight and curved daggerboard configurations will be analysed based on the hydrodynamic results which were obtained by the towing tank tests. The hydrodynamic parameters are Drag, Lift and Side Force values. The calculations have been performed based on a sample spreadsheet which was provided by the Solent University. It was adjusted for the desired experimental tests during this thesis.

- Drag Analyses with the straight and curved daggerboard configurations
- Lift Analyses with the straight and curved daggerboard configurations
- Side Force Analyses with the straight and curved daggerboard configurations
- 0° and 40° Canting Keel Analyses according to effective draft and Gz values
- Effective Draft Comparisons according to different foil configurations
- Finding the better daggerboard configuration at some particular heel angles and velocity values (Froude number) in the upwind condition

Table 5-1: Full scale foil specifications of the 1/2 - full straight and curved daggerboard configurations

Full Scale Full Straight Foil	
Chord	0,50
Span	3,36
WSA	3,39
t/c	0,1
(1+k)	1,21
Full Scale 1/2 Straight Foil	
Span	1,68

Full Scale Full Curved Foil	
Chord1	0,38
Span1	1,74
Chord2	0,57
Span2	1,82
Avg Chord	0,47
WSA	3,37
t/c	0,12
(1+k)	1,25
Full Scale 1/2 Curved Foil	
Span1	0,87

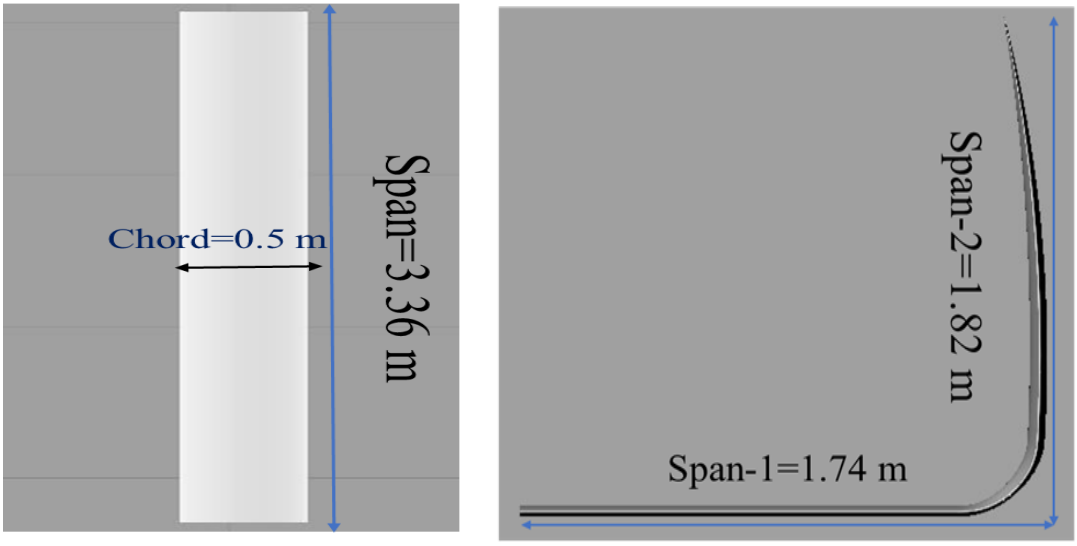

Figure 5-1: Full-Size Straight Foil Configuration (Left) & Full-Size Curved Foil Configuration (Right) [23]

5.1 The Sailing Yacht Resistance and Effective Draft Method

5.1.1 The Sailing Yacht Resistance

As explained earlier, the sailboats also have two main resistance parts which are frictional and wave making resistances. In the towing tank tests, the two resistance components can be obtained for both model and full scales separately. The wave resistance parts are assumed to be same for both scales based on Froude number similarity [2], and it can be scaled from model to full size easily. On the other hand, the viscous resistances can be computed for both model and full scales according to scaled dimensions and different Reynolds numbers. Additionally, the sailing yacht resistance has the heel and induced drag components. The induced drag occurs because of side force which is generated by the hull, dagger board, and keel and rudder sections. The side force is an important parameter for sailboat stability. The sailboat also has heel resistance when it heels to one side. The heel resistance consists of frictional and wave drags like upright resistance. Based on ITTC methods [2], the total resistance can be scaled from model size to full size according to the similarity assumptions consequently. The total resistance is divided into three parts [6]:

- **Upright Resistance (consisting of frictional and wave making resistances)**
- **Heel Resistance (when the boat is heeled, it will contain the resistance components due to the heeling)**
- **Induced Resistance (the drag due to total side force generated by hull/appendages – associated with Froude number)**

$$\boldsymbol{Rtotal = Rupright + Rheel + Rinduced} \qquad (16)$$

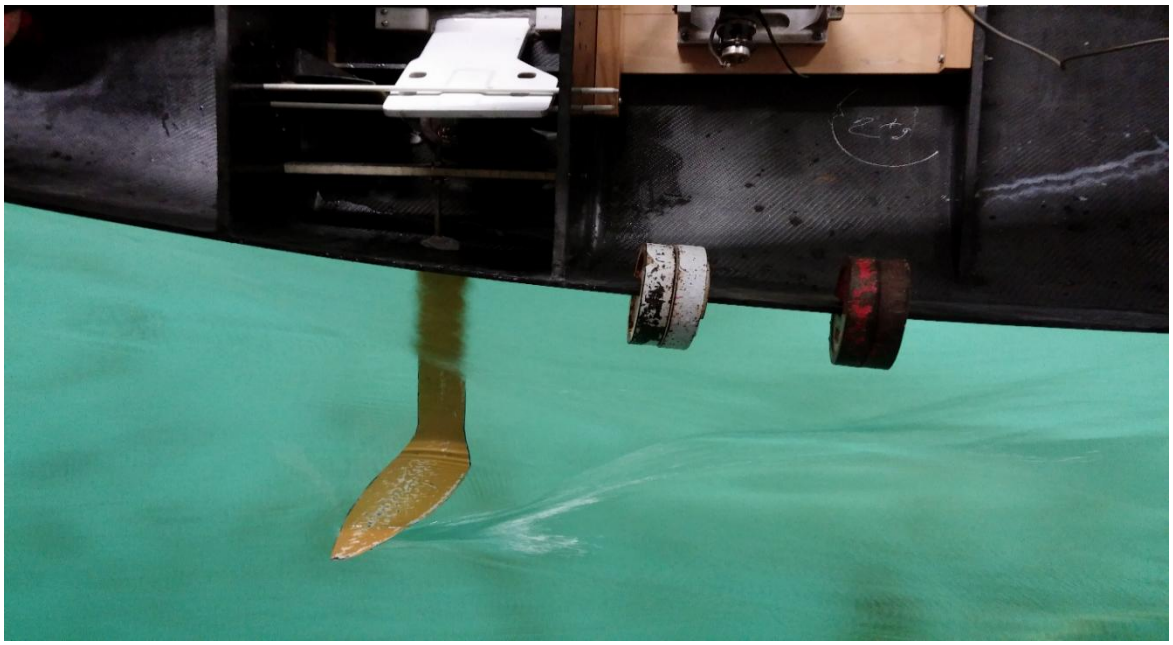

Figure 5-2: The boat heeling situation with hull and appendages

5.1.2 The Effective Draft Method

The tank test matrix is created for the all the towing tank tests, and the test matrix includes various configurations with different velocities, heel and leeway angles. Firstly, the upright resistance line at 0° leeway can be plotted according to certain velocities (or Froude number). Moreover, then the boat is heeled to port or starboard side with a particular heel angle and the boat is towed with different leeway angles at a particular velocity value. This process is repeated for desired sailing conditions, and the necessary hydrodynamic components are obtained based on the test matrix.

The total resistance (Rt) and side force squared (SF^2) values obtained at various leeway angles are used to draw a graph which enables to determine the effective draft and induced drag variables at a given heel angle and velocity value [6]. The intercept of this graph gives the sum of the upright and heel resistances, and the heel drag can be found by subtracting the upright drag from the intercept value. The slope of this regression line enables to obtain the induced drag component. As mentioned before, the total resistance consists of upright, heel and induced drag components. According to the graph, there is a relation between the induced drag and side force squared and the effective draft value can be calculated based on the relation. The effective draft formulation is shown below. [Te=Effective draft, V=Velocity, SF=Side force, Fh=Heel force]:

$$\boldsymbol{Slope}\ \ \frac{\boldsymbol{y}}{\boldsymbol{x}} = \frac{\boldsymbol{Induced\ Drag}}{\boldsymbol{F_h{}^2\ (SF^2)}} = \frac{\mathbf{1}}{\boldsymbol{T_e{}^2 * \pi * \rho\ * V^2}} \qquad (\mathbf{17})$$

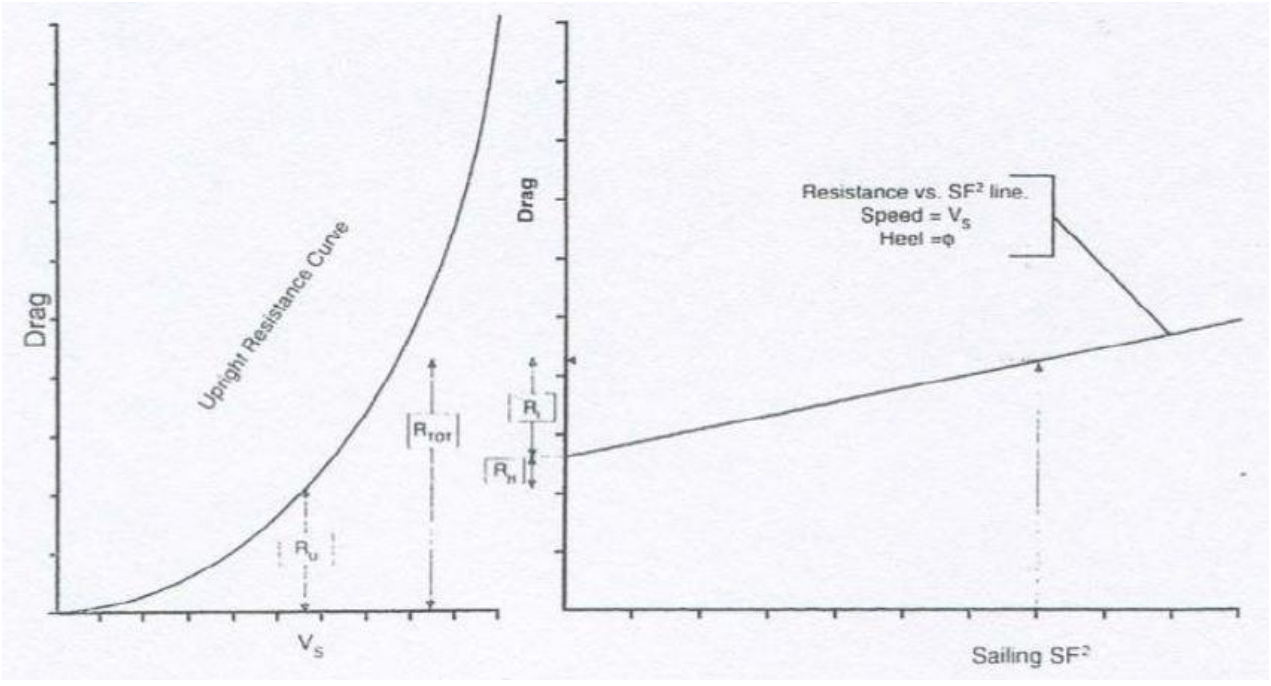

Figure 5-3: Total resistance versus side force squared graph for the effective draft calculation [6]

5.2 0° and 40° Canted Keel Analysis

In this section, the 0° and 40° canting keel configurations will be compared based on effective draft and GZ (Righting Arm) values. The advantages and disadvantages of the two different keel positions will be analysed to get critical results before the straight and curved daggerboard analyses. The towing tank tests are performed without the foil at the 0° and 40° keel canting angles and the side force and drag values are obtained by towing the model boat with certain velocity values at various leeway and heel angles. The hydrodynamic model results are scaled to full scale, and the effective draft values are determined by plotting the graphs for each sailing condition. Some model boat views with the canting keel are presented in the following pictures.

Figure 5-4: View of 40° canting keel

Figure 5-5: View of 40° canting keel below

5.2.1 0° Canted Keel Analysis

5.2.1.1 Effective Draft of 0° Canting Keel at 0° Heel Angle & 0.30 FN

Table 5-2: Effective Draft of 0° Canting Keel at 0° Heel Angle & 0.30 FN

Keel Position	Heel	Leeway	Clock No	V-Full Size (m/s)	FN	Full Size Total-Rt (kN)	SF² (kN)	Ri (kN)
0°	0°	1°	350	4,0	0,30	1,98	56,81	0,13
0°	0°	2°	350	4,0	0,30	2,07	89,82	0,20
0°	0°	3°	350	4,0	0,30	2,14	124,52	0,28

Ru+Rh (kN)	Slope	Te²	Te (m)
1,86	0,0022	8,66	2,94

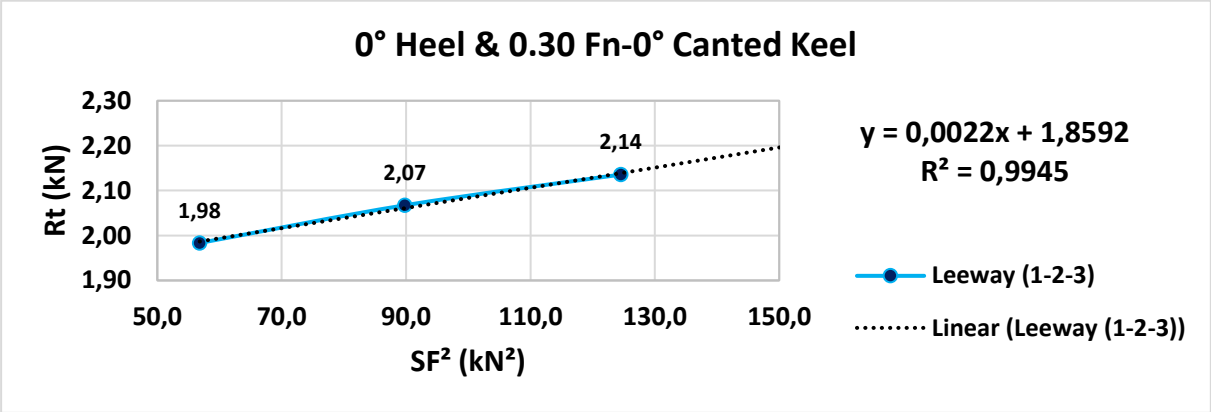

Figure 5-6: Graph of 0° canted keel at 0° heel angle and 0.30 Froude number

5.2.1.2 Effective Draft of 0° Canting Keel at 0° Heel Angle & 0.39 FN

Table 5-3: Effective Draft of 0° Canting Keel at 0° Heel Angle & 0.39 FN

Keel Position	Heel	Leeway	Clock No	V-Full Size (m/s)	FN	Full Size Total-Rt (kN)	SF² (kN)	Ri (kN)
0°	0°	1°	450	5,13	0,39	3,25	90,41	0,17
0°	0°	2°	450	5,13	0,39	3,42	208,92	0,38
0°	0°	3°	450	5,13	0,39	3,69	357,33	0,66
0°	0°	4°	450	5,13	0,39	3,99	499,53	0,92

Ru+Rh (kN)	Slope	Te²	Te (m)
3,06	0,0018	6,44	2,54

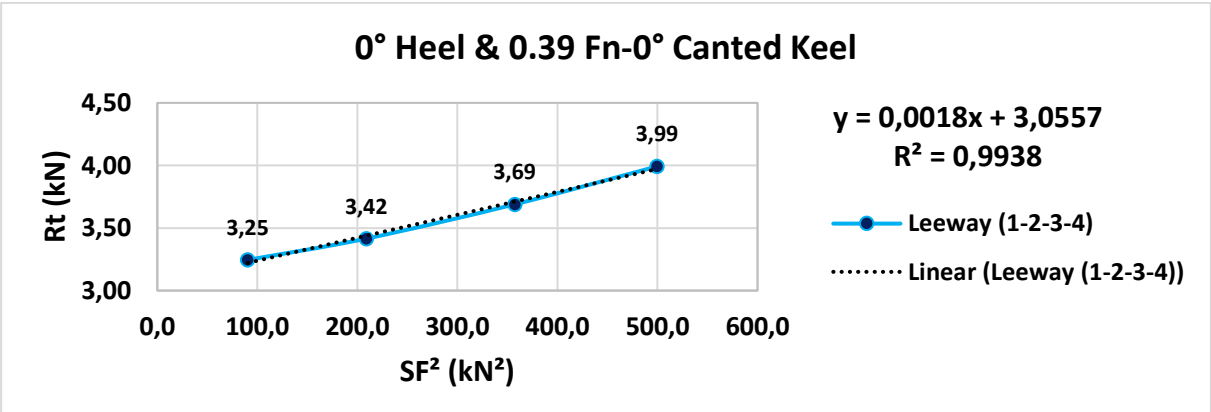

Figure 5-7: Graph of 0° canted keel at 0° heel angle and 0.39 Froude number

5.2.1.3 Effective Draft of 0° Canting Keel at 15° Heel Angle & 0.30 FN

Table 5-4: Effective Draft of 0° Canting Keel at 15° Heel Angle & 0.30 FN

Keel Position	Heel	Leeway	Clock No	V-Full Size (m/s)	FN	Full Size Total-Rt (kN)	SF² (kN)	Ri (kN)
0°	15°	1°	350	4,0	0,30	2,02	25,66	0,07
0°	15°	2°	350	4,0	0,30	2,11	57,02	0,15
0°	15°	3°	350	4,0	0,30	2,20	96,06	0,25

Ru+Rh (kN)	Slope	Te²	Te (m)
1,95	0,0026	7,46	2,73

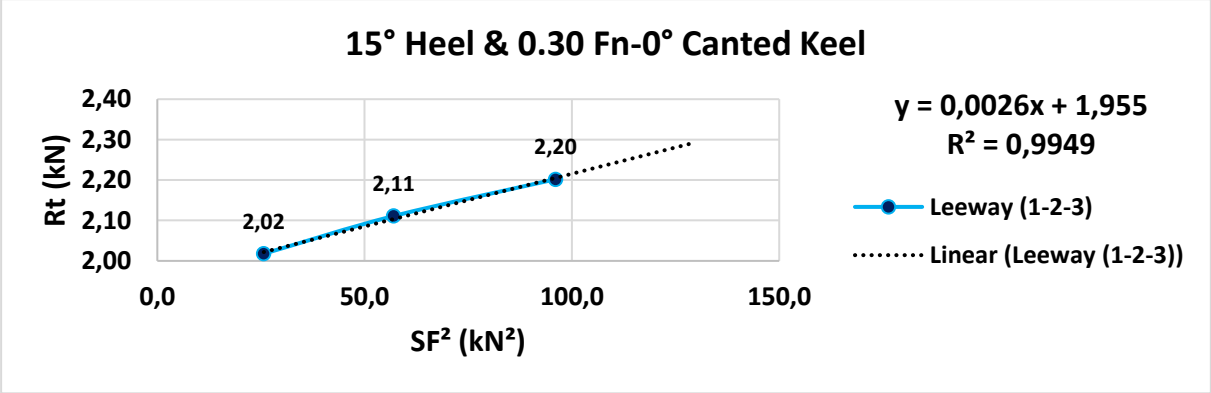

Figure 5-8: Graph of 0° canted keel at 15° heel angle and 0.30 Froude number

5.2.1.4 Effective Draft of 0° Canting Keel at 15° Heel Angle & 0.39 FN

Table 5-5: Effective Draft of 0° Canting Keel at 15° Heel Angle & 0.39 FN

Keel Position	Heel	Leeway	Clock No	V-Full Size (m/s)	FN	Full Size Total-Rt (kN)	SF² (kN)	Ri (kN)
0°	15°	1°	450	5,13	0,39	3,32	55,28	0,13
0°	15°	2°	450	5,13	0,39	3,50	132,38	0,32
0°	15°	3°	450	5,13	0,39	3,81	255,65	0,62

Ru+Rh (kN)	Slope	Te²	Te (m)
3,19	0,0024	4,86	2,21

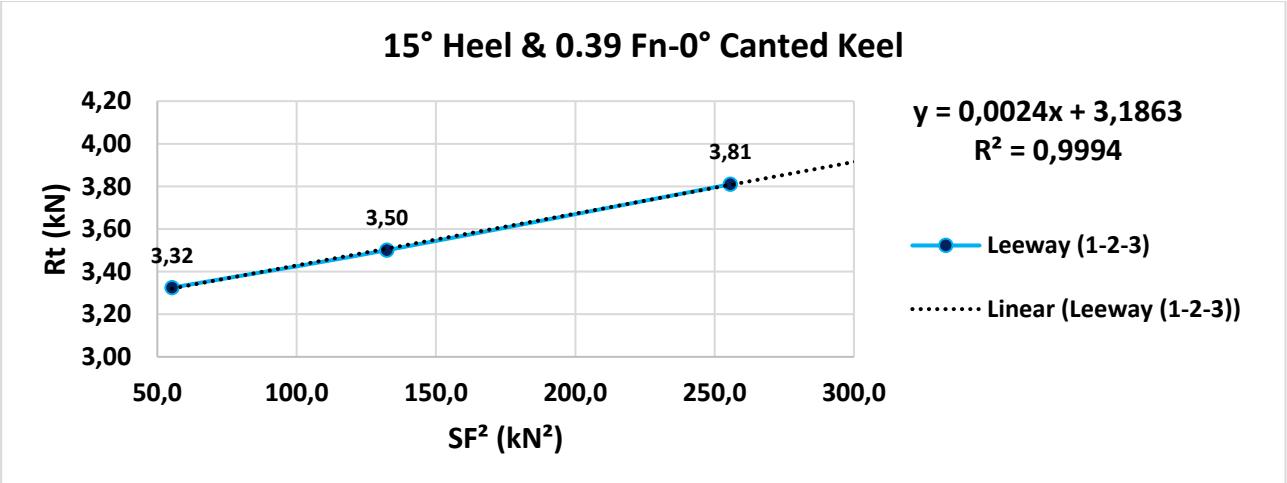

Figure 5-9: Graph of 0° canted keel at 15° heel angle and 0.39 Froude number

5.2.1.5 Effective Draft of 0° Canting Keel at 20° Heel Angle & 0.30 FN

Table 5-6: Effective Draft of 0° Canting Keel at 20° Heel Angle & 0.30 FN

Keel Position	Heel	Leeway	Clock No	V-Full Size (m/s)	FN	Full Size Total-Rt (kN)	SF² (kN)	Ri (kN)
0°	20°	1°	350	4,0	0,30	2,04	6,34	0,02
0°	20°	2°	350	4,0	0,30	2,10	29,24	0,08
0°	20°	4°	350	4,0	0,30	2,28	90,97	0,26

Ru+Rh (kN)	Slope	Te²	Te (m)
2,02	0,0029	6,73	2,59

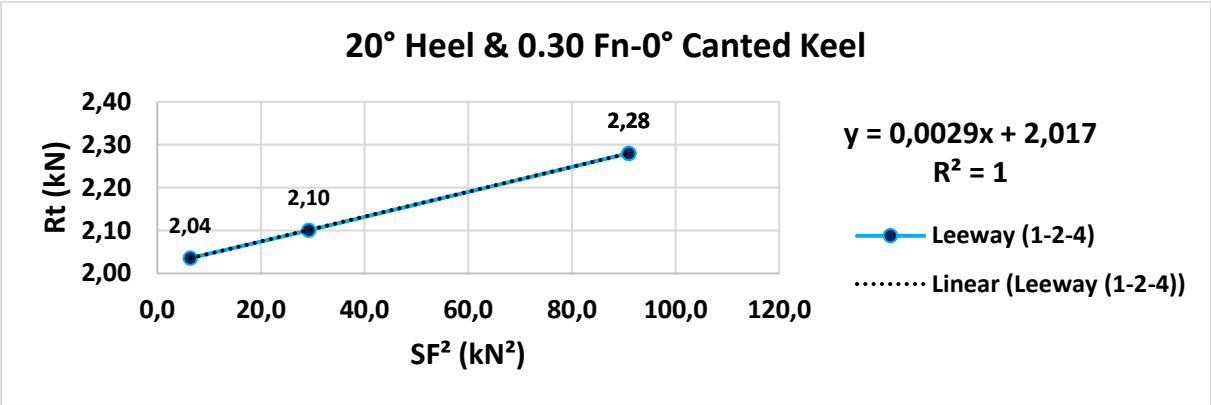

Figure 5-10: Graph of 0° canted keel at 20° heel angle and 0.30 Froude number

5.2.1.6 Effective Draft of 0° Canting Keel at 20° Heel Angle & 0.39 FN

Table 5-7: Effective Draft of 0° Canting Keel at 20° Heel Angle & 0.39 FN

Keel Position	Heel	Leeway	Clock No	V-Full Size (m/s)	FN	Full Size Total-Rt (kN)	SF² (kN)	Ri (kN)
0°	20°	1°	450	5,13	0,39	3,32	27,40	0,09
0°	20°	2°	450	5,13	0,39	3,48	80,95	0,26
0°	20°	3°	450	5,13	0,39	3,76	164,90	0,52
0°	20°	4°	450	5,13	0,39	4,01	246,55	0,78

Ru+Rh (kN)	Slope	Te²	Te (m)
3,23	0,0032	3,71	1,93

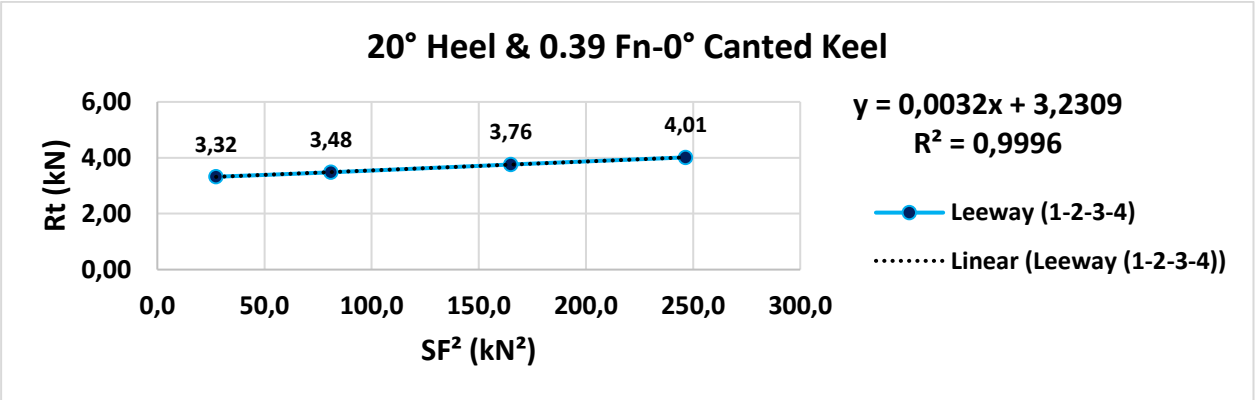

Figure 5-11: Graph of 0° canted keel at 20° heel angle and 0.39 Froude number

5.2.1.7 Overall Results of the 0° Canting Keel

After the effective draft calculations, the overall full-scale results are presented in the following tables. According to these results, it is noted that there are some energy losses when the keel/hull combination generates the side force at different conditions during sailing. The assessment of the general situation is done for 0° canted keel according to these results:

- The effective draft values decrease due to the ratio of the induced drag (energy losses) and side force squared when the Froude number is increased. When the leeway angle (angle of attack) is increased, the side force squared has increment based on foil theory.
- The amount of the side force values decreases due to change of 3D side force vector direction when the boat is heeled at a particular angle; therefore, the effective draft values fall due to more induced drag. The highest value is obtained at 0° heel angle and lowest velocity (0.3 FN).

Table 5-8: Effective draft results of the 0° canting keel

Effective Draft Results of O° Canted Keel		
Conditions	Fn	
	0,3	0,4
O° Cant - O° Heel Angle	2,94	2,54
O° Cant - 15° Heel Angle	2,73	2,21
O° Cant - 20° Heel Angle	2,59	1,93

Table 5-9: Effective draft / maximum draft results of the 0° canting keel

O° Canted Keel		
Effective Draft / Max. Draft		
FN	0,3	0,4
0° Heel	0,65	0,56
15° Heel	0,61	0,49
20° Heel	0,58	0,43
Max. Draft = 4.5 m		

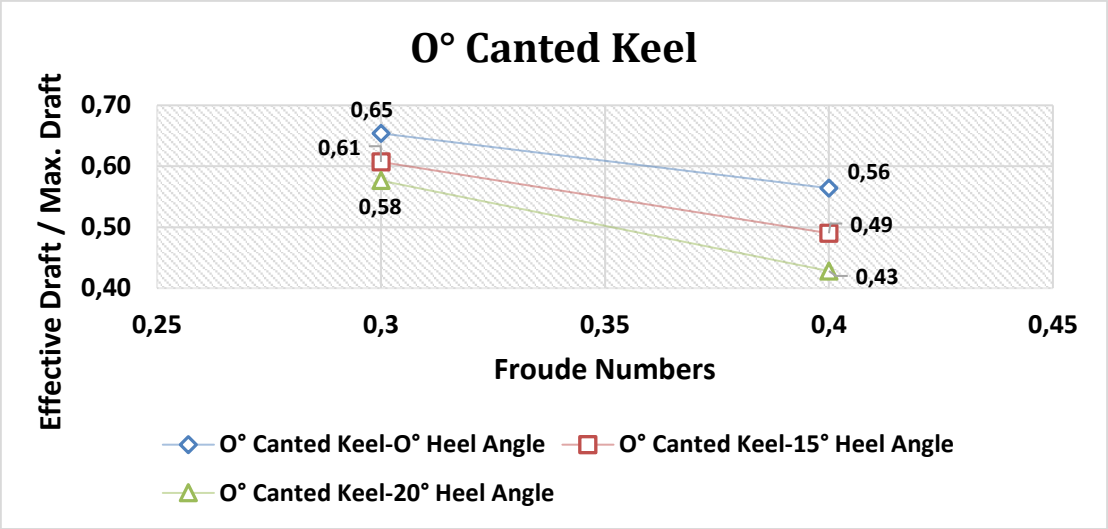

Figure 5-12: Effective draft / Max. Draft graph of 0° canted keel

5.2.2 40° Canted Keel Analysis

5.2.2.1 Effective Draft of 40° Canted Keel at 0° Heel Angle & 0.30 FN

Table 5-10: Effective Draft of 40° Canted Keel at 0° Heel Angle & 0.30 FN

Keel Position	Heel	Leeway	Clock No	V-Full Size (m/s)	FN	Full Size Total-Rt (kN)	SF² (kN)	Ri (kN)
40°	0°	4°	350	4,0	0,30	2,09	35,46	0,21
40°	0°	6°	350	4,0	0,30	2,30	75,44	0,46
40°	0°	8°	350	4,0	0,30	2,48	102,71	0,62
40°	0°	10°	350	4,0	0,30	2,70	136,11	0,82

Ru+Rh (kN)	Slope	Te²	Te (m)
1,87	0,0060	3,22	1,79

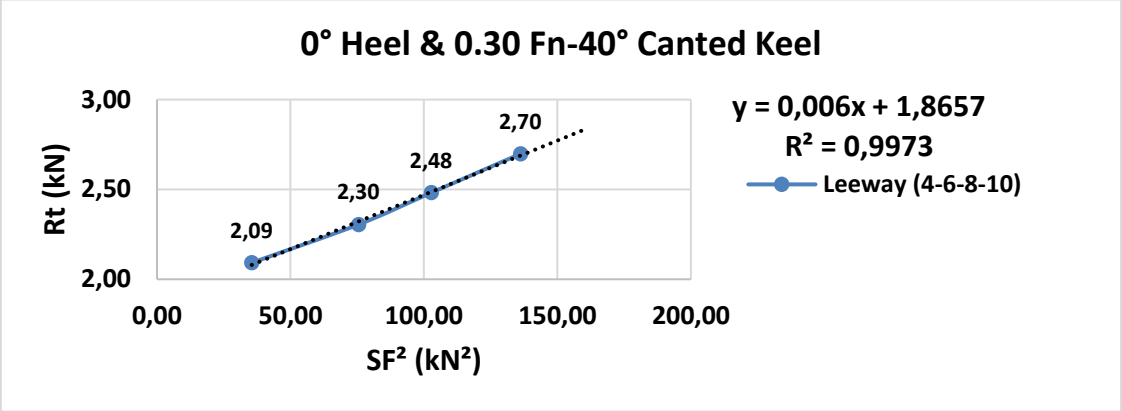

Figure 5-13: Graph of 40° canted keel at 0° heel angle and 0.30 Froude number

5.2.2.2 Effective Draft of 40° Canted Keel at 0° Heel Angle & 0.39 FN

Table 5-11: Effective Draft of 40° Canted Keel at 0° Heel Angle & 0.39 FN

Keel Position	Heel	Leeway	Clock No	V-Full Size (m/s)	FN	Full Size Total-Rt (kN)	SF² (kN)	Ri (kN)
40°	0°	4°	450	5,13	0,39	3,28	78,86	0,38
40°	0°	6°	450	5,13	0,39	3,89	208,43	1,00
40°	0°	8°	450	5,13	0,39	4,25	288,46	1,39
40°	0°	10°	450	5,13	0,39	4,71	373,14	1,79

Ru+Rh (kN)	Slope	Te²	Te (m)
2,89	0,0048	2,46	1,57

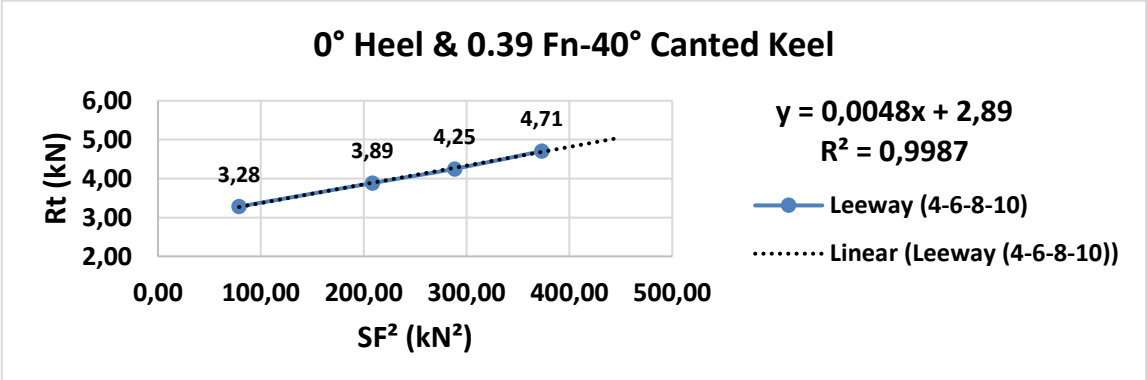

Figure 5-14: Graph of 40° canted keel at 0° heel angle and 0.39 Froude number

5.2.2.3 *Effective Draft of 40° Canted Keel at 15° Heel Angle & 0.30 FN*

Table 5-12: Effective Draft of 40° Canted Keel at 15° Heel Angle & 0.30 FN

Keel Position	Heel	Leeway	Clock No	V-Full Size (m/s)	FN	Full Size Total-Rt (kN)	SF² (kN)	Ri (kN)
40°	15°	4°	350	4,0	0,30	2,15	1,43	0,02
40°	15°	8°	350	4,0	0,30	2,61	37,99	0,49
40°	15°	9°	350	4,0	0,30	2,72	44,79	0,57

Ru+Rh (kN)	Slope	Te²	Te (m)
2,13	0,0128	1,52	1,23

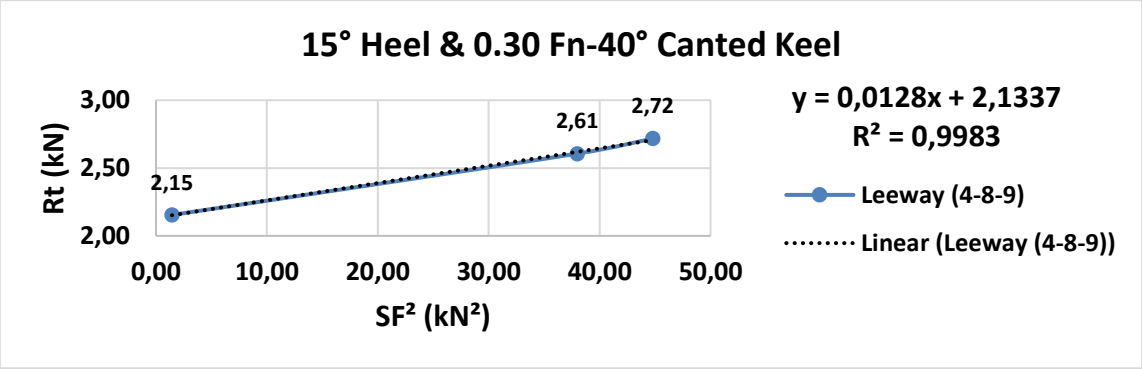

Figure 5-15: Graph of 40° canted keel at 15° heel angle and 0.30 Froude number

5.2.2.4 *Effective Draft of 40° Canted Keel at 15° Heel Angle & 0.39 FN*

Table 5-13: Effective Draft of 40° Canted Keel at 15° Heel Angle & 0.39 FN

Keel Position	Heel	Leeway	Clock No	V-Full Size (m/s)	FN	Full Size Total-Rt (kN)	SF² (kN)	Ri (kN)
40°	15°	6°	450	5,13	0,39	3,93	49,06	0,64
40°	15°	8°	450	5,13	0,39	4,55	98,46	1,29
40°	15°	9°	450	5,13	0,39	4,88	121,13	1,58

Ru+Rh (kN)	Slope	Te²	Te (m)
3,29	0,0131	0,90	0,95

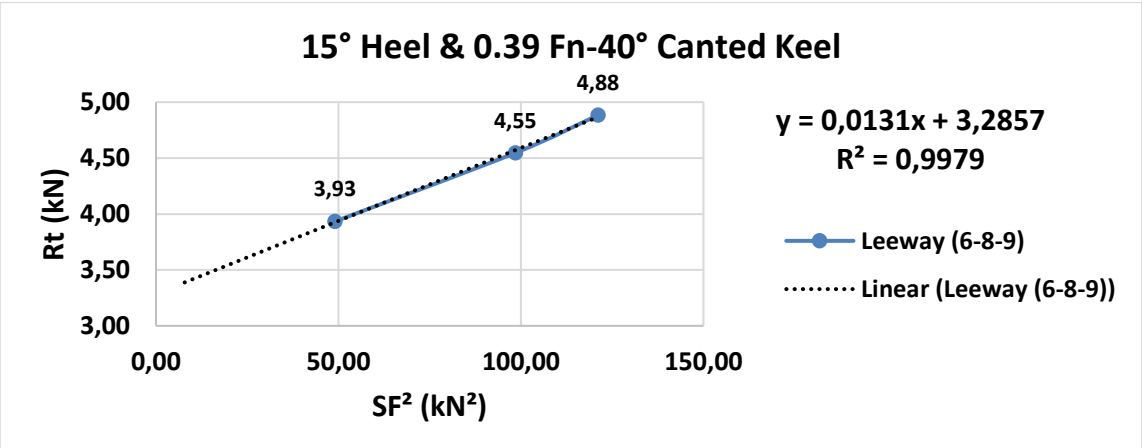

Figure 5-16: Graph of 40° canted keel at 15° heel angle and 0.39 Froude number

5.2.2.5 *Effective Draft of 40° Canted Keel at 20° Heel Angle & 0.30 FN*

Table 5-14: Effective Draft of 40° Canted Keel at 20° Heel Angle & 0.30 FN

Keel Position	Heel	Leeway	Clock No	V-Full Size (m/s)	FN	Full Size Total-Rt (kN)	SF² (kN)	Ri (kN)
40°	20°	6°	350	4,0	0,30	2,33	2,13	0,06
40°	20°	7°	350	4,0	0,30	2,46	6,46	0,17
40°	20°	8°	350	4,0	0,30	2,61	12,52	0,34

Ru+Rh (kN)	Slope	Te²	Te (m)
2,28	0,0268	0,73	0,85

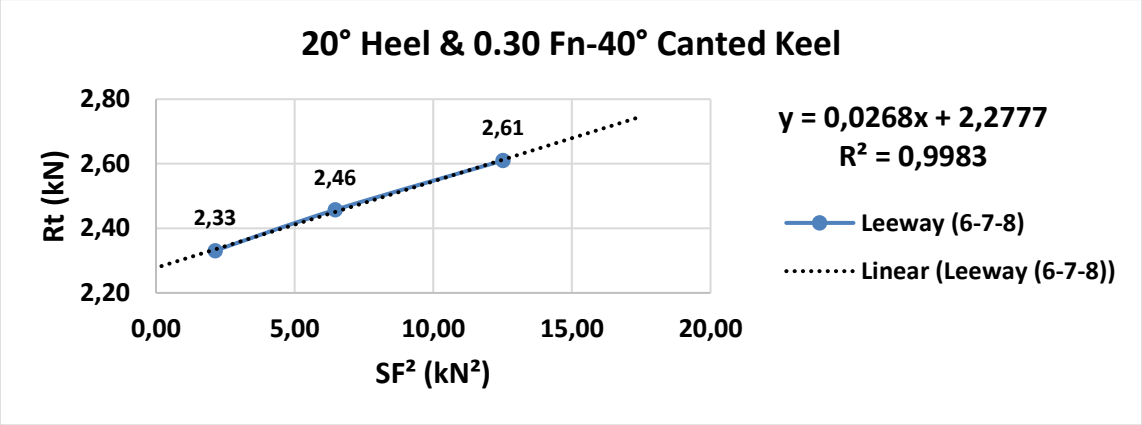

Figure 5-17: Graph of 40° canted keel at 20° heel angle and 0.30 Froude number

5.2.2.6 *Effective Draft of 40° Canted Keel at 20° Heel Angle & 0.39 FN*

Table 5-15: Effective Draft of 40° Canted Keel at 20° Heel Angle & 0.39 FN

Keel Position	Heel	Leeway	Clock No	V-Full Size (m/s)	FN	Full Size Total-Rt (kN)	SF² (kN)	Ri (kN)
40°	20°	6°	450	5,13	0,39	3,89	14,38	0,25
40°	20°	7°	450	5,13	0,39	4,20	31,28	0,54
40°	20°	8°	450	5,13	0,39	4,57	53,72	0,93
40°	20°	9°	450	5,13	0,39	4,83	68,21	1,18

Ru+Rh (kN)	Slope	Te²	Te (m)
3,65	0,0174	0,68	0,82

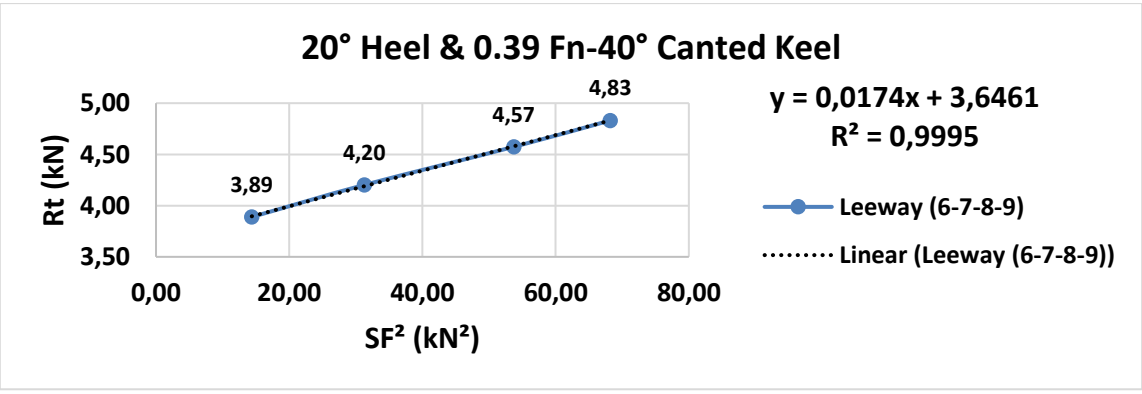

Figure 5-18: Graph of 40° canted keel at 20° heel angle and 0.39 Froude number

5.2.2.7 Overall Results of the 40° Canted Keel

- The effective draft values decrease energy losses (induced drag) when the Froude number is increased. When the leeway angle (angle of attack) is increased, the side force squared (SF^2) component and induced drag values have increased.
- The amount of the side force values decrease due to 3D energy losses at the same leeway angle when the boat is heeled with increasing heel angles so the effective draft values go down. The highest value is obtained at 0° heel angle and lowest velocity (0.30 FN).

Note: Effective Draft Graphs and Tables of 40° Canting Keel at 10° and 25° Heel Angles & 0.30 and 0.39 Froude Numbers is presented in the Appendix-C section.

Table 5-16: Effective draft results of the 40° canting keel

The Effective Draft Results of 40° Canted Keel		
Conditions	Fn	
	0,30	0,39
40° Cant Angle-0° Heel	1,79	1,57
40° Cant Angle-10° Heel	1,26	1,14
40° Cant Angle-15° Heel	1,23	0,95
40° Cant Angle-20° Heel	0,85	0,82
40° Cant Angle-25° Heel	0,55	0,61

Table 5-17: Effective draft / maximum draft results of the 40° canting keel

40° Canted Keel		
Effective Draft / Max. Draft		
FN	0,30	0,39
0° Heel	0,40	0,35
10° Heel	0,28	0,25
15° Heel	0,27	0,21
20° Heel	0,19	0,18
25° Heel	0,12	0,14
Max. Draft = 4.5 m		

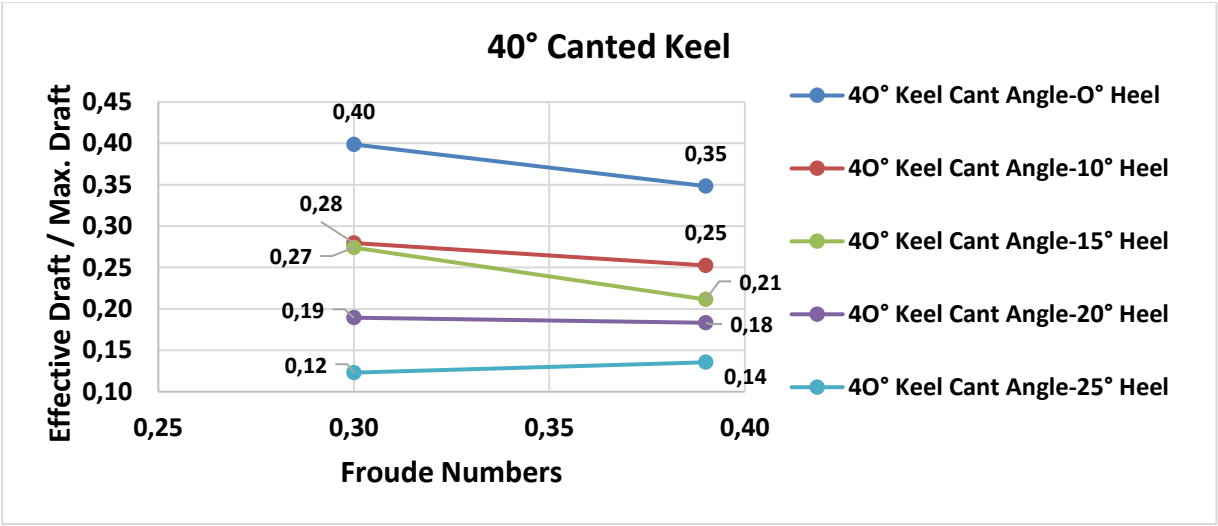

Figure 5-19: Effective draft / Max. Draft graph of the 40° canted keel

5.2.3 Comparison between 0° and 40° Canted Keel Conditions

After the effective draft calculations, the approximate GZ values were determined for each canting keel condition in Hydromax [20] and the representative righting moment was calculated according to a certain displacement situation to compare both keel conditions. In addition, the heeling arm (distance between CE (Centre of Effort) and CLR (Centre of Lateral Resistance-[40% of the draft] [6]) was estimated according to approximate rig dimensions [24]. The heel force was obtained with the values estimated at 15° heel angle approximately based on the hydrodynamic (FHy) and aerodynamic force (FAy) heel=side force equilibrium formulation which is presented below:

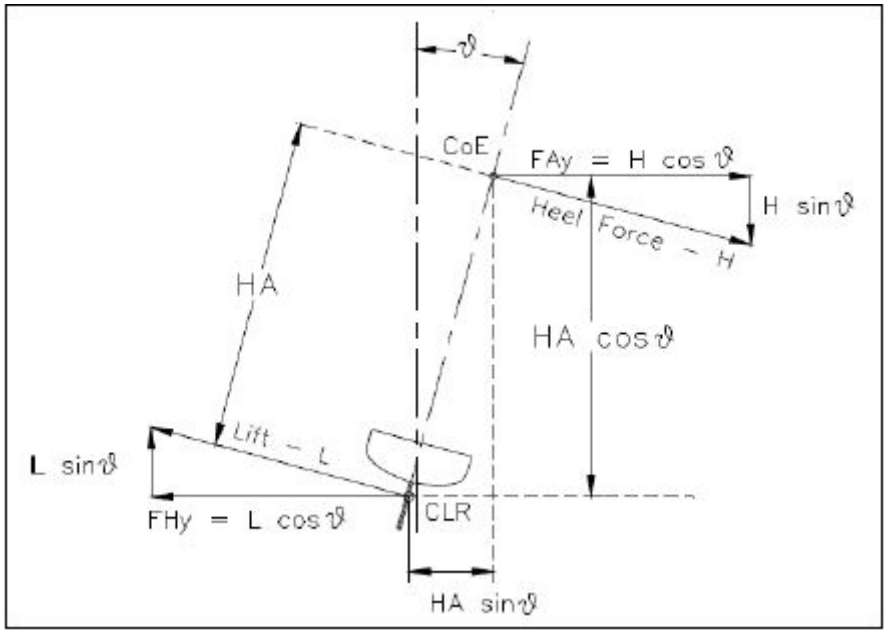

Figure 5-20: Heeling Moment Equilibrium [6]

$$FHy = \frac{RM}{HA}\cos\theta \qquad [18]$$

GZ= Righting Arm - HA=Heeling Arm- RM=Righting (Heeling) Moment – FH= Heel Force

Table 5-18: Static righting arm table of the 0° canting keel & water ballast

0° Canted Keel+Water Ballast					
Heel Angle	Displacement (kg)	GZ (m)	HA (m)	RM (kg.m)	FH-N
15°	9260	1,58	16,6	14594	8330

Table 5-19: Static righting arm table of the 40° canting keel & water ballast

40° Canted Keel+Water Ballast					
Heel Angle	Displacement (kg)	GZ (m)	HA (m)	RM (kg.m)	FH-N
15°	6544	2,23	16,6	14594	8330

According to these results above, the 40° canted keel configuration has GZ advantage thanks to the bulb weight (about 3 tonnes) [16] as compared with the centre keel (0° cant angle) to obtain the same righting moment value. The keel/bulb moves to windward side with the 40° keel cant angle that increases the GZ value (horizontal distance between Centre of Gravity-CG and Centre of Buoyancy-CB). In other words, it can generate the certain righting moment value with less displacement. This situation could be a benefit for competitors with having less weight to get less resistance and higher boat speed [25].

Table 5-20: The overall effective draft results of the 0° and 40° canting keel

The Effective Draft Results of 40° Canted Keel		
Conditions	Fn	
	0,30	0,39
40° Cant Angle-0° Heel	1,79	1,57
40° Cant Angle-10° Heel	1,26	1,14
40° Cant Angle-15° Heel	1,23	0,95
40° Cant Angle-20° Heel	0,85	0,82
40° Cant Angle-25° Heel	0,55	0,61

Effective Draft Results of 0° Canted Keel		
Conditions	Fn	
	0,3	0,4
0° Cant - 0° Heel Angle	2,94	2,54
0° Cant - 15° Heel Angle	2,73	2,21
0° Cant - 20° Heel Angle	2,59	1,93

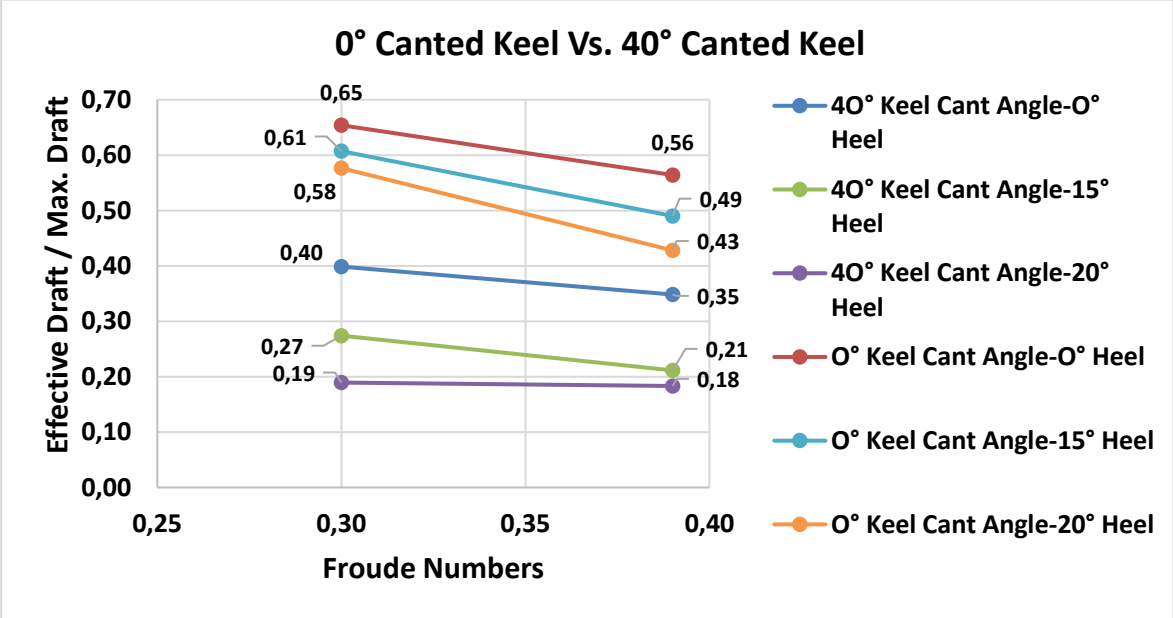

Figure 5-21: Overall Effective Draft / Max. Draft graph of 0° and 40° canted keel

However, the 40° canted keel is not effective to generate the side force as compared with the centre keel; therefore, it requires extra foil configuration on the leeward side to produce necessary side force for sailboat stability. For this reason, the Open 60 sailboats are employed with 40° canting keel and straight or curved daggerboard configurations. The dagger board configurations complete the deficient part of the canting keel with producing lift and side force. The straight and curved foil configurations will be analysed in the upwind condition with 40° canted keel in next sections.

5.3 The Straight Daggerboard Analysis

In this section, the model hull was towed together with appendages (keel/bulb, straight daggerboard) at different heel and yaw angles according to particular boat speeds. All conditions will be presented with drag, side force and effective draft components in further parts. The 40° canted keel was employed to get the results, and it was considered that the rudders might modify the leeway angle (so side force) therefore they were not used during this tests to prevent additional direction changes or other effects. The general specifications of the model and full-scale hull are shown based on heel angles in the following tables.

Table 5-21: Model hull specifications in the upright condition, 15° and 20° heel angles

MODEL -Upright		Unit	MODEL -15° Heel		Unit	MODEL -20° Heel		Unit
Length	2,286	m	Length	2,286	m	Length	2,286	m
WSA	0,88	m^2	WSA	0,67	m^2	WSA	0,62	m^2
Density-ρ	1000	kg/m^3	Density-ρ	1000	kg/m^3	Density-ρ	1000	kg/m^3
Viscosity-μ	1,14E-03	(Pa·s)	Viscosity-μ	1,14E-03	(Pa·s)	Viscosity-μ	1,14E-03	(Pa·s)
(1+k)	1,32	-	(1+k)	1,19	-	(1+k)	1,13	-
Scale Factor	8	-	Scale Factor	8	-	Scale Factor	8	-

Table 5-22: Full size hull specifications in the upright condition, 15° and 20° heel angles

Full Scale-Upright		Unit	Full Scale-15° Heel		Unit	Full Scale-20° Heel		Unit
Length	18,288	m	Length	18,288	m	Length	18,288	m
WSA	56,25	m^2	WSA	42,97	m^2	WSA	39,85	m^2
Density-ρ	1025	kg/m^3	Density-ρ	1025	kg/m^3	Density-ρ	1025	kg/m^3
Viscosity-μ	1,19E-03	(Pa·s)	Viscosity-μ	1,19E-03	(Pa·s)	Viscosity-μ	1,19E-03	(Pa·s)
(1+k)	1,32	-	(1+k)	1,19	-	(1+k)	1,13	-
Scale Factor	8	-	Scale Factor	8	-	Scale Factor	8	-

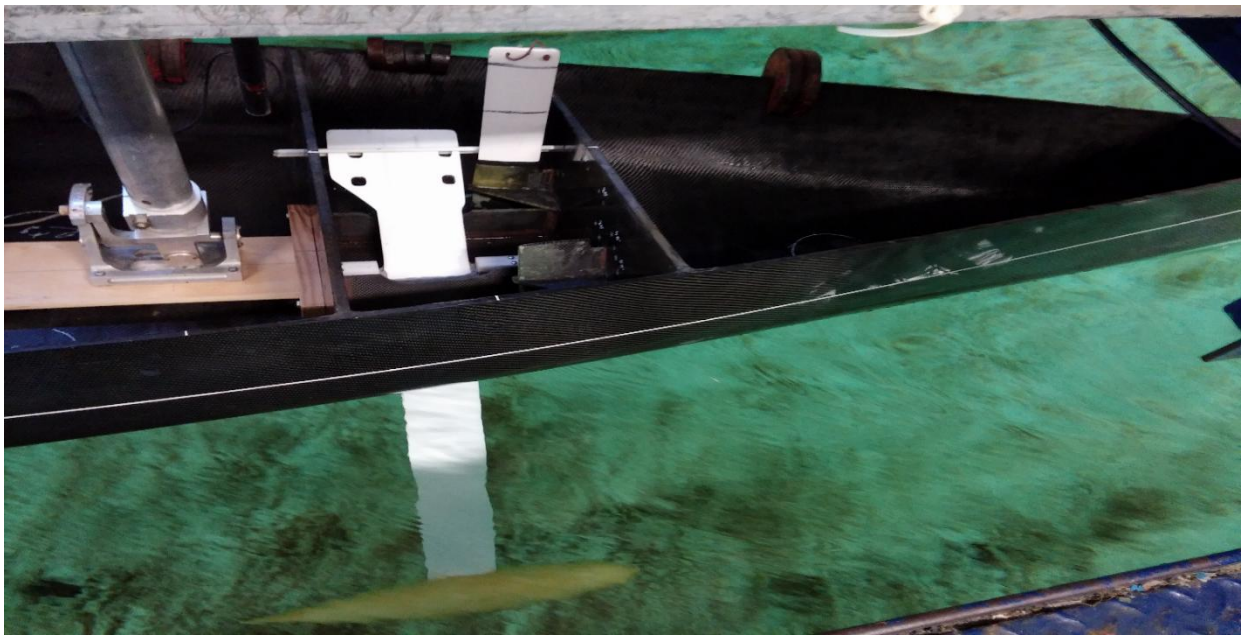

Figure 5-22: View of the model hull with the straight daggerboard configuration & 40° canting keel.

5.3.1 Upright Resistance

Table 5-23: Upright resistance table of the 1/2-straight daggerboard configuration

Keel Position	DBD Position	% DBD	Heel	Leeway	Clock No	V-Full Size (m/s)	FN	Full Size Total-R (kN)
40°	1/2 DBD	50	0	0	350	4,00	0,30	1,87
40°	1/2 DBD	50	0	0	400	4,56	0,34	2,50
40°	1/2 DBD	50	0	0	450	5,13	0,39	3,27
40°	1/2 DBD	50	0	0	500	5,71	0,43	4,13

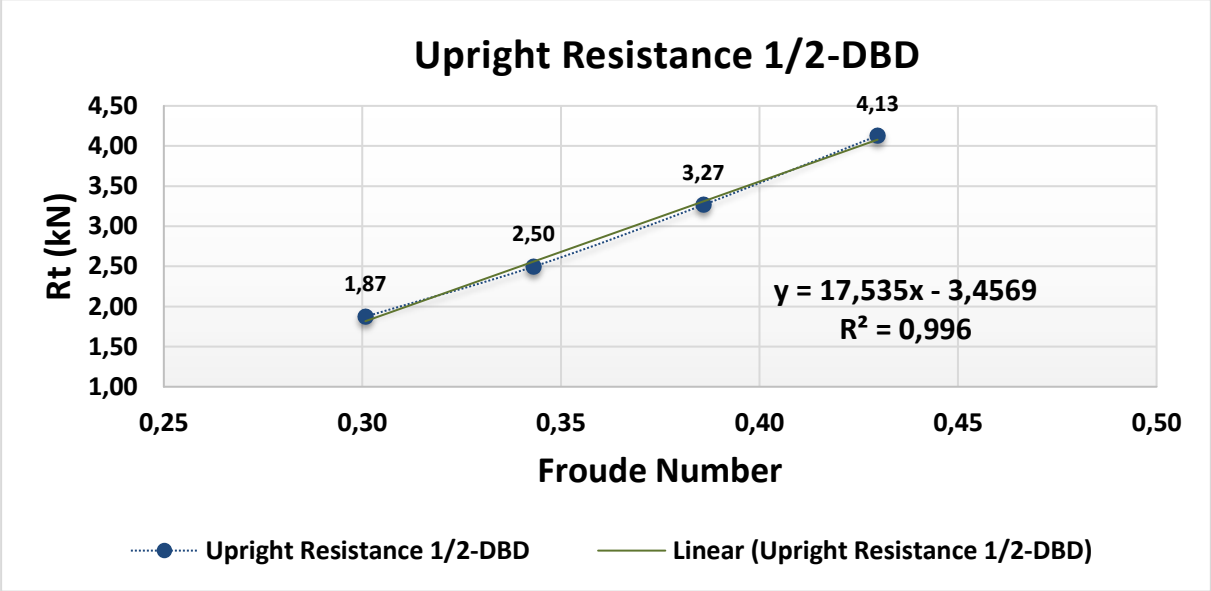

Figure 5-23: Upright resistance graph of the 1/2-straight daggerboard configuration

Table 5-24: Upright resistance table of the full-straight daggerboard configuration

Keel Position	DBD Position	% DBD	Heel	Leeway	Clock No	V-Full Size (m/s)	FN	Full Size Total-R (kN)
40°	Full DBD	100	0	0	350	4,00	0,30	1,95
40°	Full DBD	100	0	0	400	4,56	0,34	2,52
40°	Full DBD	100	0	0	450	5,13	0,39	3,28
40°	Full DBD	100	0	0	500	5,71	0,43	4,23

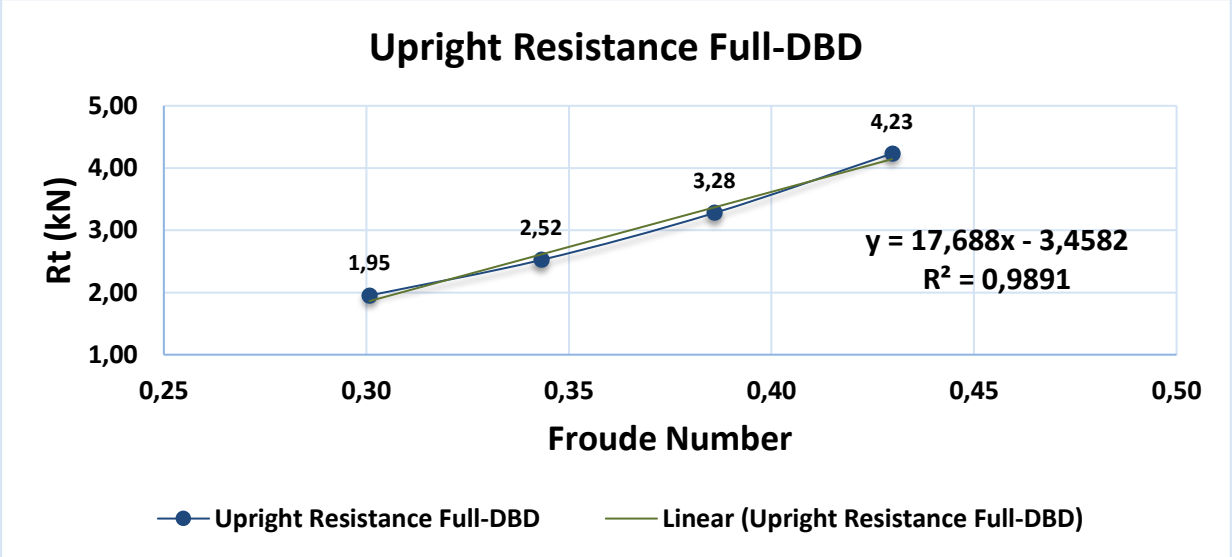

Figure 5-24: Upright resistance graph of the full-straight daggerboard configuration

5.3.2 *Effective Draft of 1/2 DBD at 15° Heel Angle & 0.30 FN*

Table 5-25: Effective Draft of 1/2 DBD at 15° Heel Angle & 0.30 FN

Keel Position	DBD Position	% DBD	Heel	Leeway	Clock No	V-Full Size (m/s)	FN	Full Size Total-Rt (kN)	SF² (kN)	Ri (kN)
40°	1/2 DBD	50	15°	2,25°	350	4	0,30	2,50	19,70	0,33
40°	1/2 DBD	50	15°	2,75°	350	4	0,30	2,69	30,53	0,52
40°	1/2 DBD	50	15°	4	350	4	0,30	3,20	60,90	1,03

Ru+Rh (kN)	Slope	Te²	Te (m)
2,17	0,0170	1,14	1,07

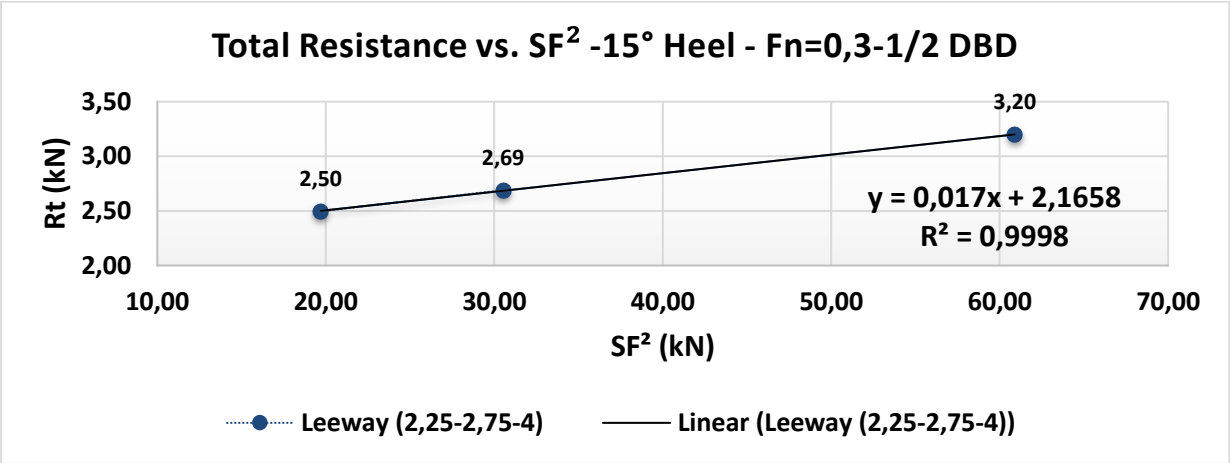

Figure 5-25: Graph of 1/2-straight daggerboard at 15° heel angle and 0.30 Froude number

5.3.3 *Effective Draft of 1/2 DBD at 15° Heel Angle & 0.39 FN*

Table 5-26: Effective Draft of 1/2 DBD at 15° Heel Angle & 0.39 FN

Keel Position	DBD Position	% DBD	Heel	Leeway	Clock No	V-Full Size (m/s)	FN	Full Size Total-Rt (kN)	SF² (kN)	Ri (kN)
40°	1/2 DBD	50	15°	2,75°	450	5,13	0,39	4,81	122,23	1,70
40°	1/2 DBD	50	15°	3,25°	450	5,13	0,39	5,18	147,52	2,05
40°	1/2 DBD	50	15°	4°	450	5,13	0,39	5,55	175,57	2,44

Ru+Rh (kN)	Slope	Te²	Te (m)
3,12	0,0139	0,85	0,92

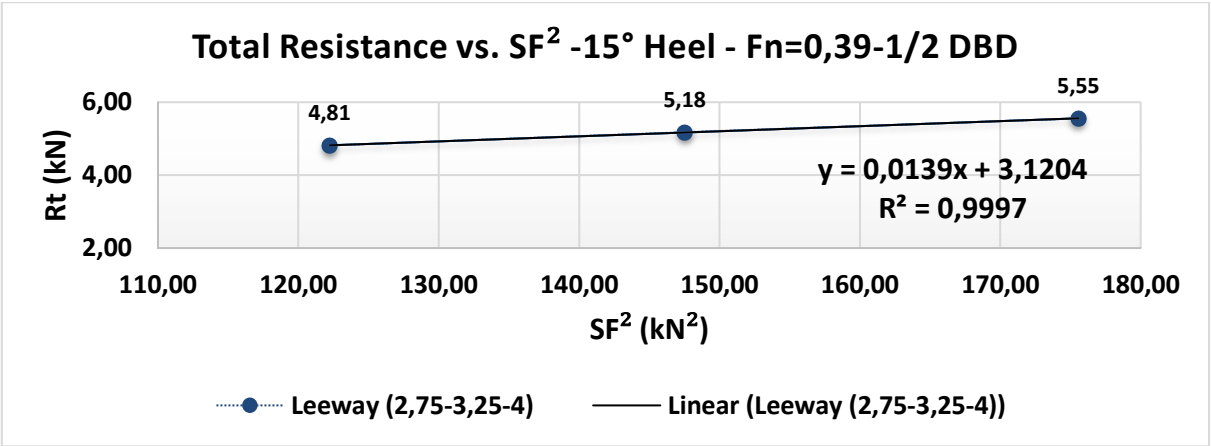

Figure 5-26: Graph of 1/2-straight daggerboard at 15° heel angle and 0.39 Froude number

5.3.4 Effective Draft of Full DBD at 15° Heel Angle & 0.30 FN

Table 5-27: Effective Draft of Full DBD at 15° Heel Angle & 0.30 FN

Keel Position	DBD Position	% DBD	Heel	Leeway	Clock No	V-Full Size (m/s)	FN	Full Size Total-Rt (kN)	SF² (kN)	Ri (kN)
40°	Full DBD	100	15°	1°	350	4,0	0,30	2,33	19,14	0,20
40°	Full DBD	100	15°	2°	350	4,0	0,30	2,60	45,80	0,48
40°	Full DBD	100	15°	2,75°	350	4,0	0,30	3,31	112,38	1,18

Ru+Rh (kN)	Slope	Te²	Te (m)
2,13	0,0105	1,86	1,36

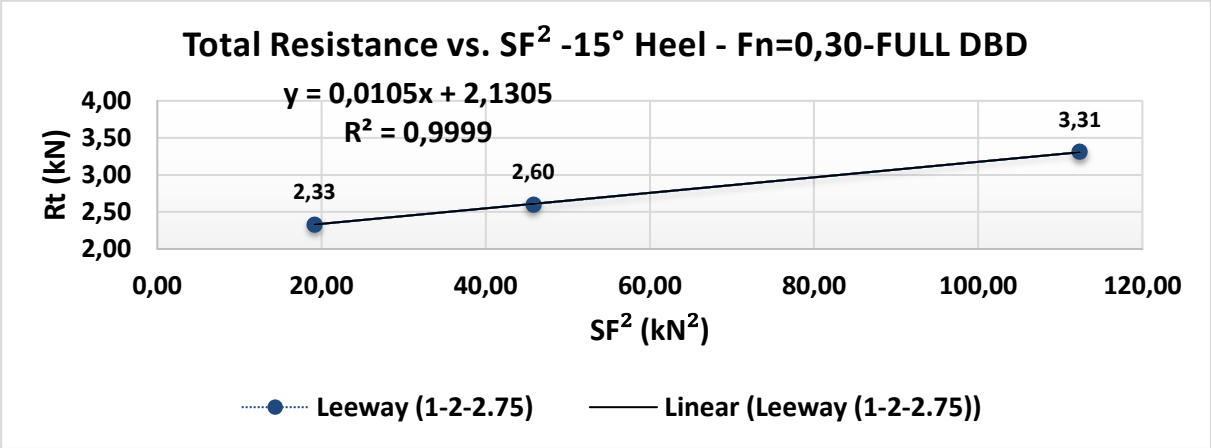

Figure 5-27: Graph of full-straight daggerboard at 15° heel angle and 0.30 Froude number

5.3.5 Effective Draft of Full DBD at 15° Heel Angle & 0.39 FN

Table 5-28: Effective Draft of Full DBD at 15° Heel Angle & 0.39 FN

Keel Position	DBD Position	% DBD	Heel	Leeway	Clock No	V-Full Size (m/s)	FN	Full Size Total-Rt (kN)	SF² (kN)	Ri (kN)
40°	Full DBD	100	15°	1°	450	5,13	0,39	3,93	90,29	0,81
40°	Full DBD	100	15°	1,5°	450	5,13	0,39	4,33	141,13	1,26
40°	Full DBD	100	15°	2,75°	450	5,13	0,39	5,98	321,52	2,87

Ru+Rh (kN)	Slope	Te²	Te (m)
3,10	0,0089	1,32	1,15

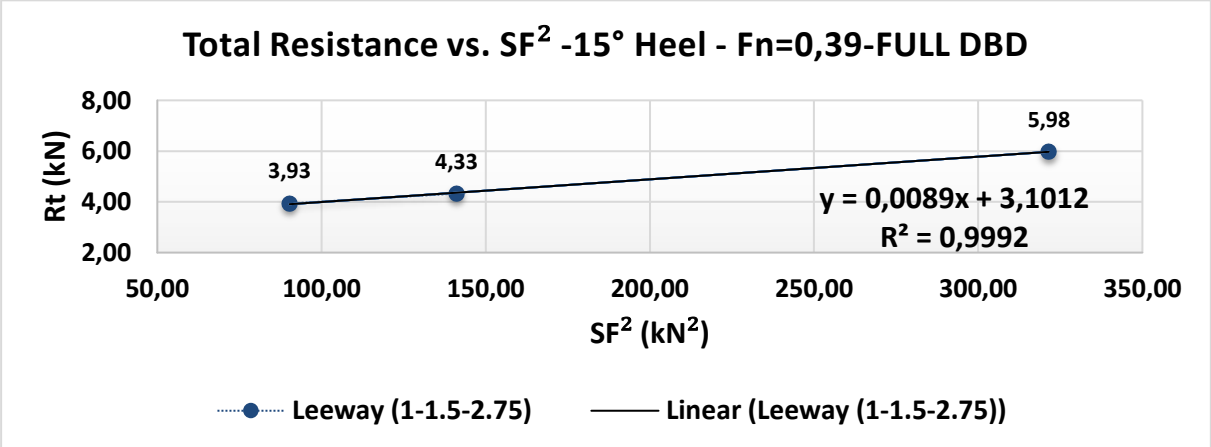

Figure 5-28: Graph of full-straight daggerboard at 15° heel angle and 0.39 Froude number

5.3.6 Effective Draft of 1/2 DBD at 20° Heel Angle & 0.39 and 0.43 FN

Table 5-29: Effective Draft of 1/2 DBD at 20° Heel Angle & 0.39 FN

Keel Position	DBD Position	% DBD	Heel	Leeway	Clock No	V-Full Size (m/s)	FN	Full Size Total-Rt (kN)	SF² (kN)	Ri (kN)
40°	1/2 DBD	50	20°	2,25°	450	5,13	0,39	4,32	46,19	0,86
40°	1/2 DBD	50	20°	2,75°	450	5,13	0,39	4,79	72,24	1,34
40°	1/2 DBD	50	20°	3,25°	450	5,13	0,39	5,12	88,94	1,65

Ru+Rh (kN)	Slope	Te²	Te (m)
3,46	0,0186	0,63	0,80

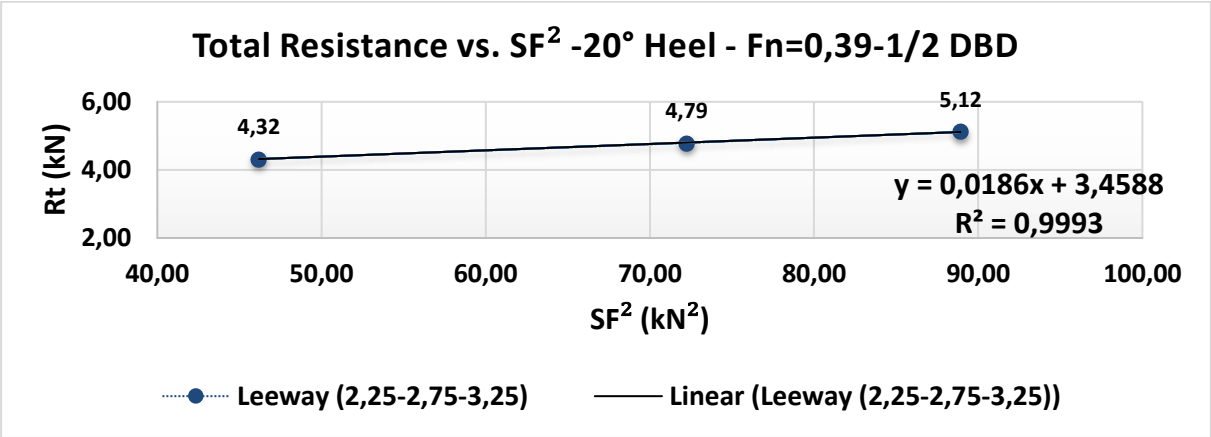

Figure 5-29: Graph of 1/2-straight daggerboard at 20° heel angle and 0.39 Froude number

Table 5-30: Effective Draft of 1/2 DBD at 20° Heel Angle & 0.43 FN

Keel Position	DBD Position	% DBD	Heel	Leeway	Clock No	V-Full Size (m/s)	FN	Full Size Total-Rt (kN)	SF² (kN)	Ri (kN)
40°	1/2 DBD	50	20°	2,25°	500	5,71	0,43	5,56	84,93	1,35
40°	1/2 DBD	50	20°	3,25°	500	5,71	0,43	7,00	174,76	2,79
40°	1/2 DBD	50	20°	4°	500	5,71	0,43	7,39	199,59	3,18

Ru+Rh (kN)	Slope	Te²	Te (m)
4,21	0,0159	0,60	0,77

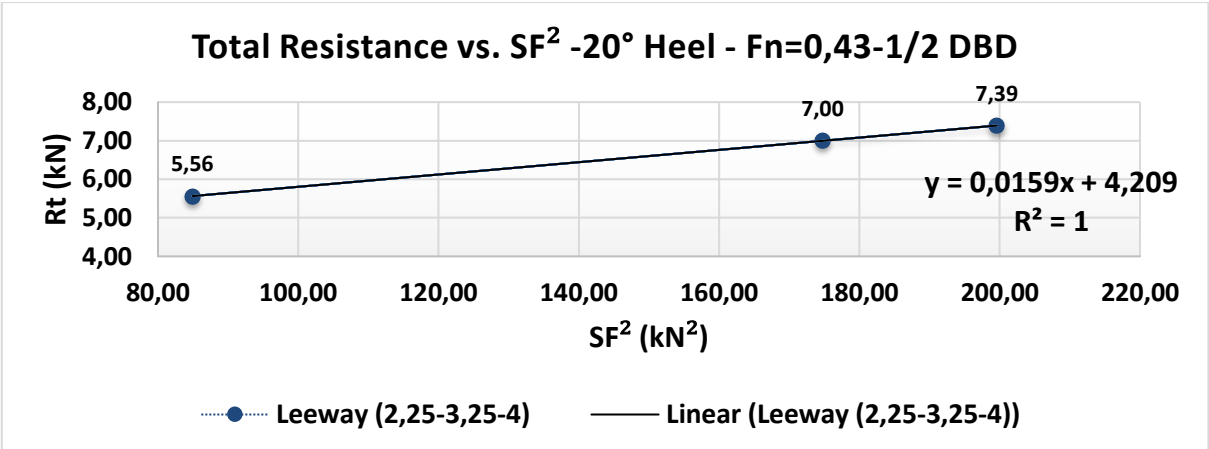

Figure 5-30: Graph of 1/2-straight daggerboard at 20° heel angle and 0.43 Froude number

5.3.7 Effective Draft of Full DBD at 20° Heel Angle & 0.39 and 0.43 FN

Table 5-31: Effective Draft of Full DBD at 20° Heel Angle & 0.39 FN

Keel Position	DBD Position	% DBD	Heel	Leeway	Clock No	V-Full Size (m/s)	FN	Full Size Total-Rt (kN)	SF² (kN)	Ri (kN)
40°	Full DBD	100	20°	1°	450	5,13	0,39	3,92	65,37	0,79
40°	Full DBD	100	20°	1,5°	450	5,13	0,39	4,34	112,46	1,36
40°	Full DBD	100	20°	2,75°	450	5,13	0,39	6,05	245,07	2,96

Ru+Rh (kN)	Slope	Te²	Te (m)
3,07	0,0121	0,98	0,99

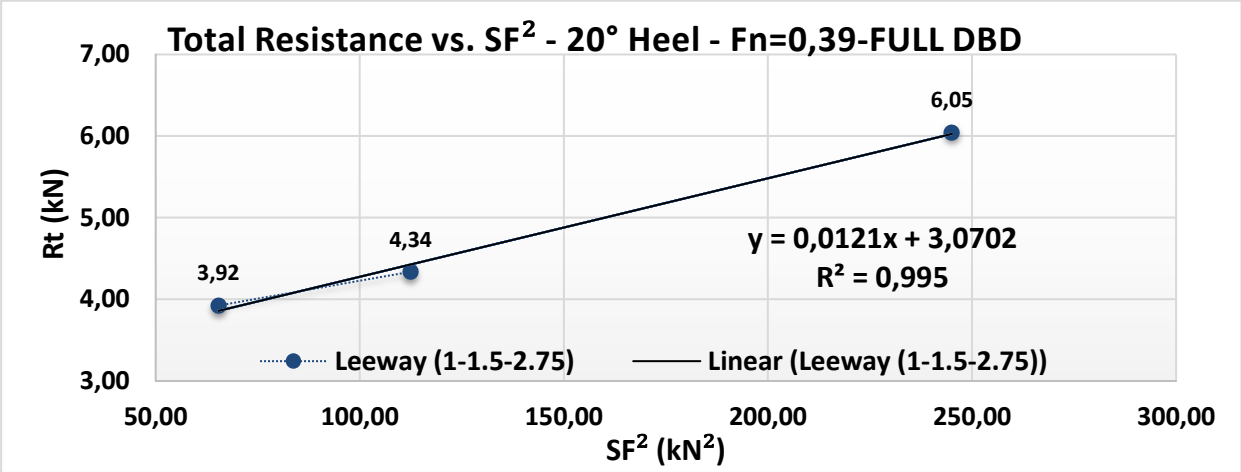

Figure 5-31: Graph of full-straight daggerboard at 20° heel angle and 0.39 Froude number

Table 5-32: Effective Draft of Full DBD at 20° Heel Angle & 0.43 FN

Keel Position	DBD Position	% DBD	Heel	Leeway	Clock No	V-Full Size (m/s)	FN	Full Size Total-Rt (kN)	SF² (kN)	Ri (kN)
40°	Full DBD	100	20°	1°	500	5,71	0,43	5,29	165,86	1,80
40°	Full DBD	100	20°	1,5°	500	5,71	0,43	5,80	240,17	2,61
40°	Full DBD	100	20°	2,75°	500	5,71	0,43	8,15	436,27	4,74

Ru+Rh (kN)	Slope	Te²	Te (m)
3,37	0,0109	0,88	0,94

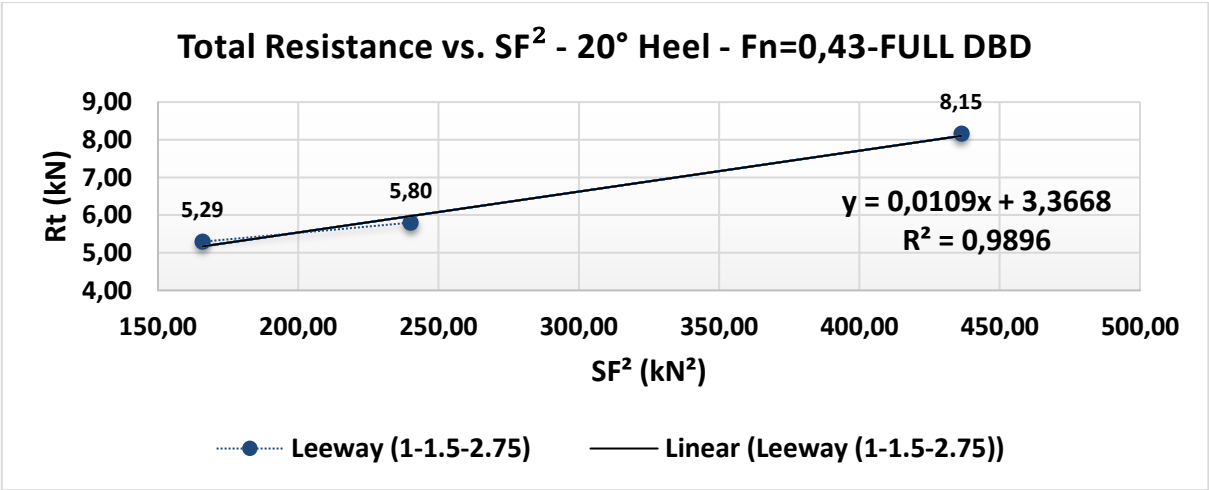

Figure 5-32: Graph of full-straight daggerboard at 20° heel angle and 0.43 Froude number

5.3.8 Overall Effective Draft Analysis of Full and 1/2 Straight Dagger Boards

After all these calculations, the overall table is created for each heel and straight dagger board configuration at different Froude numbers. According to the tables, the some significant notes are realized about these results:

- The effective draft values decrease when the Froude number is increased generally.
- The highest effective draft value is determined with full daggerboard configuration at lowest heel angle (15°) and Froude number (0.3 Fn).
- The lowest effective draft value is determined with 1/2 daggerboard configuration at highest heel angle (20°) and Froude number (0.43 Fn).

Note: Effective Draft Graphs and Tables of 1/2-Full Straight Daggerboards & 40° Canting Keel at 15° Heel Angle & 0.34 and 0.43 Froude Numbers is presented in the Appendix-D section.

Table 5-33: The overall effective draft results of the straight daggerboard configurations

Straight Dagger Board Configuration				
Table of Effective Drafts For Each Heel & Daggerboad Configuration				
Fn	15° & 1/2 DBD	15° & Full DBD	20° & 1/2 DBD	20° & Full DBD
0,3	1,07	1,36	-	-
0,34	1,00	1,33	-	-
0,4	0,92	1,15	0,80	0,99
0,43	0,81	1,07	0,77	0,94

Table 5-34: The overall effective draft / Max. draft results of the straight daggerboard configurations

Effective Draft / Max. Draft-STRAIGHT DAGGER BOARD (Max. Draft= 4.5 m)				
FN	0,3	0,34	0,4	0,43
15° Heel-1/2DBD - 40° Cant Angle	0,24	0,22	0,20	0,18
15° Heel-FULL DBD - 40° Cant Angle	0,303	0,295	0,26	0,24
20° Heel-1/2DBD - 40° Cant Angle	-	-	0,18	0,17
20° Heel-FULL DBD - 40° Cant Angle	-	-	0,22	0,21

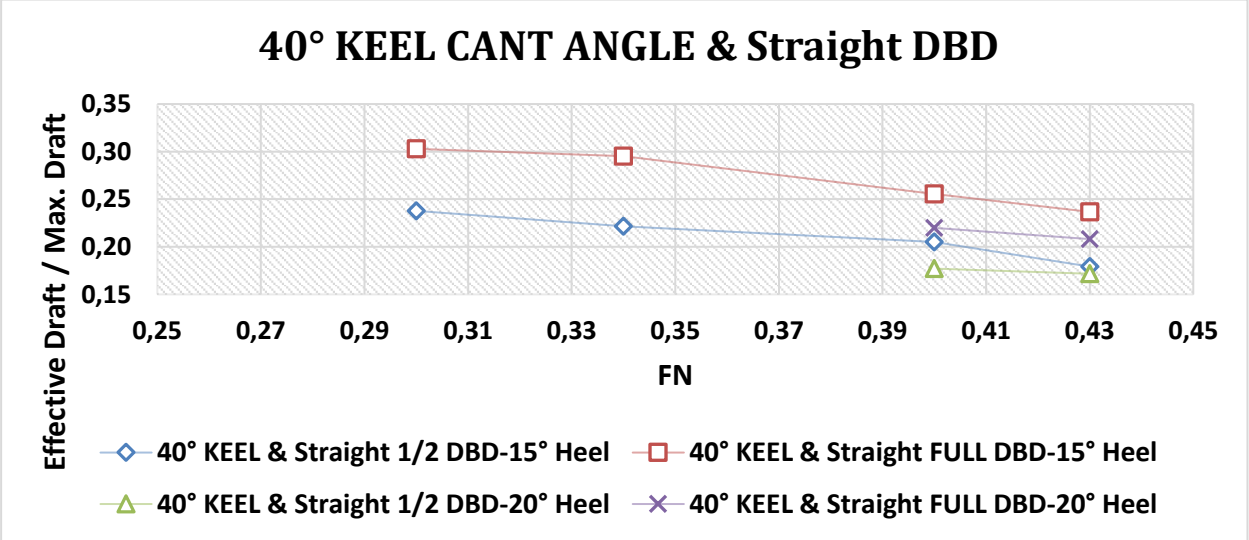

Figure 5-33: Overall Effective Draft / Max. Draft graph of 1/2 and full straight foils & 40° canting keel

5.4 The Curved Daggerboard Analysis

The tank tests were performed at some heel and leeway angles, Froude numbers with the curved daggerboard configuration. The half and full curved daggerboard configurations will be presented in this section based on the drag, side force and effective draft values. The 40° canting keel was used as an appendage during these tests again. The obtained results will be compared with straight foil shape and between each other in next sections. According to heel angles, the model and full-scale hull specifications are shown in the following tables.

Table 5-35: Model hull specifications in the upright condition, 10°, 15°, 20° and 25° heel angles

MODEL -Upright		MODEL -10° Heel		MODEL -15° Heel		MODEL -20° Heel		MODEL -25° Heel		Unit
Length	2,286	Length	2,286	Length	2,286	Length	2,286	Length	2,286	m
WSA	0,88	WSA	0,74	WSA	0,67	WSA	0,62	WSA	0,59	m^2
Density-ρ	1000	Density-ρ	1000	Density-ρ	1000	Density-ρ	1000	Density-ρ	1000	kg/m^3
Viscosity-μ	1,14E-03	Viscosity-μ	1,14E-03	Viscosity-μ	1,14E-03	Viscosity-μ	1,14E-03	Viscosity-μ	1,14E-03	(Pa·s)
(1+k)	1,32	(1+k)	1,26	(1+k)	1,19	(1+k)	1,13	(1+k)	1,12	-
Scale Factor	8	Scale Factor	8	Scale Factor	8	Scale Factor	8	Scale Factor	8	-

Table 5-36: Full size hull specifications in the upright condition, 10°, 15°, 20° and 25° heel angles

Full Scale -Upright		Full Scale -10° Heel		Full Scale -15° Heel		Full Scale -20° Heel		Full Scale -25° Heel		Unit
Length	18,288	Length	18,288	Length	18,288	Length	18,288	Length	18,288	m
WSA	56,25	WSA	47,58	WSA	42,97	WSA	39,85	WSA	37,69	m^2
Density-ρ	1025	Density-ρ	1025	Density-ρ	1025	Density-ρ	1025	Density-ρ	1025	kg/m^3
Viscosity-μ	1,19E-03	Viscosity-μ	1,19E-03	Viscosity-μ	1,19E-03	Viscosity-μ	1,19E-03	Viscosity-μ	1,19E-03	(Pa·s)
(1+k)	1,32	(1+k)	1,26	(1+k)	1,19	(1+k)	1,13	(1+k)	1,12	-
Scale Factor	8	Scale Factor	8	Scale Factor	8	Scale Factor	8	Scale Factor	8	-

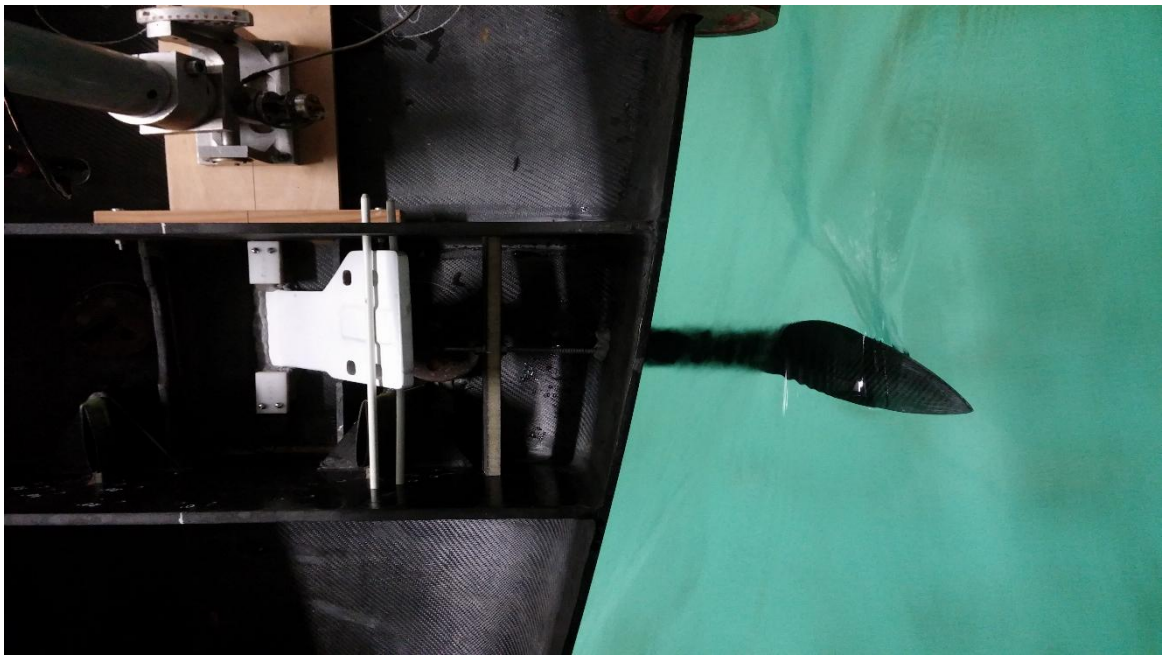

Figure 5-34: View of model hull with 1/2-curved daggerboard & 40° canting keel

5.4.1 Upright Resistance

Note: The half-daggerboard does not touch the water when the hull is towed in the upright condition during the tests; therefore, the percentage of the foil is seen as % 0 in the following table.

Table 5-37: Upright resistance table of the 1/2-curved daggerboard configuration

Keel Position	DBD Position	% DBD	Heel	Leeway	Clock No.	V-Full Size (m/s)	FN	Full Size Total-R (kN)
40°	1/2 DBD	0	0	0	350	4,00	0,30	1,73
40°	1/2 DBD	0	0	0	450	5,13	0,39	2,86

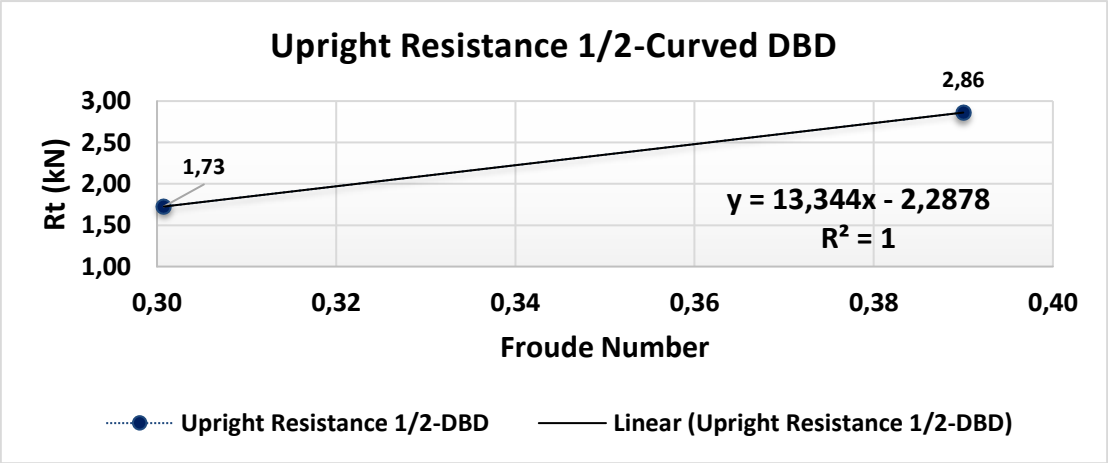

Figure 5-35: Upright resistance graph of 1/2-curved daggerboard

Note: The % 50 part of the full-daggerboard touched the water approximately when the hull was towed in the upright condition during the tests, and the only % 50 of the total wetted surface area of the curved foil is taken into account to determine the total resistance value.

Table 5-38: Upright resistance table of full-curved daggerboard configuration

Keel Position	DBD Position	% DBD	Heel	Leeway	Clock No.	V-Full Size (m/s)	FN	Full Size Total-R (kN)
40°	Full DBD	50	0	0	350	4,00	0,30	1,80
40°	Full DBD	50	0	0	450	5,13	0,39	2,98

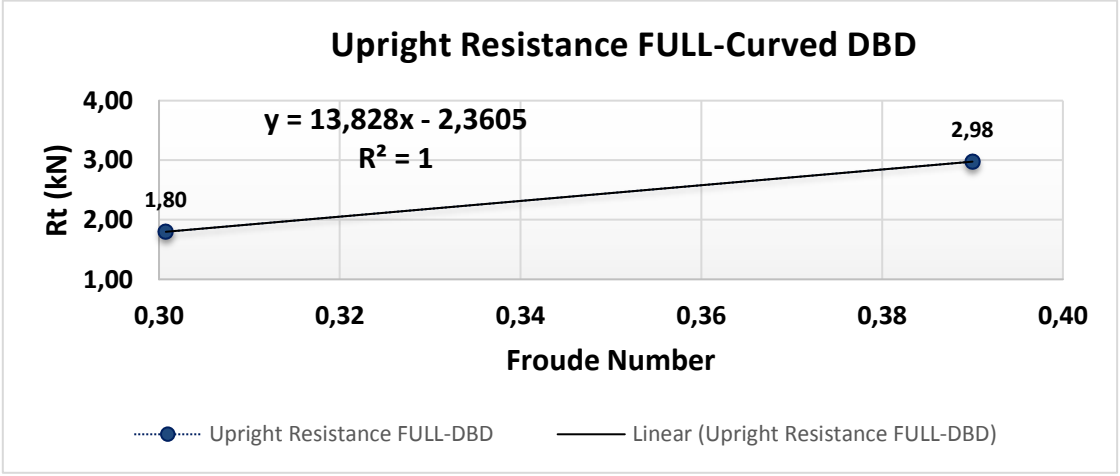

Figure 5-36: Upright resistance graph of full-curved daggerboard

5.4.2 *Effective Draft of 1/2 DSS at 15° Heel Angle & 0.30 FN*

Table 5-39: Effective Draft of 1/2 DSS at 15° Heel Angle & 0.30 FN

Keel Position	DBD Position	% DBD	Heel	Leeway	Clock No	V-Full Size (m/s)	FN	Full Size Total-Rt (kN)	SF² (kN)	Ri (kN)
40°	1/2 DBD	40	15°	3°	350	4,0	0,30	2,42	3,81	0,05
40°	1/2 DBD	40	15°	4°	350	4,0	0,30	2,66	20,94	0,26
40°	1/2 DBD	40	15°	5°	350	4,0	0,30	2,94	48,76	0,61
40°	1/2 DBD	40	15°	6°	350	4,0	0,30	3,35	75,53	0,95

Ru+Rh (kN)	Slope	Te²	Te (m)
2,37	0,0126	1,54	1,24

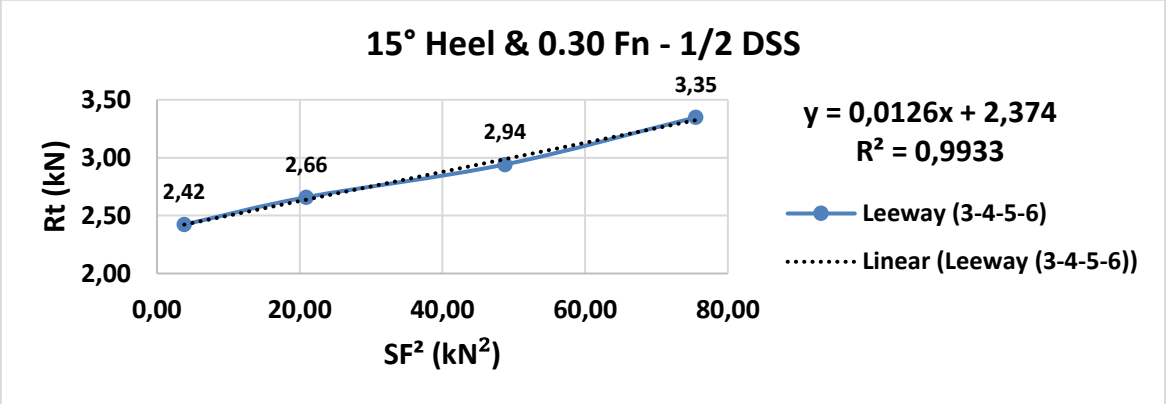

Figure 5-37: Graph of 1/2-curved daggerboard at 15° heel angle & 0.30 Froude number

5.4.3 *Effective Draft of 1/2 DSS at 15° Heel Angle & 0.39 FN*

Table 5-40: Effective Draft of 1/2 DSS at 15° Heel Angle & 0.39 FN

Keel Position	DBD Position	% DBD	Heel	Leeway	Clock No	V-Full Size (m/s)	FN	Full Size Total-Rt (kN)	SF² (kN)	Ri (kN)
40°	1/2 DBD	40	15°	3°	450	5,13	0,39	3,84	7,35	0,07
40°	1/2 DBD	40	15°	4°	450	5,13	0,39	4,00	26,19	0,26
40°	1/2 DBD	40	15°	5°	450	5,13	0,39	4,27	51,24	0,50
40°	1/2 DBD	40	15°	6°	450	5,13	0,39	4,55	81,16	0,79

Ru+Rh (kN)	Slope	Te²	Te (m)
3,76	0,0097	1,21	1,10

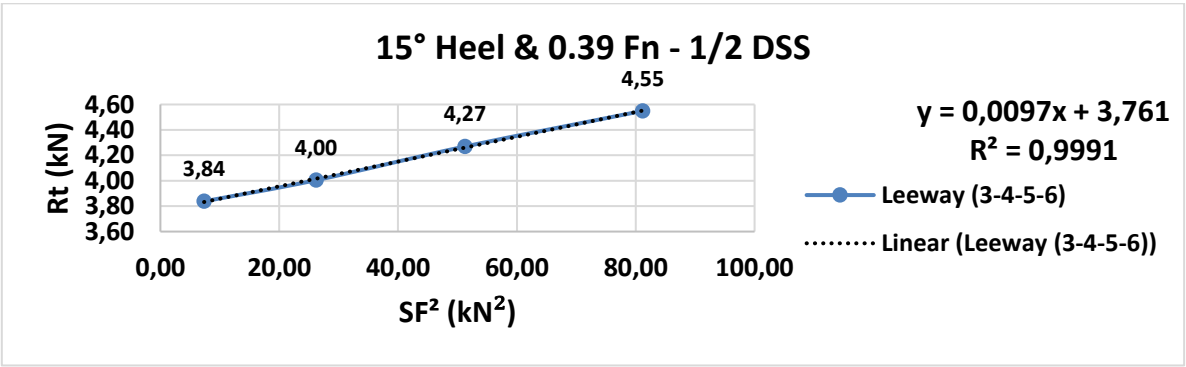

Figure 5-38: Graph of 1/2-curved daggerboard at 15° heel angle & 0.39 Froude number

5.4.4 *Effective Draft of 1/2 DSS at 20° Heel Angle & 0.30 FN*

Table 5-41: Effective Draft of 1/2 DSS at 20° Heel Angle & 0.30 FN

Keel Position	DBD Position	% DBD	Heel	Leeway	Clock No	V-Full Size (m/s)	FN	Full Size Total-Rt (kN)	SF² (kN)	Ri (kN)
40°	1/2 DBD	45	20°	5°	350	4,0	0,30	2,58	4,58	0,07
40°	1/2 DBD	45	20°	7°	350	4,0	0,30	2,87	20,55	0,33
40°	1/2 DBD	45	20°	9°	350	4,0	0,30	3,17	41,30	0,66

Ru+Rh (kN)	Slope	Te²	Te (m)
2,52	0,0159	1,22	1,11

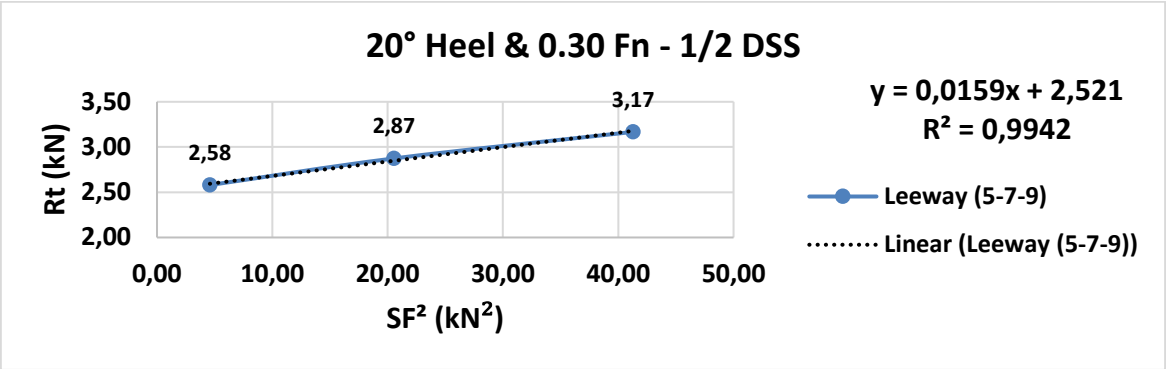

Figure 5-39: Graph of 1/2-curved daggerboard at 20° heel angle & 0.30 Froude number

5.4.5 *Effective Draft of 1/2 DSS at 20° Heel Angle & 0.39 FN*

Table 5-42: Effective Draft of 1/2 DSS at 20° Heel Angle & 0.39 FN

Keel Position	DBD Position	% DBD	Heel	Leeway	Clock No	V-Full Size (m/s)	FN	Full Size Total-Rt (kN)	SF² (kN)	Ri (kN)
40°	1/2 DBD	45	20°	5°	450	5,13	0,39	4,31	24,37	0,29
40°	1/2 DBD	45	20°	7°	450	5,13	0,39	5,00	77,53	0,93
40°	1/2 DBD	45	20°	9°	450	5,13	0,39	5,79	147,79	1,77

Ru+Rh (kN)	Slope	Te²	Te (m)
4,03	0,0120	0,98	0,99

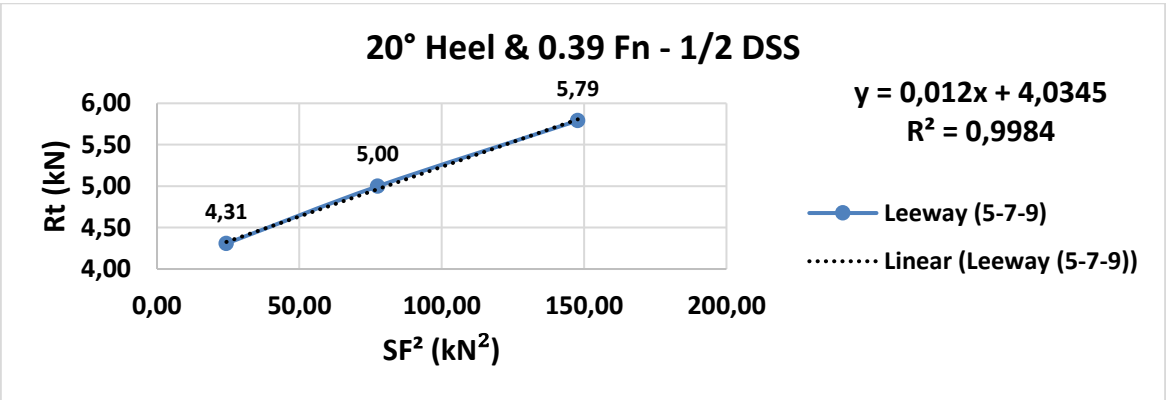

Figure 5-40: Graph of 1/2-curved daggerboard at 20° heel angle & 0.39 Froude number

5.4.6 *Effective Draft of Full DSS at 15° Heel Angle & 0.30 FN*

Table 5-43: Effective Draft of Full DSS at 15° Heel Angle & 0.30 FN

Keel Position	DBD Position	% DBD	Heel	Leeway	Clock No	V-Full Size (m/s)	FN	Full Size Total-Rt (kN)	SF² (kN)	Ri (kN)
40°	Full DBD	90	15°	6°	350	4,0	0,30	3,07	39,96	0,59
40°	Full DBD	90	15°	8°	350	4,0	0,30	3,52	77,27	1,15
40°	Full DBD	90	15°	10°	350	4,0	0,30	4,14	112,38	1,67
40°	Full DBD	90	15°	12°	350	4,0	0,30	4,55	141,53	2,10

Ru+Rh (kN)	Slope	Te²	Te (m)
2,44	0,0149	1,31	1,14

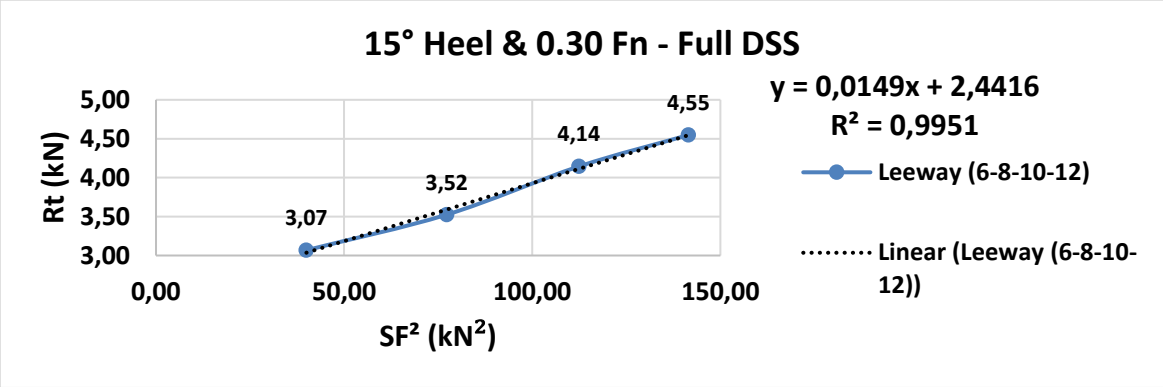

Figure 5-41: Graph of full-curved daggerboard at 15° heel angle & 0.30 Froude number

5.4.7 *Effective Draft of Full DSS at 15° Heel Angle & 0.39 FN*

Table 5-44: Effective Draft of Full DSS at 15° Heel Angle & 0.39 FN

Keel Position	DBD Position	% DBD	Heel	Leeway	Clock No	V-Full Size (m/s)	FN	Full Size Total-Rt (kN)	SF² (kN)	Ri (kN)
40°	Full DBD	90	15°	6°	450	5,13	0,39	5,45	133,91	1,46
40°	Full DBD	90	15°	8°	450	5,13	0,39	6,50	252,64	2,76
40°	Full DBD	90	15°	10°	450	5,13	0,39	7,58	338,46	3,69
40°	Full DBD	90	15°	12°	450	5,13	0,39	8,91	453,94	4,95

Ru+Rh (kN)	Slope	Te²	Te (m)
3,89	0,0109	1,08	1,04

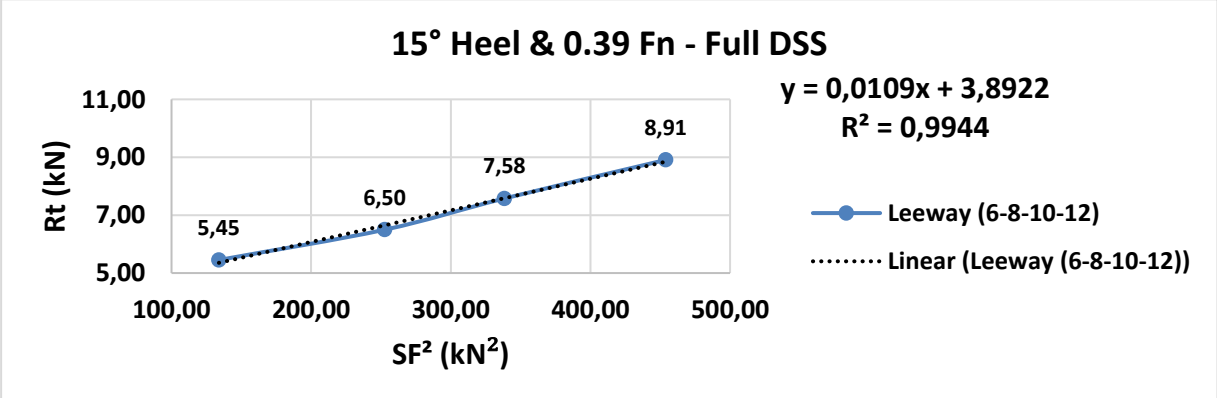

Figure 5-42: Graph of full-curved daggerboard at 15° heel angle & 0.39 Froude number

5.4.8 *Effective Draft of Full DSS at 20° Heel Angle & 0.30 FN*

Table 5-45: Effective Draft of Full DSS at 20° Heel Angle & 0.30 FN

Keel Position	DBD Position	% DBD	Heel	Leeway	Clock No	V-Full Size (m/s)	FN	Full Size Total-Rt (kN)	SF² (kN)	Ri (kN)
40°	Full DBD	95	20°	6°	350	4,0	0,30	3,29	26,10	0,44
40°	Full DBD	95	20°	8°	350	4,0	0,30	3,82	57,29	0,96
40°	Full DBD	95	20°	10°	350	4,0	0,30	4,23	84,11	1,40
40°	Full DBD	95	20°	12°	350	4,0	0,30	4,73	111,51	1,86

Ru+Rh (kN)	Slope	Te²	Te (m)
2,85	0,0167	1,17	1,08

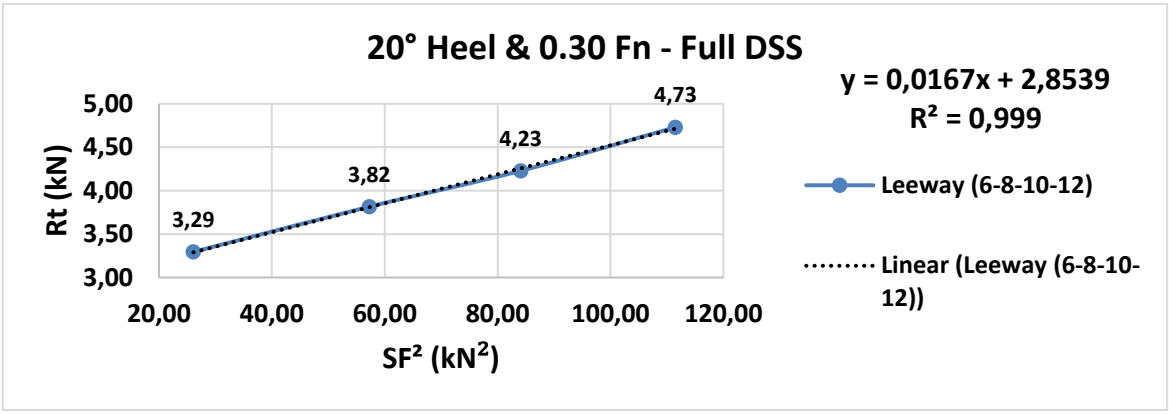

Figure 5-43: Graph of full-curved daggerboard at 20° heel angle & 0.30 Froude number

5.4.9 *Effective Draft of Full DSS at 20° Heel Angle & 0.39 FN*

Table 5-46: Effective Draft of Full DSS at 20° Heel Angle & 0.39 FN

Keel Position	DBD Position	% DBD	Heel	Leeway	Clock No	V-Full Size (m/s)	FN	Full Size Total-Rt (kN)	SF² (kN)	Ri (kN)
40°	Full DBD	95	20°	6°	450	5,13	0,39	5,83	104,49	1,25
40°	Full DBD	95	20°	8°	450	5,13	0,39	6,97	201,19	2,41
40°	Full DBD	95	20°	10°	450	5,13	0,39	7,97	290,03	3,48
40°	Full DBD	95	20°	12°	450	5,13	0,39	9,36	397,43	4,77

Ru+Rh (kN)	Slope	Te²	Te (m)
4,55	0,0120	0,98	0,99

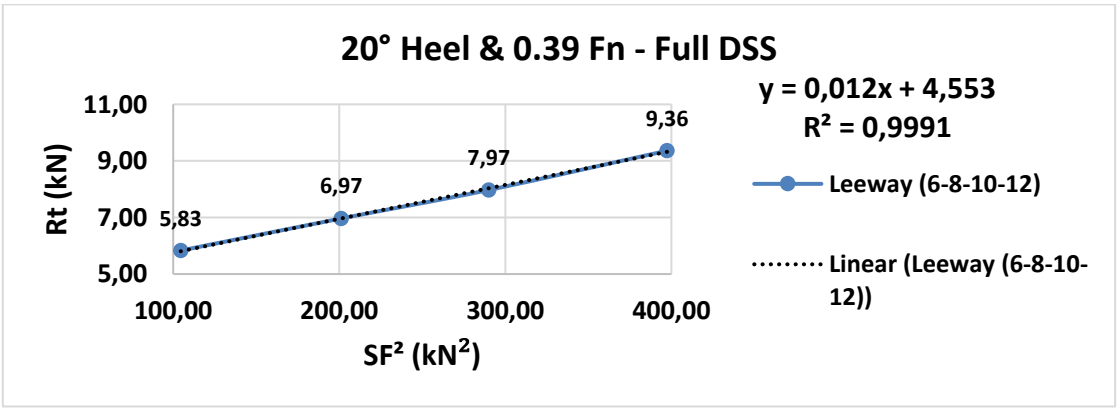

Figure 5-44: Graph of full-curved daggerboard at 20° heel angle & 0.39 Froude number

5.4.10 Overall Effective Draft Analysis of Full and 1/2 Curved Dagger Boards

The effective draft values of the half and full DSS configurations were presented at different sailing conditions singly in previous sections. According to the effective draft results, the half DSS configuration is seen as more efficient than the full configuration at some conditions. The general remarks about the overall performance are explained in the following parts.

- The highest effective draft value is determined with 1/2 daggerboard configuration at lowest heel angle (10°) and Froude number (0.30).
- The lowest effective draft value is determined with 1/2 daggerboard configuration at highest heel angle (25°) and Froude number (0.30).
- The effective draft values generally decrease when the Froude number is increased.
- The curved daggerboard configuration requires more leeway angles (angle of attack) as compared with straight foil shape.
- The curved daggerboard configurations have a bound section which joins the straight (vertical lift force part) and curved (horizontal side force part) parts of the daggerboard and it prevents the tip vortices, therefore, it has less induced drag due to the joint section.
- According to towing tank test observations, the full configuration loses the lift and side force vector directions much more than the half configuration due to its longer span-1 part when the boat is heeled.

Figure 5-45: A view of IMOCA 60 SAFRAN equipped with canting keel & curved foil configuration [26]

Table 5-47: The overall effective draft results of the curved daggerboard configurations

1/2 & Full DSS -40° Canting Keel-Effective Draft Results		
Conditions	FN	
	0,30	0,39
10° Heel & 1/2 DSS	1,42	1,28
15° Heel & 1/2 DSS	1,24	1,10
20° Heel & 1/2 DSS	1,11	0,99
25° Heel & 1/2 DSS	0,64	0,74
10° Heel & FULL DSS	1,16	1,10
15° Heel & FULL DSS	1,14	1,04
20° Heel & FULL DSS	1,08	0,99
25° Heel & FULL DSS	0,96	0,91

Note: Effective Draft Graphs and Tables of 1/2-Full Curved Daggerboards & 40° Canting Keel at 10° and 25° Heel Angle & 0.30 and 0.39 Froude Numbers is presented in the Appendix-E section.

Table 5-48: The overall effective draft / Max. draft results of the curved daggerboard configurations

1/2 & Full DSS -40° Canting Keel		
Effective Draft / Max. Draft (4.5 m)		
FN	0,30	0,39
10° Heel-1/2 DSS - 40° Canting Keel	0,31	0,28
10° Heel-FULL DSS - 40° Canting Keel	0,26	0,25
15° Heel-1/2 DSS - 40° Canting Keel	0,28	0,24
15° Heel-FULL DSS - 40° Canting Keel	0,25	0,23
20° Heel-1/2 DSS - 40° Canting Keel	0,25	0,22
20° Heel-FULL DSS - 40° Canting Keel	0,24	0,22
25° Heel-1/2 DSS - 40° Canting Keel	0,14	0,17
25° Heel-FULL DSS - 40° Canting Keel	0,21	0,20

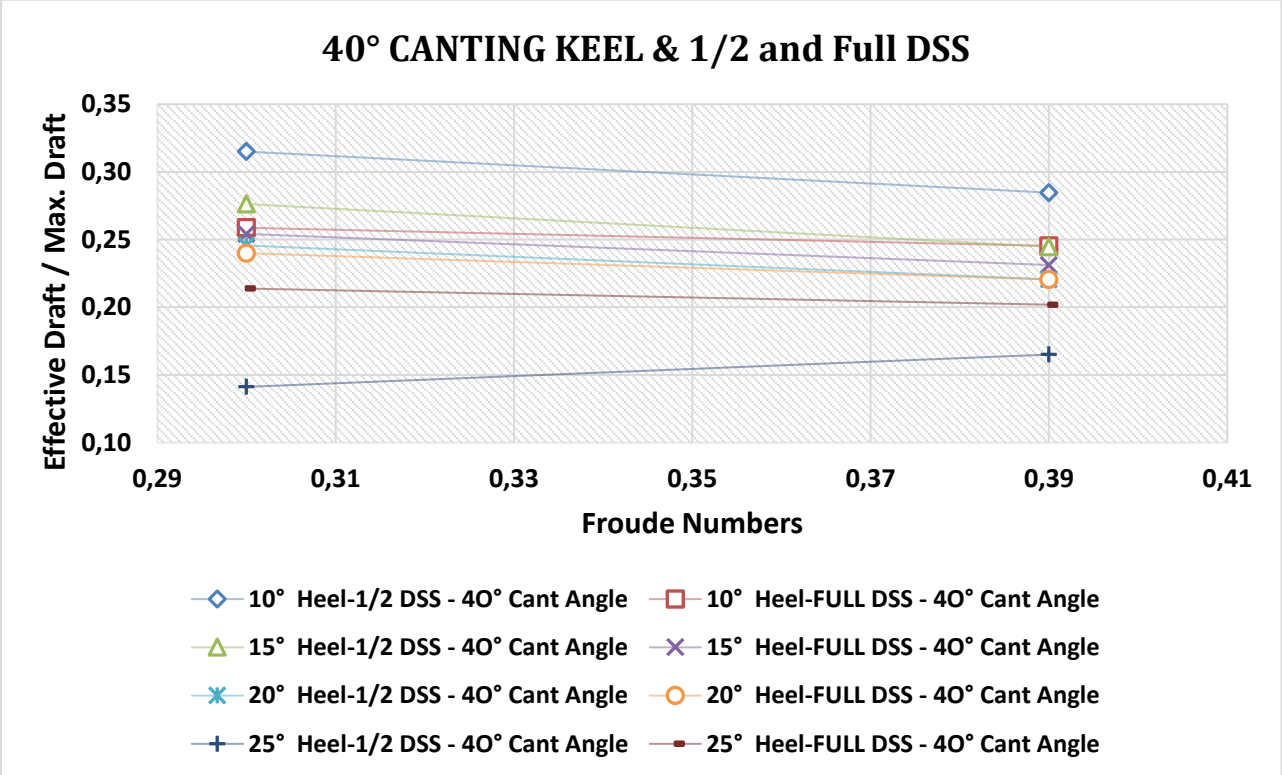

Figure 5-46: Overall graph of 1/2 and full DSS & 40° canting keel

6 OVERALL COMPARISONS BETWEEN STRAIGHT & CURVED FOIL CONFIGURATIONS

The straight and curved configurations have different aspects and shapes. The straight foil is designed for side force generation mainly, but the curved daggerboard has two distinct tasks which are lift force vertically and side force horizontally. During the towing tank tests, the total side force component is obtained from the hull, and all appendages and the total side force consists of the sum of the vertical lift force and the horizontal side force generated by hull/appendages. The same hull and keel/bulb are employed for towing tank tests, but the two different daggerboard configurations are used separately at particular sailing conditions to compare the hydrodynamic effects of them.

The effective draft results show the measure of the ratio of induced drag to side force squared. It means that the higher effective draft corresponds to less induced drag which occurs for per unit of the side force generated therefore this situation is a significant effect for boat speed at upwind condition especially.

The model heave values were analysed to see the lift force differences between both the configurations at particular conditions approximately. The average values of heave measurements obtained at the towing tank tests are taken into account for lift force calculations. There are results for 1/2 and full sizes of the straight and curved configurations. In previous sections, the effective draft values were obtained for each configuration at different sailing conditions. The straight and curved foil configurations will be compared according to certain circumstances based on the effective draft and heave values in this section, and then the overall results will be presented for all configurations.

Note: The sum of upright and heel resistances for both configurations is related to separately their particular test conditions which are shown in further sections. The curved foil has higher (Ru+Rh) because it does not generate side force (so induced drag) therefore the (Ru+Rh) of curved foil is seen as greater than the straight shape. The curved foil needs to have more angle of attack (Leeway) to generate side force at same conditions with straight foil.

6.1 Analyses of 1/2 - Straight & 1/2 - Curved Foil Configurations

6.1.1 15° Heel Angle & 0.30 Froude Number–1/2 Straight & 1/2 Curved Configurations

Table 6-1: Effective draft of the 1/2-straight daggerboard configuration at 15° Heel Angle & 0.30 FN

Keel Position	DBD Position	% DBD	Heel	Leeway	Clock No	V-Full Size (m/s)	FN	Full Size Total-Rt (kN)	SF² (kN)	Ri (kN)
40°	1/2 DBD	50	15°	2,25°	350	4	0,30	2,50	19,70	0,33
40°	1/2 DBD	50	15°	2,75°	350	4	0,30	2,69	30,53	0,52
40°	1/2 DBD	50	15°	4	350	4	0,30	3,20	60,90	1,03

Ru+Rh (kN)	Slope	Te²	Te (m)
2,17	0,0170	1,14	1,07

Table 6-2: Effective draft of the 1/2-curved daggerboard configuration at 15° Heel Angle & 0.30 FN

Keel Position	DBD Position	% DBD	Heel	Leeway	Clock No	V-Full Size (m/s)	FN	Full Size Total-Rt (kN)	SF² (kN)	Ri (kN)
40°	1/2 DBD	40	15°	3°	350	4,0	0,30	2,42	3,81	0,05
40°	1/2 DBD	40	15°	4°	350	4,0	0,30	2,66	20,94	0,26
40°	1/2 DBD	40	15°	5°	350	4,0	0,30	2,94	48,76	0,61
40°	1/2 DBD	40	15°	6°	350	4,0	0,30	3,35	75,53	0,95

Ru+Rh (kN)	Slope	Te²	Te (m)
2,37	0,0126	1,54	1,24

Table 6-3: Comparison of model lift analysis results of 1/2 straight & 1/2 curved foil configurations at 15° Heel Angle & 0.30 FN

Model - Heave Analysis Values	
STRAIGHT DBD	CURVED DBD
Static Heave Value At Zero Speed (mm)	Static Heave Value At Zero Speed (mm)
15,7	0
STRAIGHT DBD	CURVED DBD
Average Sinking Value (mm)	Average Sinking Value (mm)
12,75	-1,59
STRAIGHT DBD	CURVED DBD
Average Sinking Difference (mm)	Average Sinking Difference (mm)
2,95	1,59
The Lift Difference Between Straight & Curved DBD (mm)	
Better Configuration-CURVED DBD	1,37
Full Size - Heave Analysis Values	
Scale Factor	8
Lift Difference (mm)	10,92
Water Plane Area- m²- 15° Heel	39,77
Volume Difference-m³	0,43
ρ-Density (kg/m³)	1025
g (m/s²)	9,81
Lift Force Difference (kN)	4,37
Displacement Difference (tonnes)	0,45

6.1.2 15° Heel Angle & 0.39 Froude Number-1/2-Straight and 1/2-Curved Configurations

Table 6-4: Effective draft of the 1/2-straight daggerboard configuration at 15° Heel Angle & 0.39 FN

Keel Position	DBD Position	% DBD	Heel	Leeway	Clock No	V-Full Size (m/s)	FN	Full Size Total-Rt (kN)	SF² (kN)	Ri (kN)
40°	1/2 DBD	50	15°	2,75°	450	5,13	0,39	4,81	122,23	1,70
40°	1/2 DBD	50	15°	3,25°	450	5,13	0,39	5,18	147,52	2,05
40°	1/2 DBD	50	15°	4°	450	5,13	0,39	5,55	175,57	2,44

Ru+Rh (kN)	Slope	Te²	Te (m)
3,12	0,0139	0,85	0,92

Table 6-5: Effective draft of the 1/2-curved daggerboard configuration at 15° Heel Angle & 0.39 FN

Keel Position	DBD Position	% DBD	Heel	Leeway	Clock No	V-Full Size (m/s)	FN	Full Size Total-Rt (kN)	SF² (kN)	Ri (kN)
40°	1/2 DBD	40	15°	3°	450	5,13	0,39	3,84	7,35	0,07
40°	1/2 DBD	40	15°	4°	450	5,13	0,39	4,00	26,19	0,26
40°	1/2 DBD	40	15°	5°	450	5,13	0,39	4,27	51,24	0,50
40°	1/2 DBD	40	15°	6°	450	5,13	0,39	4,55	81,16	0,79

Ru+Rh (kN)	Slope	Te²	Te (m)
3,76	0,0097	1,21	1,10

Table 6-6: Comparison of model lift analysis results of 1/2 straight & 1/2 curved foil configurations at 15° Heel Angle & 0.39 FN

Model - Heave Analysis Values	
STRAIGHT DBD	CURVED DBD
Static Heave Value At Zero Speed (mm)	Static Heave Value At Zero Speed (mm)
15,7	0
STRAIGHT DBD	CURVED DBD
Average Sinking Value (mm)	Average Sinking Value (mm)
10,01	-5,45
STRAIGHT DBD	CURVED DBD
Average Sinking Difference (mm)	Average Sinking Difference (mm)
5,69	5,45
The Lift Difference Between Straight & Curved DBD (mm)	
Better Configuration-CURVED DBD	0,24
Full Size - Heave Analysis Values	
Scale Factor	8
Lift Difference (mm)	1,9
Water Plane Area- m²- 15° Heel	39,77
Volume Difference-m³	0,08
ρ-Density (kg/m³)	1025
g (m/s²)	9,81
Lift Force Difference (kN)	0,76
Displacement Difference (tonnes)	0,08

6.1.3 20° Heel Angle & 0.39 Froude Number-1/2-Straight and 1/2-Curved Configurations

Table 6-7: Effective draft of the 1/2-straight daggerboard configuration at 20° Heel Angle & 0.39 FN

Keel Position	DBD Position	% DBD	Heel	Leeway	Clock No	V-Full Size (m/s)	FN	Full Size Total-Rt (kN)	SF² (kN)	Ri (kN)
40°	1/2 DBD	50	20°	2,25°	450	5,13	0,39	4,32	46,19	0,86
40°	1/2 DBD	50	20°	2,75°	450	5,13	0,39	4,79	72,24	1,34
40°	1/2 DBD	50	20°	3,25°	450	5,13	0,39	5,12	88,94	1,65

Ru+Rh (kN)	Slope	Te²	Te (m)
3,46	0,0186	0,63	0,80

Table 6-8: Effective draft of the 1/2-curved daggerboard configuration at 20° Heel Angle & 0.39 FN

Keel Position	DBD Position	% DBD	Heel	Leeway	Clock No	V-Full Size (m/s)	FN	Full Size Total-Rt (kN)	SF² (kN)	Ri (kN)
40°	1/2 DBD	45	20°	5°	450	5,13	0,39	4,31	24,37	0,29
40°	1/2 DBD	45	20°	7°	450	5,13	0,39	5,00	77,53	0,93
40°	1/2 DBD	45	20°	9°	450	5,13	0,39	5,79	147,79	1,77

Ru+Rh (kN)	Slope	Te²	Te (m)
4,03	0,0120	0,98	0,99

Table 6-9: Comparison of model lift analysis results of 1/2 straight & 1/2 curved foil configurations at 20° Heel Angle & 0.39 FN

Model - Heave Analysis Values	
STRAIGHT DBD	CURVED DBD
Static Heave Value At Zero Speed (mm)	Static Heave Value At Zero Speed (mm)
25,64	9,2
STRAIGHT DBD	CURVED DBD
Average Sinking Value (mm)	Average Sinking Value (mm)
17,83	1,78
STRAIGHT DBD	CURVED DBD
Average Sinking Difference (mm)	Average Sinking Difference (mm)
7,81	7,42
The Lift Difference Between Straight & Curved DBD (mm)	
Better Configuration-CURVED DBD	0,39
Full Size - Heave Analysis Values	
Scale Factor	8
Lift Difference (mm)	3,08
Water Plane Area- m²- 20° Heel	36,04
Volume Difference-m³	0,11
ρ-Density (kg/m³)	1025
g (m/s²)	9,81
Lift Force Difference (kN)	1,12
Displacement Difference (tonnes)	0,11

6.1.4 Overall Analysis of 1/2-Straight and 1/2-Curved Foil Configurations & 40° Canting Keel

Table 6-10: Effective draft comparison of the 1/2 straight & 1/2 curved foil configurations & 40° canting keel at 15° heel angle & 0.30 and 0.39 FN

Effective Draft Values at 15° Heel Angle			
Froude Number	0,30	0,39	Unit
1/2 Curved DSS & 40° Canting Keel	1,24	1,10	m
Only 40° Canting Keel	1,23	0,95	m
1/2 Straight DBD & 40° Canting Keel	1,07	0,92	m

Table 6-11: Effective draft comparison of the 1/2 straight & 1/2 curved foil configurations & 40° canting keel at 20° heel angle & 0.39 FN

Effective Draft Values at 20° Heel Angle		
Froude Number	0,39	Unit
1/2 Curved DSS & 40° Canting Keel	0,99	m
Only 40° Canting Keel	0,82	m
1/2 Straight DBD & 40° Canting Keel	0,80	m

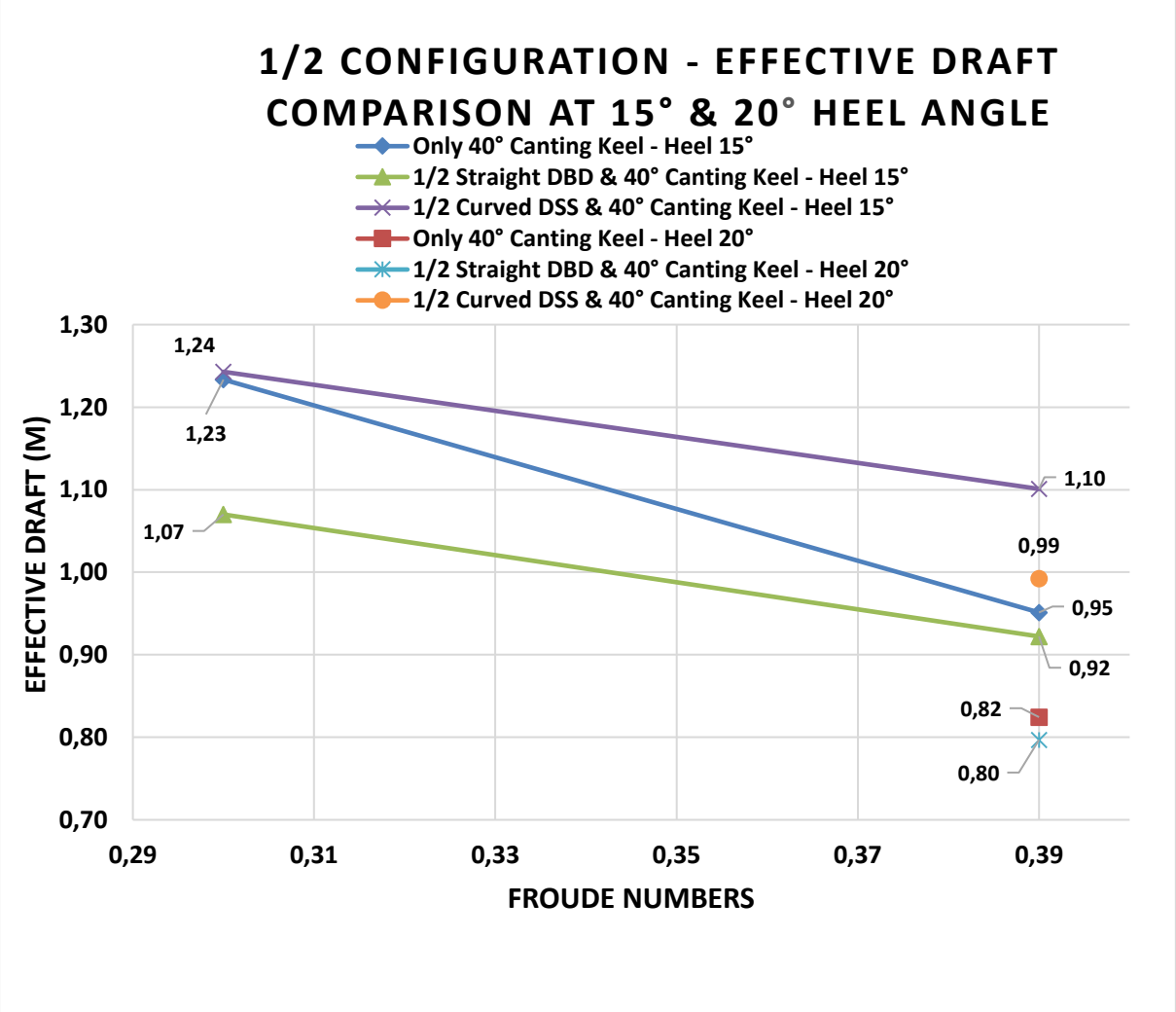

Figure 6-1: Effective draft comparison of all 1/2 configurations & 40° canting keel at 15° and 20° heel angles

6.2 Analyses of Full - Straight & Full - Curved Foil Configurations

6.2.1 15° Heel Angle & 0.30 Froude Number–Full Straight and Full Curved Configurations

Table 6-12: Effective draft of the full-straight daggerboard configuration at 15° Heel Angle & 0.30 FN

Keel Position	DBD Position	% DBD	Heel	Leeway	Clock No	V-Full Size (m/s)	FN	Full Size Total-Rt (kN)	SF² (kN)	Ri (kN)
40°	Full DBD	100	15°	1°	350	4,0	0,30	2,33	19,14	0,20
40°	Full DBD	100	15°	2°	350	4,0	0,30	2,60	45,80	0,48
40°	Full DBD	100	15°	2,75°	350	4,0	0,30	3,31	112,38	1,18

Ru+Rh (kN)	Slope	Te²	Te (m)
2,13	0,0105	1,86	1,36

Table 6-13: Effective draft of the full-curved daggerboard configuration at 15° Heel Angle & 0.30 FN

Keel Position	DBD Position	% DBD	Heel	Leeway	Clock No	V-Full Size (m/s)	FN	Full Size Total-Rt (kN)	SF² (kN)	Ri (kN)
40°	Full DBD	90	15°	6°	350	4,0	0,30	3,07	39,96	0,59
40°	Full DBD	90	15°	8°	350	4,0	0,30	3,52	77,27	1,15
40°	Full DBD	90	15°	10°	350	4,0	0,30	4,14	112,38	1,67
40°	Full DBD	90	15°	12°	350	4,0	0,30	4,55	141,53	2,10

Ru+Rh (kN)	Slope	Te²	Te (m)
2,44	0,0149	1,31	1,14

Table 6-14: Comparison of model lift analysis results of full straight & full curved foil configurations at 15° Heel Angle & 0.30 FN

Model - Heave Analysis Values	
STRAIGHT DBD	CURVED DBD
Static Heave Value At Zero Speed (mm)	Static Heave Value At Zero Speed (mm)
15,7	-0,3
STRAIGHT DBD	CURVED DBD
Average Sinking Value (mm)	Average Sinking Value (mm)
12,89	-1,80
STRAIGHT DBD	CURVED DBD
Average Sinking Difference (mm)	Average Sinking Difference (mm)
2,81	1,50
The Lift Difference Between Straight & Curved DBD (mm)	
Better Configuration-CURVED DBD	1,31
Full Size - Heave Analysis Values	
Scale Factor	8
Lift Difference (mm)	10,47
Water Plane Area- m²- 15° Heel	39,77
Volume Difference-m³	0,42
ρ-Density (kg/m³)	1025
g (m/s²)	9,81
Lift Force Difference (kN)	4,19
Displacement Difference (tonnes)	0,43

6.2.2 15° Heel Angle & 0.39 Froude Number–Full Straight and Full Curved Configurations

Table 6-15: Effective draft of the full-straight daggerboard configuration at 15° Heel Angle & 0.39 FN

Keel Position	DBD Position	% DBD	Heel	Leeway	Clock No	V-Full Size (m/s)	FN	Full Size Total-Rt (kN)	SF² (kN)	Ri (kN)
40°	Full DBD	100	15°	1°	450	5,13	0,39	3,93	90,29	0,81
40°	Full DBD	100	15°	1,5°	450	5,13	0,39	4,33	141,13	1,26
40°	Full DBD	100	15°	2,75°	450	5,13	0,39	5,98	321,52	2,87

Ru+Rh (kN)	Slope	Te²	Te (m)
3,10	0,0089	1,32	1,15

Table 6-16: Effective draft of the full-curved daggerboard configuration at 15° Heel Angle & 0.39 FN

Keel Position	DBD Position	% DBD	Heel	Leeway	Clock No	V-Full Size (m/s)	FN	Full Size Total-Rt (kN)	SF² (kN)	Ri (kN)
40°	Full DBD	90	15°	6°	450	5,13	0,39	5,45	133,91	1,46
40°	Full DBD	90	15°	8°	450	5,13	0,39	6,50	252,64	2,76
40°	Full DBD	90	15°	10°	450	5,13	0,39	7,58	338,46	3,69
40°	Full DBD	90	15°	12°	450	5,13	0,39	8,91	453,94	4,95

Ru+Rh (kN)	Slope	Te²	Te (m)
3,89	0,0109	1,08	1,04

Table 6-17: Comparison of model lift analysis results of full straight & full curved foil configurations at 15° Heel Angle & 0.39 FN

Model - Heave Analysis Values	
STRAIGHT DBD	CURVED DBD
Static Heave Value At Zero Speed (mm)	Static Heave Value At Zero Speed (mm)
15,7	-0,3
STRAIGHT DBD	CURVED DBD
Average Sinking Value (mm)	Average Sinking Value (mm)
10,19	-4,43
STRAIGHT DBD	CURVED DBD
Average Sinking Difference (mm)	Average Sinking Difference (mm)
5,51	4,13
The Lift Difference Between Straight & Curved DBD (mm)	
Better Configuration-CURVED DBD	1,38
Full Size - Heave Analysis Values	
Scale Factor	8
Lift Difference (mm)	11,07
Water Plane Area- m²- 15° Heel	39,77
Volume Difference-m³	0,44
ρ-Density (kg/m³)	1025
g (m/s²)	9,81
Lift Force Difference (kN)	4,43
Displacement Difference (tonnes)	0,45

6.2.3 20° Heel Angle & 0.39 Froude Number–Full Straight and Full Curved Configurations

Table 6-18: Effective draft of the full-straight daggerboard configuration at 20° Heel Angle & 0.39 FN

Keel Position	DBD Position	% DBD	Heel	Leeway	Clock No	V-Full Size (m/s)	FN	Full Size Total-Rt (kN)	SF² (kN)	Ri (kN)
40°	Full DBD	100	20°	1°	450	5,13	0,39	3,92	65,37	0,79
40°	Full DBD	100	20°	1,5°	450	5,13	0,39	4,34	112,46	1,36
40°	Full DBD	100	20°	2,75°	450	5,13	0,39	6,05	245,07	2,96

Ru+Rh (kN)	Slope	Te²	Te (m)
3,07	0,0121	0,98	0,99

Table 6-19: Effective draft of the full-curved daggerboard configuration at 20° Heel Angle & 0.39 FN

Keel Position	DBD Position	% DBD	Heel	Leeway	Clock No	V-Full Size (m/s)	FN	Full Size Total-Rt (kN)	SF² (kN)	Ri (kN)
40°	Full DBD	95	20°	6°	450	5,13	0,39	5,83	104,49	1,25
40°	Full DBD	95	20°	8°	450	5,13	0,39	6,97	201,19	2,41
40°	Full DBD	95	20°	10°	450	5,13	0,39	7,97	290,03	3,48
40°	Full DBD	95	20°	12°	450	5,13	0,39	9,36	397,43	4,77

Ru+Rh (kN)	Slope	Te²	Te (m)
4,55	0,0120	0,98	0,99

Table 6-20: Comparison of model lift analysis results of full straight & full curved foil configurations at 20° Heel Angle & 0.39 FN

Model - Heave Analysis Values	
STRAIGHT DBD	CURVED DBD
Static Heave Value At Zero Speed (mm)	Static Heave Value At Zero Speed (mm)
25,64	9,5
STRAIGHT DBD	CURVED DBD
Average Sinking Value (mm)	Average Sinking Value (mm)
18,16	2,76
STRAIGHT DBD	CURVED DBD
Average Sinking Difference (mm)	Average Sinking Difference (mm)
7,48	6,74
The Lift Difference Between Straight & Curved DBD (mm)	
Better Configuration-CURVED DBD	0,74
Full Size - Heave Analysis Values	
Scale Factor	8
Lift Difference (mm)	5,95
Water Plane Area- m²- 20° Heel	36,04
Volume Difference-m³	0,21
ρ-Density (kg/m³)	1025
g (m/s²)	9,81
Lift Force Difference (kN)	2,15
Displacement Difference (tonnes)	0,22

6.2.4 Overall Analysis of Full-Straight and Full-Curved Foil Configurations & 40° Canting Keel

Table 6-21: Effective draft comparison of the full straight & full curved foil configurations & 40° canting keel at 15° heel angle & 0.30 and 0.39 Fn

Effective Draft Values at 15° Heel Angle			
Froude Number	0,30	0,39	Unit
Full Straight DBD & 40° Canting Keel	1,36	1,15	m
Only 40° Canting Keel	1,23	0,95	m
Full Curved DSS & 40° Canting Keel	1,14	1,04	m

Table 6-22: Effective draft comparison of the full straight & full curved foil configurations & 40° canting keel at 20° heel angle & 0.39 Fn

Effective Draft Values at 20° Heel Angle		
Froude Number	0,39	Unit
Full Curved DSS & 40° Canting Keel	0,992	m
Full Straight DBD & 40° Canting Keel	0,989	m
Only 40° Canting Keel	0,82	m

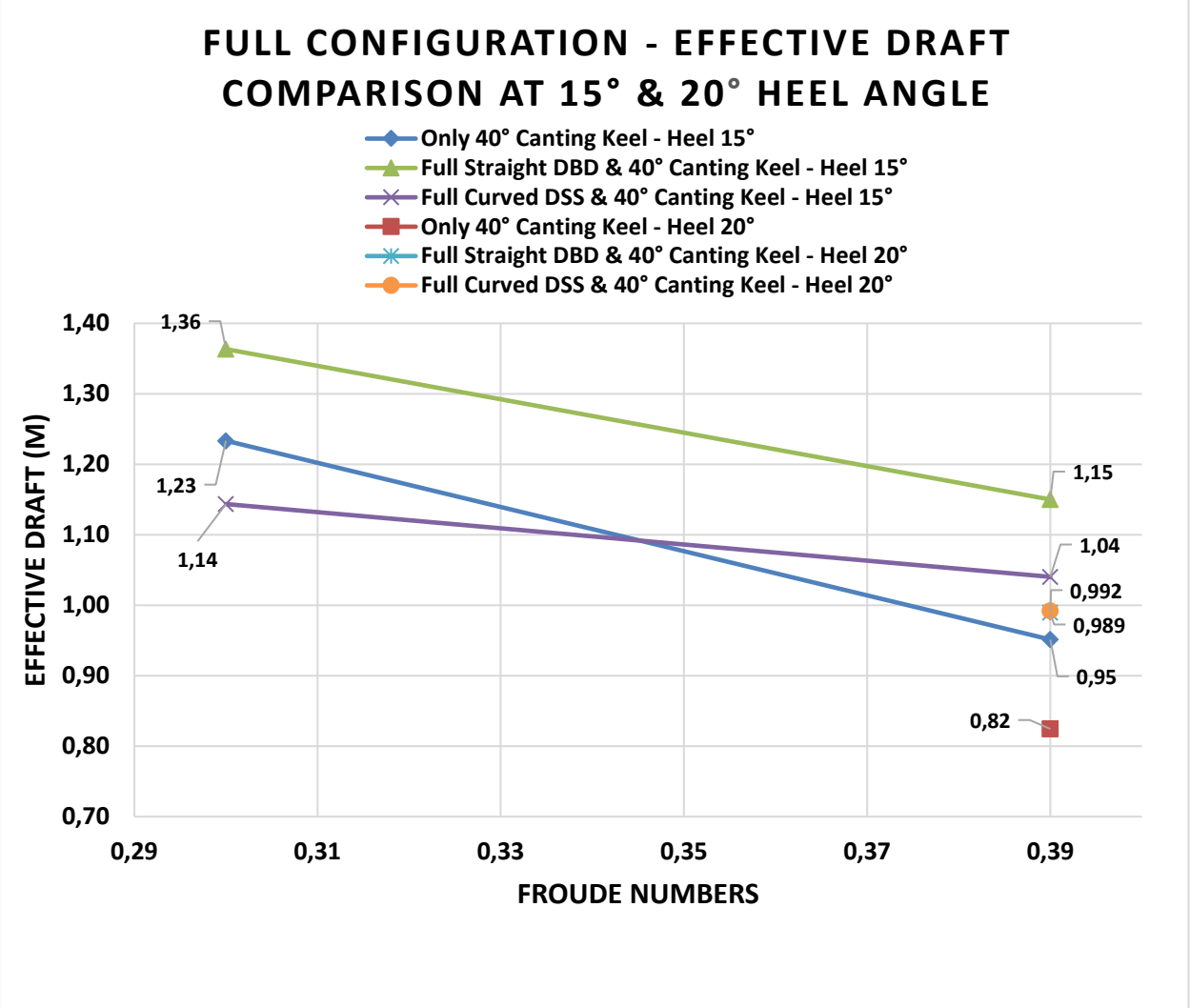

Figure 6-2: Effective draft comparison of all full configurations & 40° canting keel at 15° and 20° heel angles

6.3 Overall Analysis of Straight and Curved Foil Configurations

6.3.1 Effective Draft Analysis

Table 6-23: Overall effective draft comparison of the straight and curved foil configurations & 40° canting keel at 15° heel angle & 0.30 and 0.39 FN

Effective Draft Values at 15° Heel Angle			
Froude Number	0,30	0,39	Unit
Full Straight DBD & 40° Canting Keel	1,36	1,15	m
1/2 Curved DSS & 40° Canting Keel	1,24	1,10	m
Full Curved DSS & 40° Canting Keel	1,14	1,04	m
Only 40° Canting Keel	1,23	0,95	m
1/2 Straight DBD & 40° Canting Keel	1,07	0,92	m

Table 6-24: Overall effective draft comparison of the straight and curved foil configurations & 40° canting keel at 20° heel angle & 0.39 FN

Effective Draft Values at 20° Heel Angle		
Froude Number	0,39	Unit
Full Straight DBD & 40° Canting Keel	0,989	m
1/2 Curved DSS & 40° Canting Keel	0,992	m
Full Curved DSS & 40° Canting Keel	0,992	m
Only 40° Canting Keel	0,82	m
1/2 Straight DBD & 40° Canting Keel	0,80	m

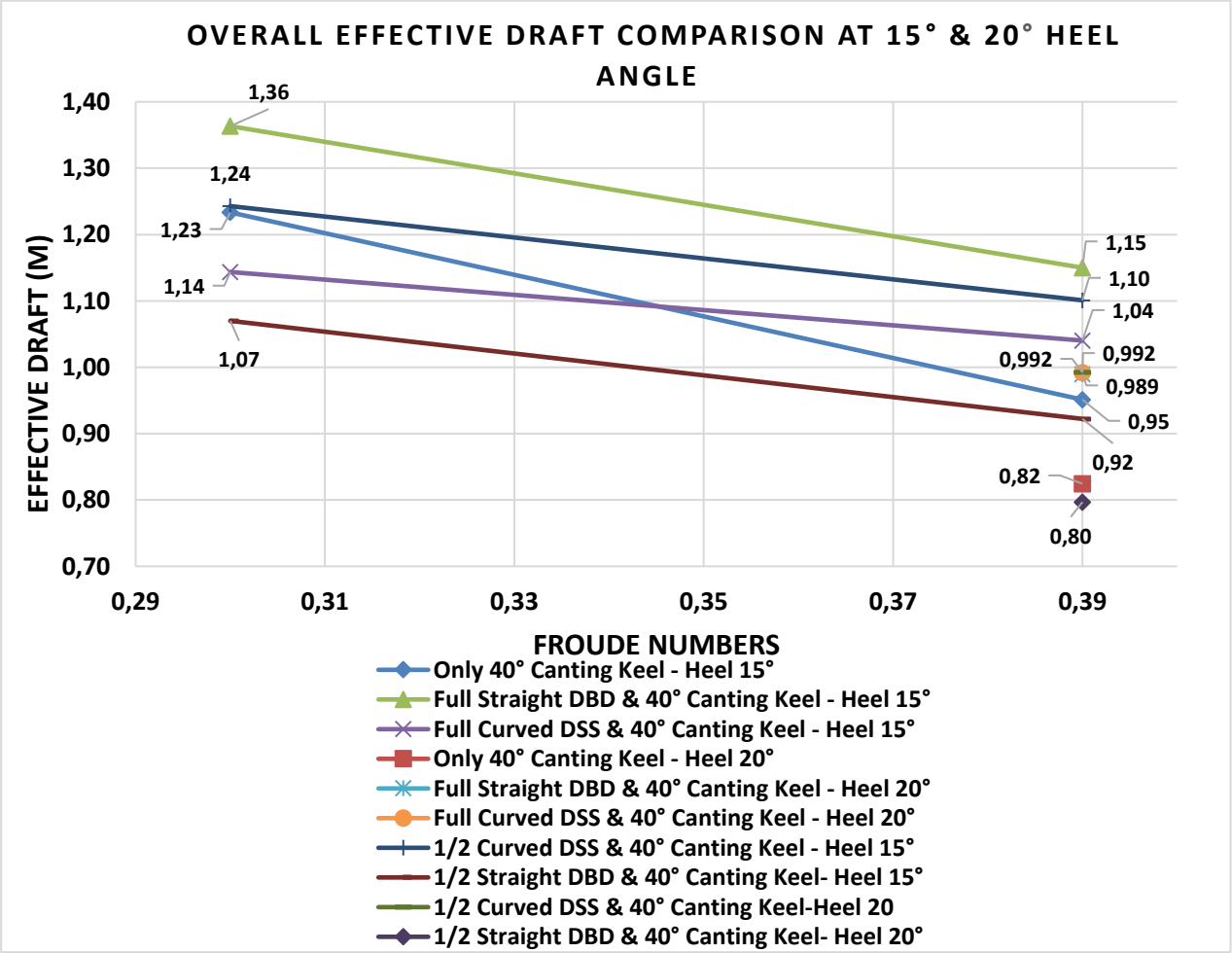

Figure 6-3: Overall effective draft comparison at 15° and 20° heel angles

Note: As stated previously, there is a % 4 total uncertainty value (uncertainty of the residual resistance coefficient) which indicates the probable maximum change of the effective draft results (as increment or decrease) based on the resistance parameters obtained from the towing tank tests. Therefore, the percentage difference between the effective draft values of the different appendage conditions should be higher than the percentage of the uncertainty to evaluate the efficiency of the tested configurations exactly. Otherwise, it will be not clear to say which one is more efficient. For instance, the effective draft results are almost same for some configurations at 20° heel angle & 0.39 Froude number, so this condition might be performed again in towing tank tests as a future work to compare the three different configurations clearly.

6.3.2 Lift Analysis between 1/2 and Full Sizes of Same Configuration Types

Table 6-25: Full-size heave analysis of 1/2 and full foil configurations at 15° heel angle & 0.30 Fn

Full Size - Heave Analysis Values at 15° Heel Angle & 0.30 Fn	
Foil Configurations - 1/2 - Straight & Full - Straight	
Lift Force Difference (kN)	0,46
Displacement Difference (tonnes)	0,05
Better Configuration	Full - Straight
Foil Configurations - 1/2 - Curved & Full - Curved	
Lift Force Difference (kN)	0,27
Displacement Difference (tonnes)	0,03
Better Configuration	Full - Curved

Table 6-26: Full-size heave analysis of 1/2 and full foil configurations at 15° heel angle & 0.39 Fn

Full Size - Heave Analysis Values at 15° Heel Angle & 0.39 Fn	
Foil Configurations - 1/2 - Straight & Full - Straight	
Lift Force Difference (kN)	0,57
Displacement Difference (tonnes)	0,06
Better Configuration	Full - Straight
Foil Configurations - 1/2 - Curved & Full - Curved	
Lift Force Difference (kN)	4,23
Displacement Difference (tonnes)	0,43
Better Configuration	Full - Curved

Table 6-27: Full-size heave analysis of 1/2 and full foil configurations at 20° heel angle & 0.39 Fn

Full Size - Heave Analysis Values at 20° Heel Angle & 0.39 Fn	
Foil Configurations - 1/2 - Straight & Full - Straight	
Lift Force Difference (kN)	0,94
Displacement Difference (tonnes)	0,10
Better Configuration	Full - Straight
Foil Configurations - 1/2 - Curved & Full - Curved	
Lift Force Difference (kN)	1,98
Displacement Difference (tonnes)	0,20
Better Configuration	Full - Curved

7 GENERAL REMARKS

7.1 Straight Daggerboard Configurations

- The primary function of the straight configuration is to generate the side force horizontally due to its shape. For that reason, the straight daggerboard produces less lift force vertically than the curved daggerboard configuration.
- It does not have a joint section like the curved foil; therefore, the tip vortex might occur more on the straight foil shape as compared with the curved configuration based on the foil theory. In general terms, 1.5 ° toe angle (angle of attack) is enough for the straight foil configuration to generate normal side force.
- The full-straight foil configuration is the most efficient configuration as compared with others in the upwind condition, and the half-straight foil is the worst configuration according to the overall experimental results. In addition, the full-straight foil generates more lift force due to its bigger foil area than the half-straight configuration in same conditions based on the lift analyses.
- According to effective draft results, the full-straight daggerboard looks better than 1/2 straight configuration. It is highly likely because of longer span dimension. Hence the fully extended configuration has less induced drag based on 2D foil theory. It can be explained that is why the full-straight foil is seen more efficient than the half-straight foil. (b=span length, c=chord length, AR= aspect ratio, Cdi=induced drag coefficient, S= foil area, lift coefficient Cl=2πα (α (angle of attack) - it is assumed that the Cl is constant) [6].

$$AR = \frac{b}{c} \rightarrow Cdi = \frac{Cl^2}{\pi . AR} - \textbf{Equation [5]} \;\&\; L = \frac{1}{2}\rho V^2 S\, Cl - \textbf{Equation [3]}$$

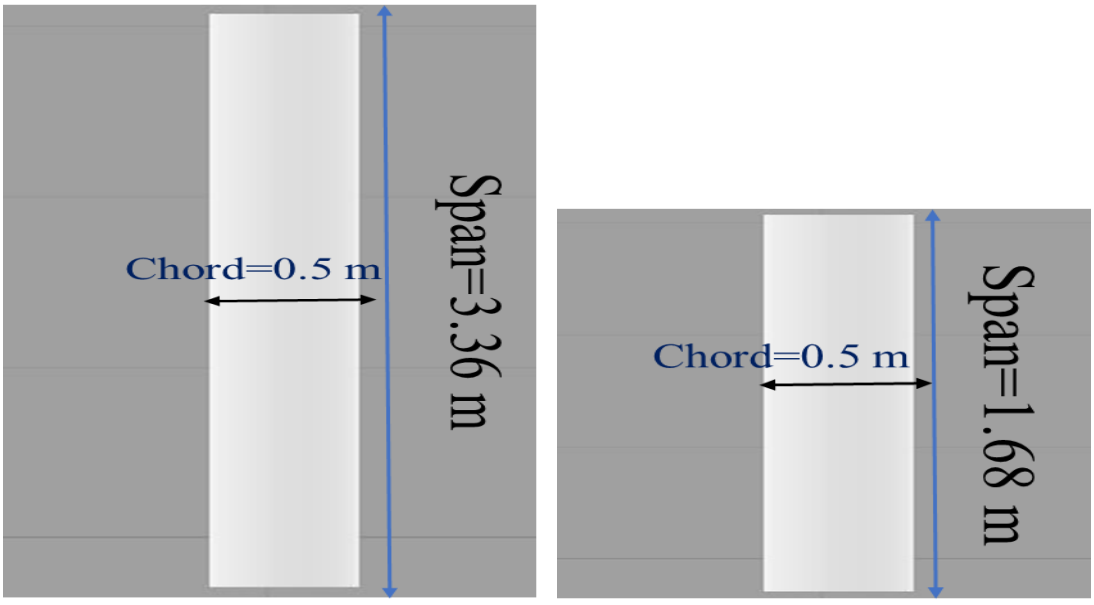

Figure 7-1: The 1/2 (right) and full (left) straight daggerboard configurations [23]

7.2 Curved Daggerboard Configurations

- The curved foil configuration has been designed to perform two tasks. One of its parts has lift function vertically differently from the straight configuration and another part (curved section) enables to generate the side force as a winglet horizontally.
- The joint section of the two parts reduces the trailing vortices of the foil when it generates the total side force (lift and side force). Hence, the induced drag due to the tip vortices could be less as compared with the straight configuration.
- The toe angle (angle of attack) was kept same with the straight configuration for the curved foil. However, the 1.5° toe angle for both parts of the curved foil was not enough to generate normal side force. Therefore, the curved foil required more leeway angle during the towing tank tests.
- It seems that the curved foil configurations do not have totally submerged sections at some low heel angles such as % 85 wetted surface area of the full-curved daggerboard at 10° heel angle. For that reason, the free surface effect occurs around the foil according to the towing tank test observations. This might cause some flow vortices and additional wave drag and it could affect the efficiency of the curved foil configurations.
- The efficiency of the both curved foil (1/2 and full) configurations are not good enough in the upwind condition as compared to the full-straight configuration based on the effective draft values. However, the curved foil configurations generate certainly more lift force than the straight foil configurations in same sailing conditions based on the model heave analyses.
- The full-curved configuration produces more lift force than the half-curved daggerboard according to the lift analyses in same sailing conditions although the full-curved foil seems slightly less efficient than the half-curved configuration based the effective draft results. Therefore, the lifting advantage of the full-curved foil is important to get less displacement (less wetted surface area and total resistance) so it provides more boat speed.
- Unexpectedly, the 1/2 curved foil configuration is seen more efficient than the full curved foil which has two times the longer span-1 length. There could be an explanation for this situation based on the test observations and 3D foil theory. The lift and side force vectors of the 1/2 curved daggerboard are closer to the normal 2D force vectors (lift and side forces) than the full curved foil. Therefore, the 1/2 configuration generates the total side force efficiently. On the other hand, the entire configuration causes more induced drag due to losing the vector directions while it produces the side force.

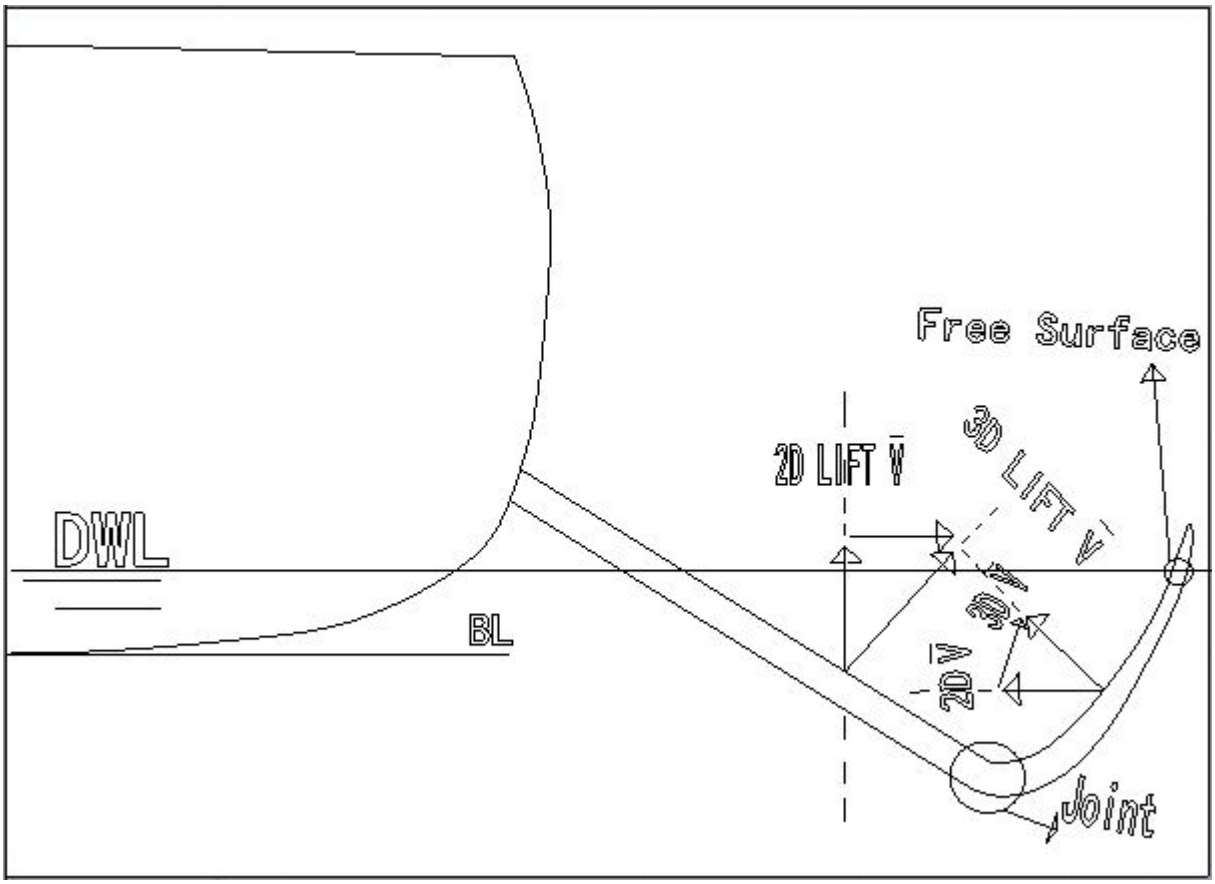

Figure 7-2: Force vector directions of the full curved daggerboard configuration [23]

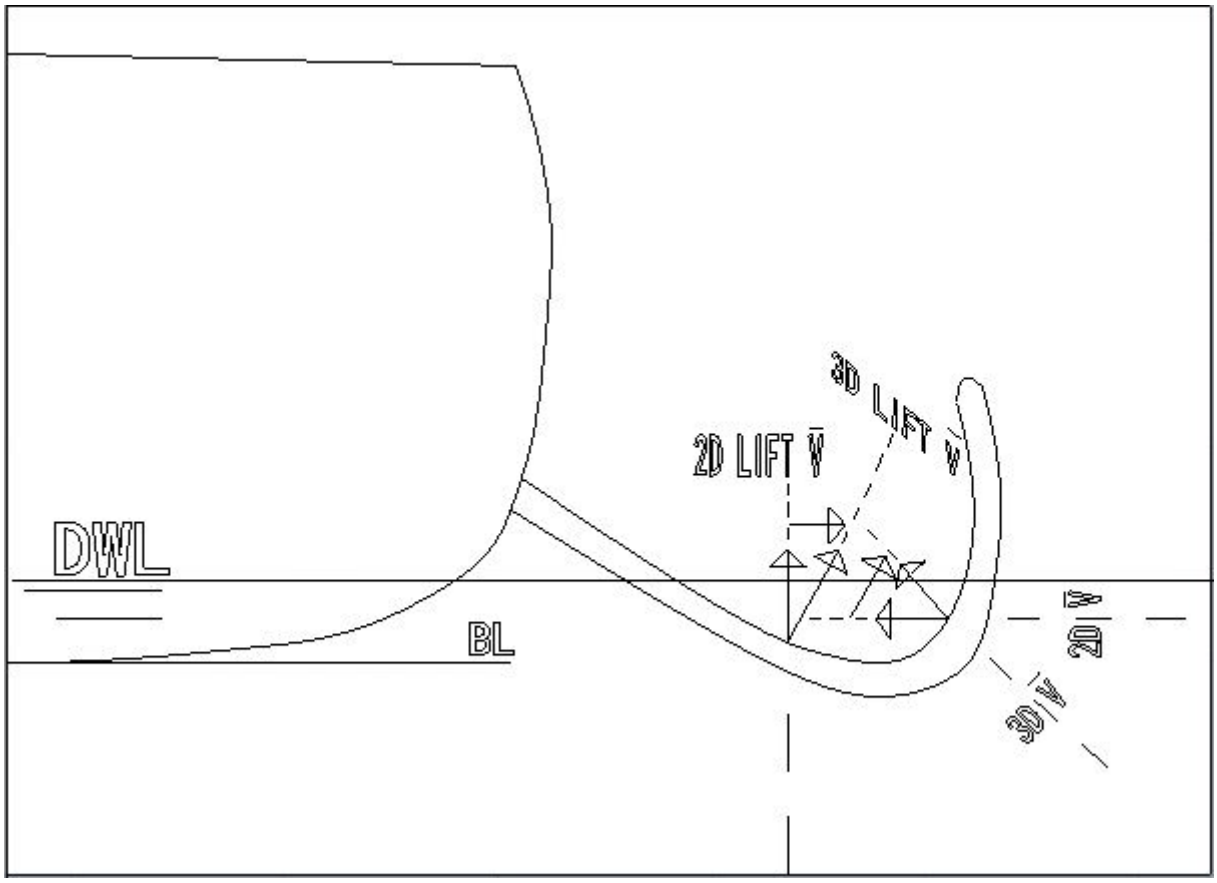

Figure 7-3: Force vector directions of the 1/2 curved daggerboard configuration [23]

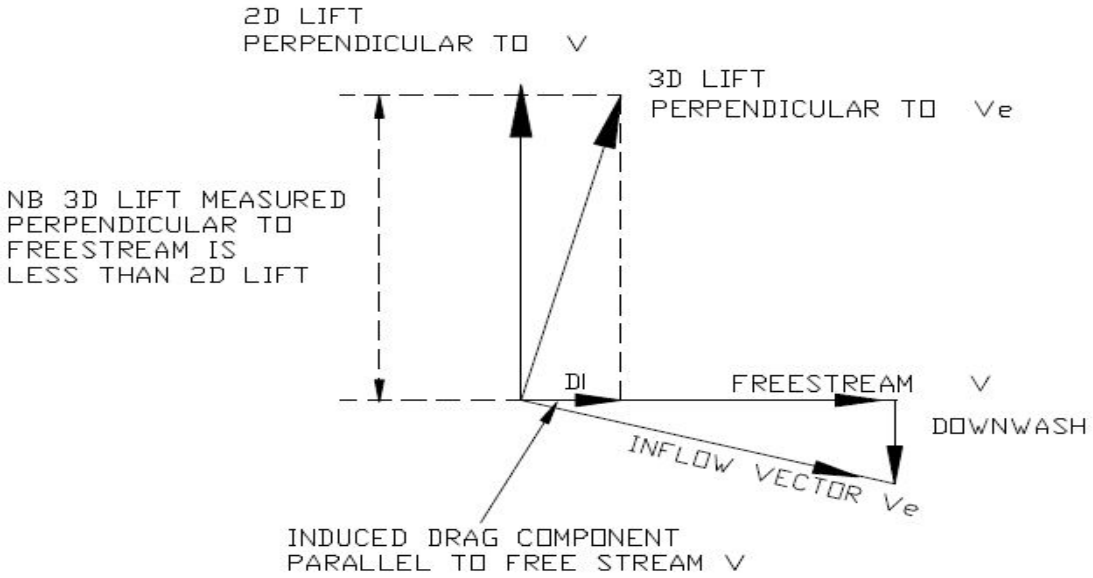

Figure 7-4: Illustration of 2D and 3D lift vector directions measured perpendicular to free stream [6]

- Based on the effective draft results, observations and the 3D foil theory, there could be a new curved foil configuration design (it is a new approach inspired by the original idea of the Canadian Open 60 project [11]) to be tested either in CFD (Computational fluid dynamics) or towing tank tests as a future work.
- The new design would also have curved lifting part (span-1) instead of the straight shape; therefore, the foil configuration might keep the 3D vector directions close to the 2D normal force vector directions (lift and side force) due to its shape. Hence it might be more efficient configuration than others. The illustration of the possible curved configuration is shown in the following Figure 7-5.

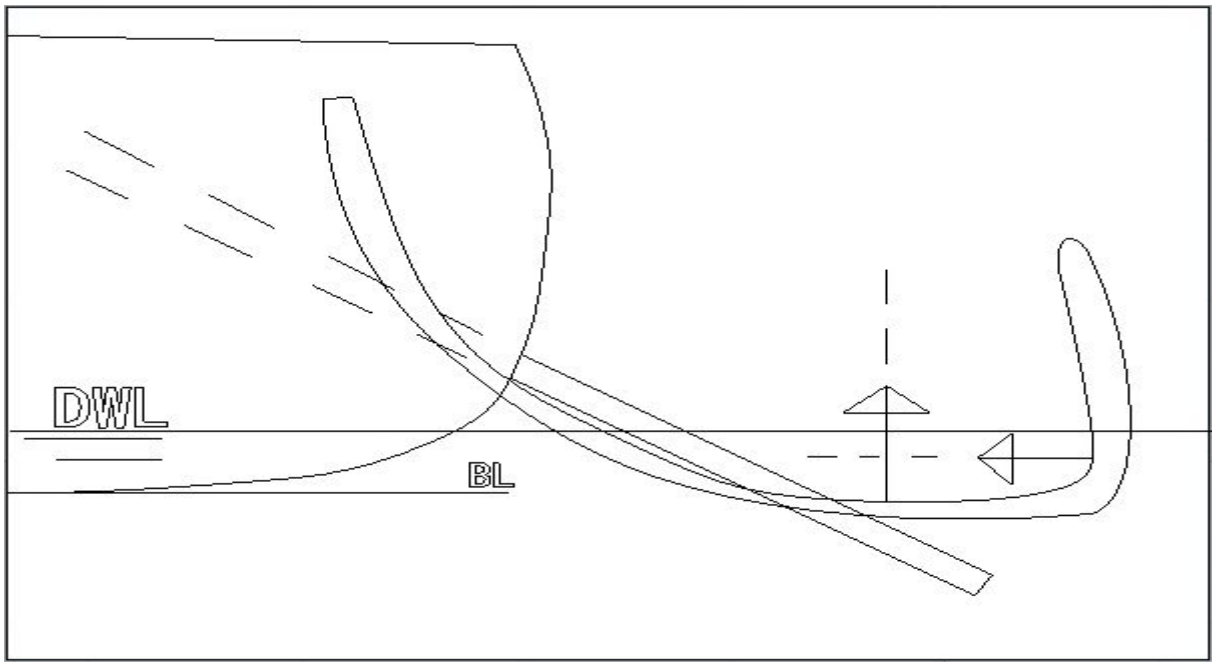

Figure 7-5: Illustration of the possible curved foil configuration design idea [11, 23]

8 CONCLUSIONS

- According to the towing tank tests performed in the upwind condition, the full straight configuration is the most efficient shape as compared with others. Hence, it might have better potential for boat speed in the upwind condition. However, there is important lifting difference between the two different configurations. The curved foil configurations have certainly lift force advantage due to their shape and function; therefore, this lift feature enables to obtain an amount of less displacement (less wetted surface area and wave resistance) for the sailboat. This lifting ability could be a very critical advantage for the speed of sailboats equipped with the curved foil configurations despite being less efficient.
- According to the model lift analyses, the full size configurations (full straight and full curved foils) of the two different shapes generate more lift force than the half configurations. That's why the skippers and designers prefer extended configurations instead of the half shapes during the race. It seems that the 1/2 curved foil configuration is more efficient than the full curved configuration based on effective draft results but the full-curved foil produced more lift force than the 1/2 curved foil configuration based on the lift analyses.
- The angle of attack was kept same for both configurations to compare them exactly. However, it was realised that the angle of attack was not great enough to generate side force for the curved daggerboards so it required more leeway angle for producing the side force. It can be recommended that the angle of attack of the curved configuration can be enhanced to generate more side force value without increasing the leeway angle in the future work. This will also enable to lift the boat more and also reduce the heel angle; therefore, the boat has more powerful and efficient sails to generate drive force and the sailboat can be sailed faster.
- Based upon the 1/2 curved foil configuration, the 3D force vectors (lift vertically and side force horizontally) of the curved foil configurations should be kept close to 2D vector directions with some mechanisms or proper positions to generate the side force effectively.
- The 0° canting keel is more efficient than the 40° canting keel according to the test results but the 40° canting keel has obviously an advantage of the static righting arm (Gz) due to the bulb weight. Therefore it can provide the necessary righting moment with less displacement value and because of this reason, designers prefer the 40° canting keel as an appendage. However, the boat needs an additional appendage (daggerboards)

to enhance efficiency of the total side force generation and get more righting moment. In general, the daggerboards together with 40° canting keel contribute to the efficiency of the side force generation and the increase of the righting moment.

- There were some very similar effective draft results, and they could not be evaluated exactly because of the uncertainty value (%4) to determine the better appendage combination. Therefore, some uncertain conditions can be performed again in the either towing tank tests or CFD simulations as a future work to make them clear.
- During the towing tank tests, there were a few restrictions to modify some variables easily such as the angle of attack of the daggerboards, viscosity of the water, the higher boat speed (downwind), the dimensions, shapes and positions of the foil configurations.
- As a future work, the lift force, side force and drag values of the different daggerboard configurations can be obtained in various sailing conditions using CFD simulations to analyse the results exactly and the CFD results can be compared with the results obtained from the towing tank tests. Also, the dimensions and shapes of them can be modified to determine the optimum configuration for the Open 60 sailboat.

Figure 8-1: A picture from the towing tank facility together with the model boat

- Based on the all towing tank test results (lift and effective draft analyses), the full-straight daggerboard is more efficient than the half and full curved foil configurations in the upwind conditions, however, the curved foils lift the hull out of the water more as compared with the straight one in the upwind condition. However, the lifting advantage and the efficiency of the foils can change positively or negatively in range of higher velocities (downwind condition). According to the tests done, it seems approximately that the effective draft differences between the two different foils are decreasing slightly in the higher velocity (0.39 Fn).
- It seems that the new generation sailboats (equipped with the curved daggerboard configurations) appear certainly top of the race ranking when the ranking list [27] of the Vendée Globe 2016-2017 is taken a look at in reality. This situation shows that the lifting advantage of the foiling monohull sailboats is a very crucial feature for the boat speed despite being less efficient in the upwind condition after all.
- The sailing record time of the Vendée Globe competition has been known as 78 days until now, and it is held by François Gabart [10]. However, according to the current distance to finish, it might be said that the time can be reduced with the new innovation foils (the curved foil configurations) at the end of the race.

Figure 8-2: The ranking list & & the elapsed time of the Vendée Globe Competition on 14 January 2017 [27]

REFERENCES

[1] MEYER, J. R., Jr. (1990). *SHIPS THAT FLY-A STORY OF THE MODERN HYDROFOIL*. Hydrofoil Technology.

[2] Architecture Navale, Génie Maritime, Navigation Intérieure et Maritime, Analyse de Systèmes de Transport (ANAST), *Towing Tank Test*, Version 1, Department of Naval Architecture of University of Liège, Belgium, November of 2010.

[3] ITTC (2011a). Recommended Procedurec and Guidelines – 7.5 – 02 – 02 – 01 / 02–01–03

[4] ITTC (2011b). Recommended Procedurec and Guidelines – 7.5 – 02 – 02 – 02.

[5] Steen, S. (2014, August). Experimental Methods in Marine Hydrodynamics. Retrieved December 21, 2016, from http://www.ivt.ntnu.no/imt/courses/tmr7/lecture/Kompendium_2014_web.pdf GENERAL MODELLING LAWS, Lecture Notes-TMR7.

[6] Barkley, G. S. (2016/2017). Advanced Naval Architecture (YEP 606). Southampton Solent University, School of Maritime Science and Engineering.

[7] Hydrofoil Basics - Configurations. (1998, May 9). Retrieved December 27, 2016, from http://www.foils.org/basfigs.htm

[8] *Rigging Small Sailboats*. (1973). Retrieved from https://www.glen-l.com/free-book/rigging-small-sailboats-10.html

[9] Tarjan, G. (2009, March 12). Multihull Keels and Daggerboards. *PUBLICATIONS & ARTICLES*. Retrieved from http://www.aeroyacht.com/2009/03/12/multihull-keels-and-daggerboards/

[10] Presentation - Vendée Globe 2016-2017. (n.d.). Retrieved November 15, 2016, from http://www.vendeeglobe.org/en/presentation

[11] Day, A., Johnston, L., Edwards, T., & O'Rourke, C. (2015, April). The Type 600 Project. Retrieved December 20, 2016, from http://www.canadianoceanracing.com/wp-content/uploads/2015/04/Open-60-Report.pdf

[12] Weather analysis-BE CAREFUL WITH THE WIND SHADOW. (2016, November 11). Retrieved November 15, 2016, from http://www.vendeeglobe.org/en/news/15967/be-careful-with-the-wind-shadow

[13] Riou, V. (2016, April 8). VINCENT RIOU: "THE MEN MAKE THE DIFFERENCE". Retrieved November 15, 2016, from http://www.vendeeglobe.org/en/news/15155/vincent-riou-the-men-make-the-difference

[14] Merfyn, O., Campbell, L., & Provinciali, G. (2013, June 28). Daggerboard evaluation for an IMOCA 60 yacht. Retrieved January 15, 2017, from http://www.owenclarkedesign.com/Daggerboard_evaluation_for_an_IMOCA_60_yacht

[15] Skippers - Vendée Globe 2016-2017. (n.d.). Retrieved December 28, 2016, from http://www.vendeeglobe.org/en/skippers

[16] The relationship between displacement, power and performance in Open 60 design. (n.d.). Retrieved December 28, 2016, from http://www.owenclarkedesign.com/The_relationship_between_displacement_power_and_pe

[17] Nielsen, P. (2015, November 04). Foiling Monohulls. Retrieved December 28, 2016, from http://www.sailmagazine.com/boats/design-and-technology/foiling-monohulls/

[18] Bunting, E. (2016, December 01). Why do the IMOCA 60 Vendee Globe boats have foils? Retrieved December 28, 2016, from http://www.yachtingworld.com/features/why-do-the-new-vendee-globe-imoca-60-yachts-have-foils-100185

[19] Sheahan, M. (Ed.). (2016, March 03). What will foiling do for you? Why foils will change sailing forever. Retrieved December 28, 2016, from http://www.empire-empire.com/yacht-empire-achives/yacht-world/what-will-foiling-do-for-you-why-foils-will-change-sailing-forever

[20] MAXSURF: Bentley. Retrieved from https://www.bentley.com/en/products/brands/maxsurf

[21] Forget the Keel: Let's Go Foiling. (n.d.). Boating Writers International. Retrieved January 1, 2017, from http://www.bwi.org/bwicontest/files/1957-foilingblanked.pdf

[22] McLeod, B. (2010). Teknologika – Moth blog. Retrieved January 01, 2017, from http://www.teknologika.com/mothblog/the-evolution-of-moth-main-hydrofoils/

[23] Rhinoceros: Retrieved from https://www.rhino3d.com/

[24] Open 60 - Rig Dimensions & Approximate Sail Area. (n.d.). Retrieved January 01, 2017, from http://www.mauripro.com/us/category/2-Open-60.html

[25] Claughton, A., & Oliver, C. (2004). Design Considerations for Canting Keel Yachts. Retrieved December 20 ,2016, from http://www.wumtia.soton.ac.uk/sites/default/files/uploads/pages/HISWA2004AC.pdf

[26] How Lifting Foils Will Help the IMOCA 60 Scuttlebutt Sailing News. (2015, September 25). Retrieved November 15, 2016, from http://www.sailingscuttlebutt.com/2015/09/25/how-lifting-foils-will-help-the-imoca-60/

[27] Ranking and race data - Vendée Globe 2016-2017. (n.d.). Retrieved January 14, 2017, from http://www.vendeeglobe.org/en/ranking-and-race-data

[28] Présentation officielle du Figaro 3. (2016, December 03). Retrieved January 14, 2017, from http://www.courseaularge.com/presentation-officielle-figaro-3.html

[29] http://www.ivt.ntnu.no/imt/courses/tmr7/resources/ITTC%20UA%20ver%2027.xls

APPENDICES

A. Appendix - Tables and Graphs of Form Factors

Upright Condition

Table- A-1: General specifications for form factor calculations of the upright condition

FORM FACTOR-Upright Condition		
Overall Submerged Length ,LOS	2,286	m
Waterline Length, LWL	2,25	m
Wetted Surface Area-Full Scale	56,25	m^2
Wetted Surface Area-Model	0,88	m^2
Density	998,31	kg/m^3
Gravity	9,81	m/s^2

Table- A-2: Values obtained from towing tank tests for form factor chart of the upright condition

Run	Clock No.	Model Speeds (m/s)	Fn	RT (N)	CT / CF	Fn^4 / CF
1	110	0,47	0,10	0,54	1,23	0,02
2	130	0,55	0,12	0,78	1,32	0,04
3	160	0,67	0,14	1,23	1,44	0,10
4	180	0,75	0,16	1,44	1,38	0,16
5	190	0,79	0,17	1,65	1,45	0,19
6	200	0,83	0,18	1,75	1,42	0,23
7	240	0,99	0,21	2,55	1,49	0,50

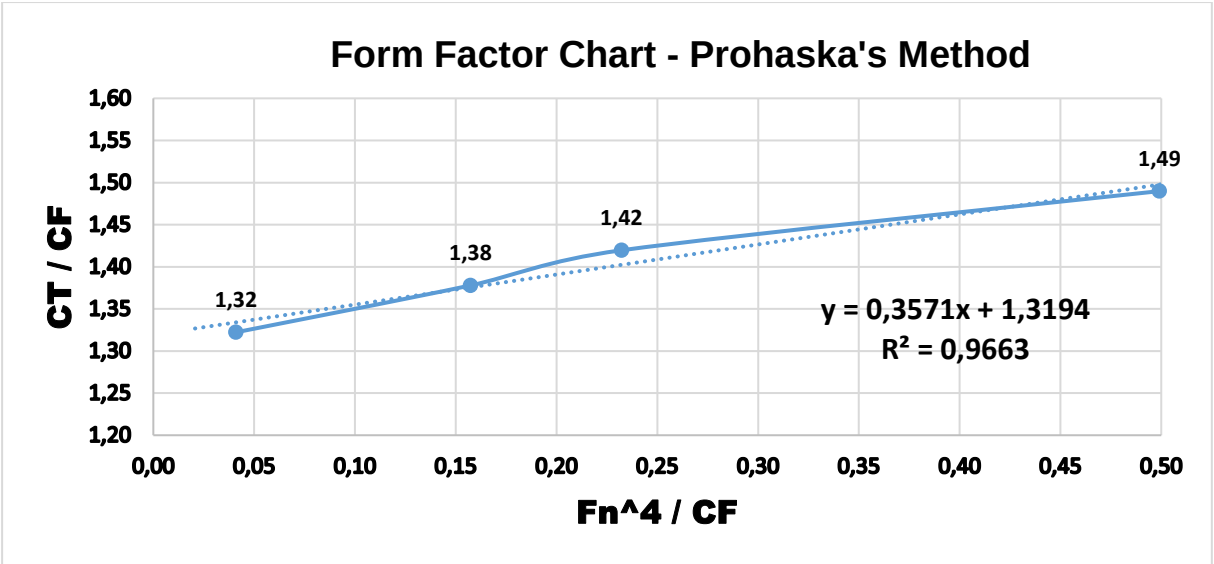

Fit intercept-1+k	1,32
Fit slope-b	0,36

Figure- A-1: Form factor graph for the upright condition.

Form Factor at 10° Heel Angle

Table- A-3: General specifications for form factor calculations of the 10° heel angle

FORM FACTOR-10° Heel Angle		
Overall Submerged Length ,LOS	2,286	m
Waterline Length, LWL	2,25	m
Wetted Surface Area-Full Scale	47,58	m^2
Wetted Surface Area-Model	0,74	m^2
Density	998,31	kg/m^3
Gravity	9,81	m/s^2

Table- A-4: Values obtained from towing tank tests for form factor chart of the 10° heel angle

Run	Clock No.	Model Speeds (m/s)	Fn	RT (N)	CT / CF	Fn^4 / CF
1	110	0,47	0,10	0,45	1,20	0,02
2	130	0,55	0,12	0,65	1,31	0,04
3	160	0,67	0,14	1,02	1,43	0,10
4	180	0,75	0,16	1,29	1,47	0,16
5	190	0,79	0,17	1,41	1,48	0,19
6	200	0,83	0,18	1,66	1,60	0,23
7	240	0,99	0,21	2,44	1,69	0,50

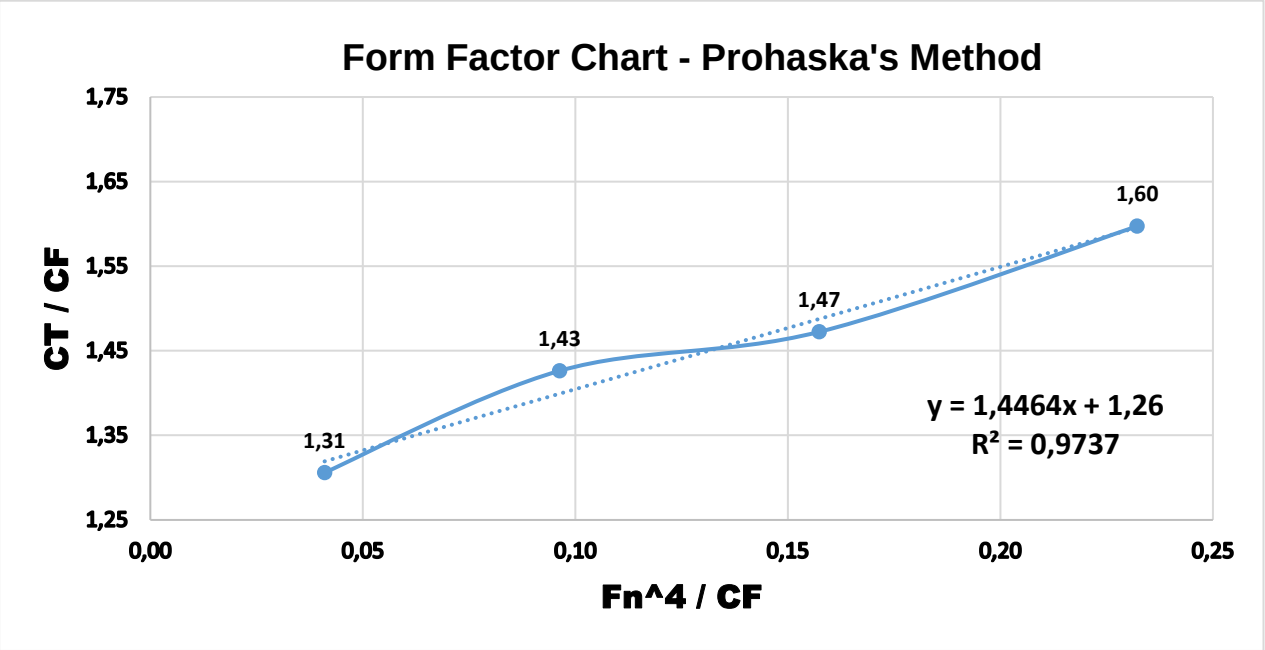

Fit intercept-1+k	1,26
Fit slope-b	1,45

Figure- A-2: Form factor graph for the 10° heel angle

Form Factor at 15° Heel Angle

Table- A-5: General specifications for form factor calculations of the 15° heel angle

FORM FACTOR-15° Heel Angle		
Overall Submerged Length ,LOS	2,286	m
Waterline Length, LWL	2,25	m
Wetted Surface Area-Full Scale	42,97	m^2
Wetted Surface Area-Model	0,67	m^2
Density	998,31	kg/m^3
Gravity	9,81	m/s^2

Table- A-6: Values obtained from towing tank tests for form factor chart of the 15° heel angle

Run	Clock No.	Model Speeds (m/s)	Fn	RT (N)	CT / CF	Fn^4 / CF
1	110	0,47	0,10	0,37	1,09	0,02
2	130	0,55	0,12	0,57	1,27	0,04
3	160	0,67	0,14	0,92	1,43	0,10
4	180	0,75	0,16	1,21	1,52	0,16
5	190	0,79	0,17	1,31	1,52	0,19
6	200	0,83	0,18	1,44	1,54	0,23
7	240	0,99	0,21	2,16	1,66	0,50

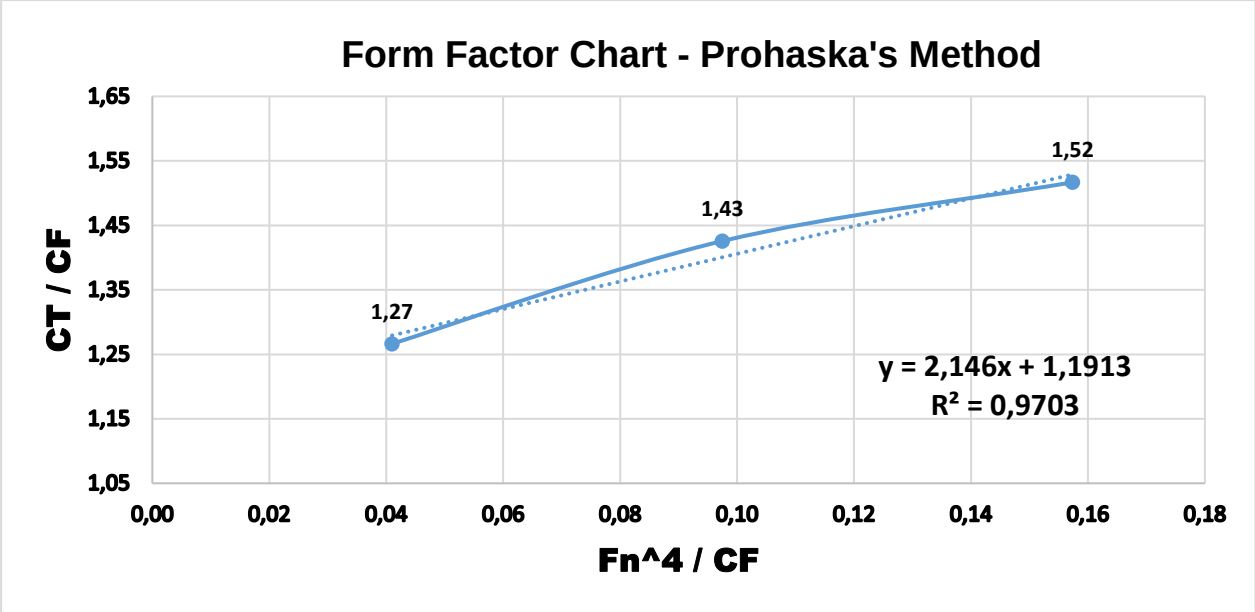

Fit intercept-1+k	1,19
Fit slope-b	2,15

Figure- A-3: Form factor graph for the 15° heel angle

Form Factor at 20° Heel Angle

Table- A-7: General specifications for form factor calculations of the 20° heel angle

FORM FACTOR-20° Heel Angle		
Overall Submerged Length ,LOS	2,286	m
Waterline Length, LWL	2,25	m
Wetted Surface Area-Full Scale	39,85	m^2
Wetted Surface Area-Model	0,62	m^2
Density	998,31	kg/m^3
Gravity	9,81	m/s^2

Table- A-8: Values obtained from towing tank tests for form factor chart of the 20° heel angle

Run	Clock No.	Model Speeds (m/s)	Fn	RT (N)	CT / CF	Fn^4 / CF
1	110	0,47	0,10	0,31	0,99	0,02
2	130	0,55	0,12	0,47	1,13	0,04
3	160	0,67	0,14	0,74	1,24	0,10
4	180	0,75	0,16	1,09	1,48	0,16
5	190	0,79	0,17	1,24	1,55	0,19
6	200	0,83	0,18	1,32	1,52	0,23
7	240	0,99	0,21	2,08	1,73	0,50

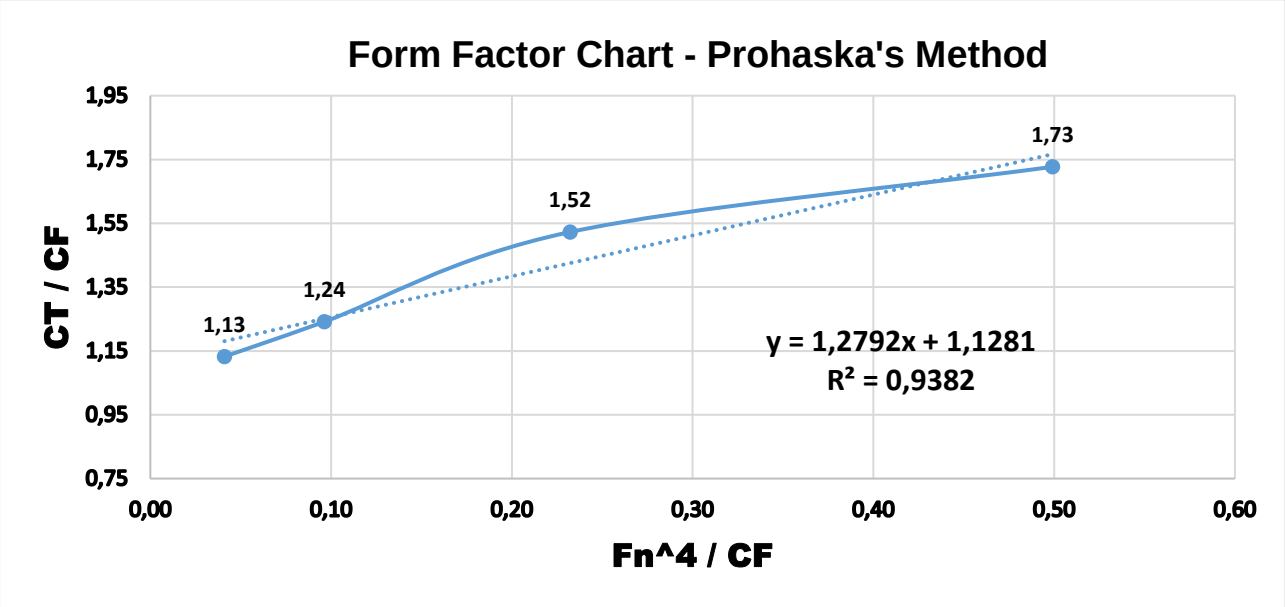

Fit intercept-1+k	1,13
Fit slope-b	1,28

Figure- A-4: Form factor graph for the 20° heel angle

Form Factor at 25° Heel Angle

Table- A-9: General specifications for form factor calculations of the 25° heel angle

FORM FACTOR-25° Heel Angle		
Overall Submerged Length ,LOS	2,286	m
Waterline Length, LWL	2,25	m
Wetted Surface Area-Full Scale	37,69	m^2
Wetted Surface Area-Model	0,59	m^2
Density	998,31	kg/m^3
Gravity	9,81	m/s^2

Table- A-10: Values obtained from towing tank tests for form factor chart of the 25° heel angle

Run	Clock No.	Model Speeds (m/s)	Fn	RT (N)	CT / CF	Fn^4 / CF
1	110	0,47	0,10	0,28	0,96	0,02
2	130	0,55	0,12	0,40	1,01	0,04
3	160	0,67	0,14	0,75	1,31	0,10
4	180	0,75	0,16	1,03	1,47	0,16
5	190	0,79	0,17	1,15	1,51	0,19
6	200	0,83	0,18	1,27	1,54	0,23
7	240	0,99	0,21	1,98	1,73	0,50

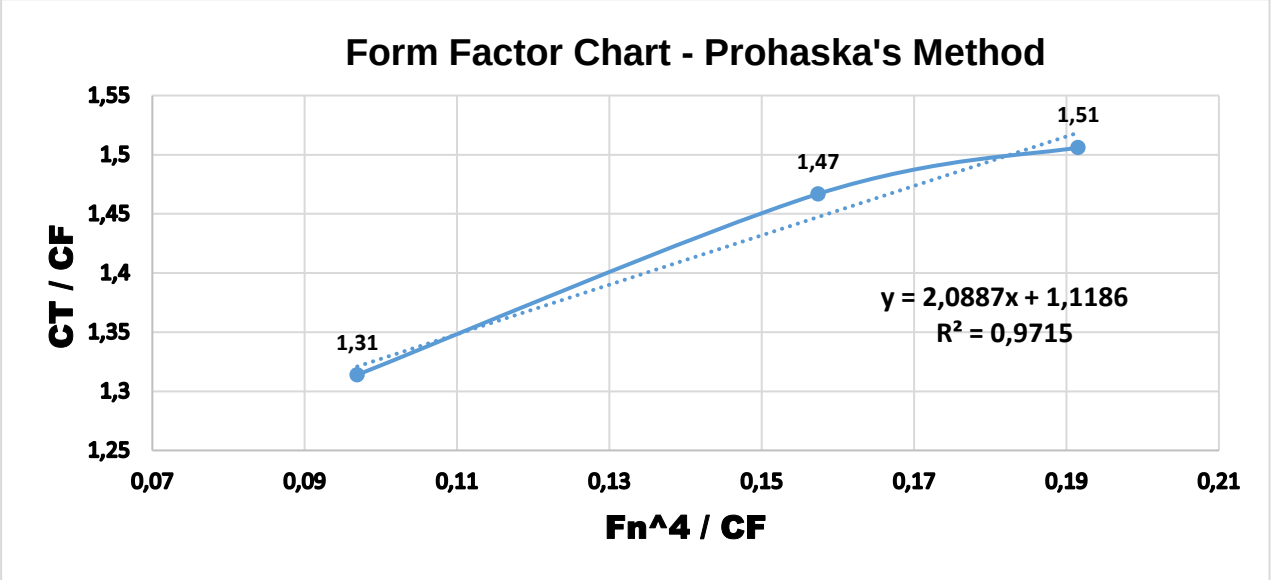

Fit intercept-1+k	1,12
Fit slope-b	2,09

Figure- A-5: Form factor graph for the 25° heel angle

Form Factor in an extended range at 15° Heel Angle

For the form factor calculations, there might be a difference between the Froude number range of the ITTC procedures and some towing tank tests in practice. In this section, the Prohaska's method was performed in an extended range (0.2≤Fn≤0.3 instead of 0.1≤Fn≤0.2) to see the form factor change. Therefore, it can be said that there is a quite big difference because of the changing range based on the new range. This situation will not change the effective draft results, but it will modify some resistance variables. For that reason, the Froude number range is a critical term for the form factor calculations. It is specified that the range of the ITTC procedure [4] was used for the resistance calculations during this master thesis.

Table- A-11: Values obtained from towing tank tests in an extended range for form factor chart of the 15° heel angle

Run	Clock No.	Model Speeds (m/s)	Fn	RT (N)	CT / CF	Fn^4 / CF
1	240	0,99	0,21	2,16	1,66	0,50
2	280	1,15	0,24	2,99	1,77	0,92
3	320	1,30	0,28	3,89	1,84	1,55
4	360	1,46	0,31	4,92	1,89	2,50

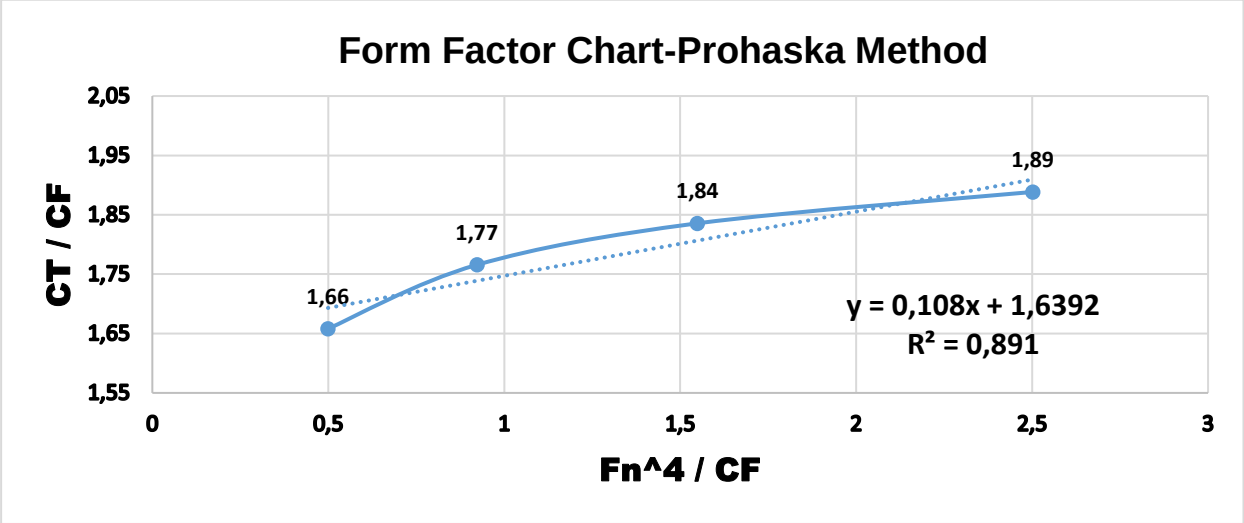

Fit intercept-1+k	1,64
Fit slope-b	0,11

Figure- A-6: Form Factor graph in an extended range for 15° Heel Angle

B. Appendix - Uncertainty Analysis Calculations

Type A – Precision (Repetition Tests)

Test-Run	Rt - N	V - m/s	T - °C	CT - Total Resistance Coefficient	Viscosity - v - m^2/s	CF - Frictional Resistance Coefficient	CR - Residual Resistance Coefficient
1	6,177	1,613	19,5	5,40E-03	1,02E-06	3,61E-03	6,35E-04
2	6,198	1,612	19,6	5,42E-03	1,01E-06	3,61E-03	6,61E-04
3	6,172	1,613	19,4	5,39E-03	1,02E-06	3,61E-03	6,31E-04
Average Value	6,18	1,613	19,5	5,40E-03	1,01E-06	3,61E-03	6,42E-04
Standard Deviation	0,013	5,77E-04	0,1	1,55E-05	1,44E-09	7,31E-07	1,65E-05
Deviation %	0,22	0,04	0,51	0,29	0,14	0,02	2,57
Precision (Single)	0,027	0,001	0,2	3,11E-05	2,89E-09	1,46E-06	3,30E-05
Deviation %	0,43	0,07	1,03	0,57	0,28	0,04	5,14
Precision (Multiple)-uA-uRt	0,015	6,67E-04	1,15E-01	1,79E-05	1,67E-09	8,45E-07	1,90E-05
Deviation %	0,25	0,04	0,59	0,33	0,16	2,34E-02	2,97

Type B

TEMPERATURE	19,5	°C
Accuracy of Thermometer	0,1	°C
Ut	0,1	°C
%	0,5	%
Density of Fresh Water		
Ucρ ± For 19,5 °C	0,030	kg/m³
Ucρ ± %	0,0030	%
Viscosity of Fresh Water		
Ucv ± For 19,5 °C	1,29E-08	m²/sn
Ucv ± %	1,13	%
Model Waterline Length-LWL		
Waterline Length, LWL	2,255	m
Length Manufacturing Tolerance	0,001	m
Total Expanded Uncertainty for Length	0,002	m
%	0,1	%
Model Length Overall Submerged-LOS		
Length Submerged,LOS	2,286	m
Length Manufacturing Tolerance	0,001	m
Total Expanded Uncertainty for Length	0,002	m
%	0,1	%

Wetted Surface Area		
Wetted Surface Area	0,88	m^2
Length Tolerance (X)	0,001	m
Waterline Length-LWL	2,26	m
Expanded Waterline Length-LWL	4,51	m
Density - ρ	998,31	kg/m^3
Ucρ ± For 19,5 °C	0,030	kg/m^3
Area of Model Hull Water-Plane - Aw	0,86	m^2
Model Displacement - Δ	16,85	kg
Uncertainty of Model Displacement Due to Ballasting	0,11	kg
Total Uncertainty	5,91E-04	m^2
%	0,1	%

Speed		
Speed	1,613	m/s
Diameter of Wheel-D	0,4	m
Time Interval-Δt	0,15	s
Number of Pulses Per Revolution-p	4000	pulse
Number of Pulses-n	770	pulse
Error of Curve Fit	0,25	pulse
Error of the Encoder	1,5	pulse
Error of DA Conversion	2	pulse
Error of AD Conversion	2	pulse
Error of Pulse Count	3,21	pulse
Sensitivity Coefficient of Pulse Count	0,0021	
Uncertainty Due to Pulse Count-un	6,73E-03	m/s
Error of Time Interval	1,03E-05	s
Sensitivity Coefficient of Time Interval	-10,75	
Uncertainty of Time Interval-uΔt	-1,10E-04	m/s
Error of Diameter of Wheel	1,15E-04	m
Sensitivity Coefficient of Wheel Diameter	4,03	
Uncertainty of Wheel Diameter-uD	4,64E-04	m/s
Total Uncertainty	2,21E-03	m/s
%	0,14	%

Froude Number		0,34
Speed	1,61	m/s
Uncertainty of Speed	2,21E-03	m/s
Waterline Length-LWL	2,255	m
Uncertainty of LWL	0,002	m
Acceleration of Gravity	9,81	m/s^2
Uncertainty of Acceleration of Gravity	0,01	m/s^2
Total Froude Uncertainty	5,23E-04	
%	0,15	%
Reynolds Number		**3,63E+06**
Speed	1,61	m/s
Uncertanity of Speed	2,21E-03	m/s
Length Overall Submerged-LOS	2,286	m
Uncertainty of LOS	0,002	m
Ut	0,1	°C
∂v/∂t	-3,00E-08	$(m^2/s \cdot °C)$
ν	1,02E-06	(m^2/s)
Total Reynolds Uncertainty	1,22E+04	
%	0,34	%
Coefficient of Frictional Resistance-Cf		**3,61E-03**
Reynolds Number	3,63E+06	
Uncertainty of Reynolds Number	1,22E+04	
Total Uncertainty of Coefficient of Frictional Resistance	2,32E-06	
%	0,1	%

Total Resistance-Rt	6,18	N
u1(F)	0,01	N
SEE-Standard Deviation	3,48E-07	-
2*SEE	6,96E-07	-
u2(F)	6,96E-07	N
u(F)-uB	0,01	N
Total Resistance Uncertainty-U-Rt	0,02	N
%	0,3	%
Coefficient of Total Resistance-Ct		5,40E-03
Ut	0,1	°C
∂ρ/∂t	-0,15071	(kg/m³·°C)
ρ	998,31	kg/m³
V	1,613	m/s
Uncertainty of Speed-V	2,21E-03	m/s
Rt	6,18	N
Total Resistance Uncertainty-U-Rt	0,02	N
Wetted Surface Area-S	0,88	m²
Uncertainty of Wetted Surface Area	5,91E-04	m²
Total Uncertainty of Coefficient of Total Resistance-Ct	2,27E-05	-
%	0,4	%

Form Factor - 1+k	1,32
Uncertainty of Coefficient of Total Resistance-Ct	2,27E-05
Coefficient of Frictional Resistance-Cf	3,61E-03
Uncertainty of Coefficient of Frictional Resistance	2,32E-06
ukb	0,01
uka	0,01
uk-Total	8,47E-03
%	2,7
Coefficient of Residuary Resistance-Cr	6,42E-04
Uncertainty of Coefficient of Total Resistance-Ct	2,27E-05
1+k	1,32
Uncertainty of Coefficient of Frictional Resistance	2,32E-06
uk-Total	0,01
Uncertainty of Coefficient of Residuary Resistance	2,29E-05
%	3,6

C. Appendix - Effective Draft Graphs and Tables of 40° Canting Keel at 10° and 25° Heel Angles & 0.30 and 0.39 Froude Numbers

Effective Draft of 40° Canted Keel at 10° Heel Angle & 0.30 Fn

Table- C-1: Effective draft table of 40° canted keel at 10° heel Angle & 0.30 Fn

Keel Position	Heel	Leeway	Clock No	V-Full Size (m/s)	FN	Full Size Total-Rt (kN)	SF² (kN)	Ri (kN)
40°	10°	8°	350	4,0	0,30	2,67	61,42	0,75
40°	10°	10°	350	4,0	0,30	2,90	82,68	1,02
40°	10°	12°	350	4,0	0,30	3,19	104,07	1,28

Ru+Rh (kN)	Slope	Te²	Te (m)
1,90	0,0123	1,58	1,26

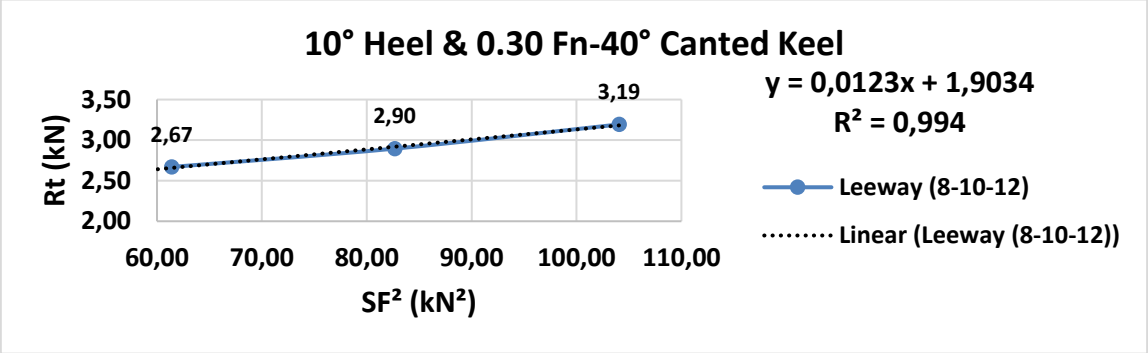

Figure- C-1: Graph of 40° canted keel at 10° heel angle and 0.30 Froude number

Effective Draft of 40° Canted Keel at 10° Heel Angle & 0.39 Fn

Table- C-2: Effective draft table of 40° canted keel at 10° heel angle & 0.39 Fn

Keel Position	Heel	Leeway	Clock No	V-Full Size (m/s)	FN	Full Size Total-Rt (kN)	SF² (kN)	Ri (kN)
40°	10°	6°	450	5,13	0,39	4,00	96,97	0,89
40°	10°	8°	450	5,13	0,39	4,61	166,62	1,52
40°	10°	10°	450	5,13	0,39	5,21	238,41	2,18
40°	10°	12°	450	5,13	0,39	5,91	302,95	2,77

Ru+Rh (kN)	Slope	Te²	Te (m)
3,09	0,0091	1,29	1,14

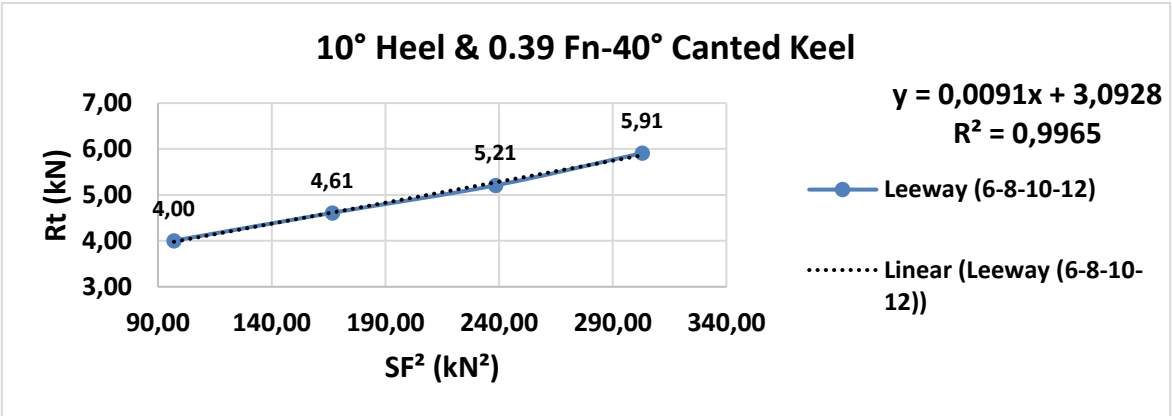

Figure- C-2: Graph of 40° canted keel at 10° heel angle and 0.39 Froude number

Effective Draft of 40° Canted Keel at 25° Heel Angle & 0.30 Fn

Table- C-3: Effective draft table of 40° canted keel at 25° heel angle & 0.30 Fn

Keel Position	Heel	Leeway	Clock No	V-Full Size (m/s)	FN	Full Size Total-Rt (kN)	SF² (kN)	Ri (kN)
40°	25°	7°	350	4,0	0,30	2,47	0,52	0,03
40°	25°	8°	350	4,0	0,30	2,61	2,42	0,15
40°	25°	9°	350	4,0	0,30	2,73	4,60	0,29

Ru+Rh (kN)	Slope	Te²	Te (m)
2,44	0,0635	0,31	0,55

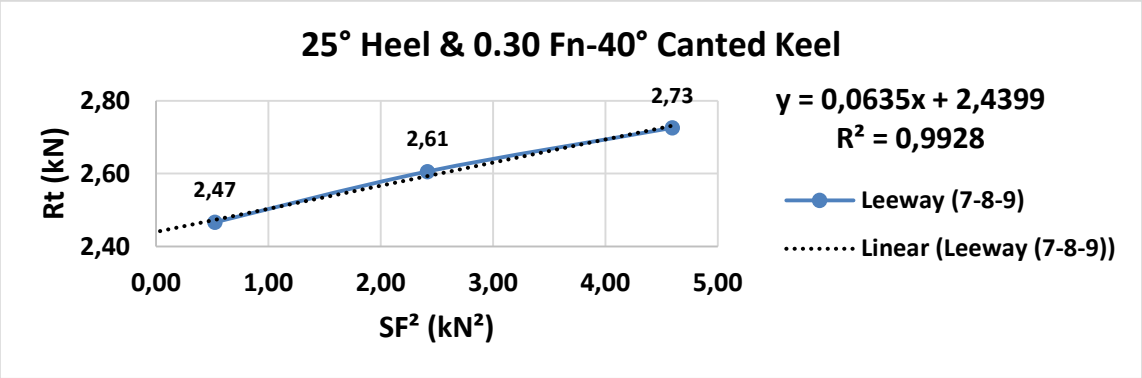

Figure- C-3: Graph of 40° canted keel at 25° heel angle and 0.30 Froude number

Effective Draft of 40° Canted Keel at 25° Heel Angle & 0.39 Fn

Table- C-4: Effective draft table of 40° canted keel at 25° heel angle & 0.39 Fn

Keel Position	Heel	Leeway	Clock No	V-Full Size (m/s)	FN	Full Size Total-Rt (kN)	SF² (kN)	Ri (kN)
40°	25°	6°	450	5,13	0,39	3,97	3,11	0,10
40°	25°	8°	450	5,13	0,39	4,50	19,53	0,62
40°	25°	9°	450	5,13	0,39	4,81	29,65	0,94

Ru+Rh (kN)	Slope	Te²	Te (m)
3,87	0,0318	0,37	0,61

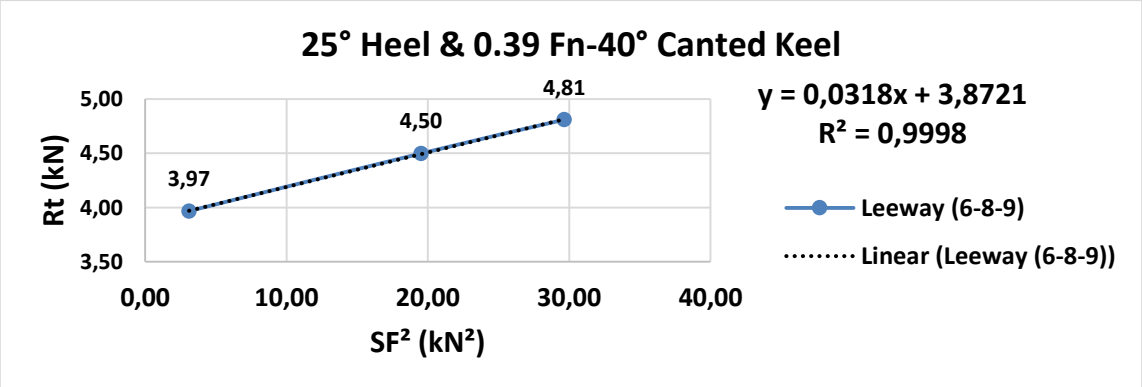

Figure- C-4: Graph of 40° canted keel at 25° heel angle and 0.39 Froude number

D. Appendix - Effective Draft Graphs and Tables of 1/2-Full Straight Daggerboards & 40° Canting Keel at 15° Heel Angle & 0.34 and 0.43 Froude Numbers

Effective Draft of 1/2 DBD at 15° Heel Angle & 0.34 Fn

Table- D-1: Effective draft table of 1/2 DBD at 15° Heel Angle & 0.34 Fn

Keel Position	DBD Position	% DBD	Heel	Leeway	Clock No	V-Full Size (m/s)	FN	Full Size Total-Rt (kN)	SF² (kN)	Ri (kN)
40°	1/2 DBD	50	15°	2,75°	400	4,56	0,34	3,56	73,67	1,11
40°	1/2 DBD	50	15°	3,25°	400	4,56	0,34	3,72	83,24	1,25
40°	1/2 DBD	50	15°	4°	400	4,56	0,34	4,12	110,47	1,66

Ru+Rh (kN)	Slope	Te²	Te (m)
2,46	0,0150	1,00	1,00

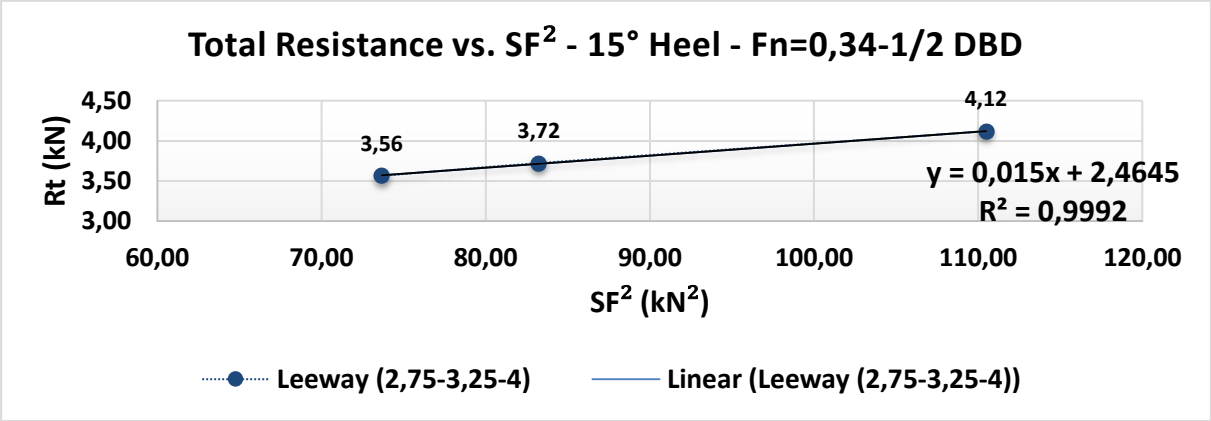

Figure- D-1: Graph of 1/2-straight daggerboard at 15° heel angle and 0.34 Froude number

Effective Draft of 1/2 DBD at 15° Heel Angle & 0.43 Fn

Table- D-2: Effective draft table of 1/2 DBD at 15° heel angle & 0.43 Fn

Keel Position	DBD Position	% DBD	Heel	Leeway	Clock No	V-Full Size (m/s)	FN	Full Size Total-Rt (kN)	SF² (kN)	Ri (kN)
40°	1/2 DBD	50	15°	2,25°	500	5,71	0,43	5,27	137,17	2,01
40°	1/2 DBD	50	15°	2,75°	500	5,71	0,43	6,28	203,72	2,98
40°	1/2 DBD	50	15°	3,25°	500	5,71	0,43	6,77	240,30	3,52

Ru+Rh (kN)	Slope	Te²	Te (m)
3,27	0,0146	0,65	0,81

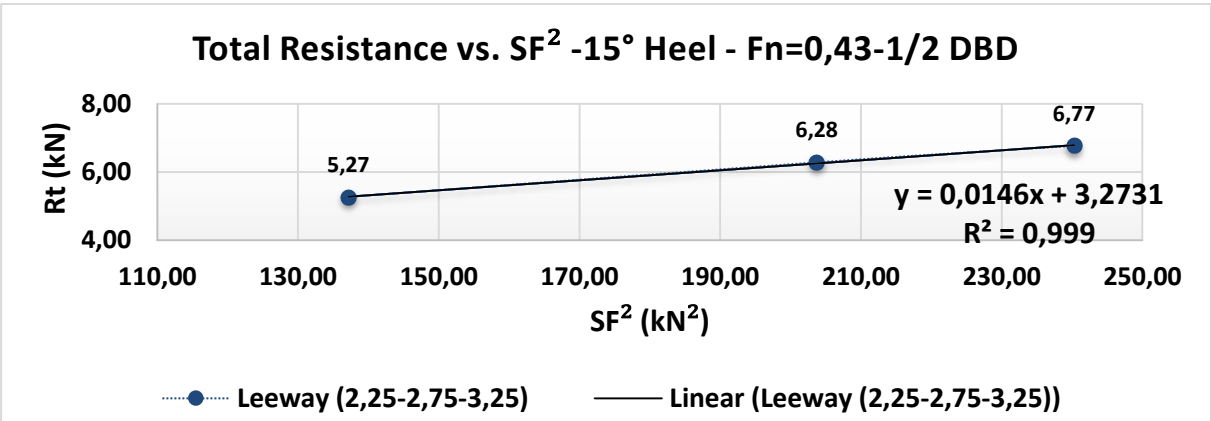

Figure- D-2: Graph of 1/2-straight daggerboard at 15° heel angle and 0.43 Froude number

Effective Draft of Full DBD at 15° Heel Angle & 0.34 FN

Table- D-3: Effective draft table of Full DBD at 15° heel angle & 0.34 FN

Keel Position	DBD Position	% DBD	Heel	Leeway	Clock No	V-Full Size (m/s)	FN	Full Size Total-Rt (kN)	SF² (kN)	Ri (kN)
40°	Full DBD	100	15°	1°	400	4,6	0,34	3,05	40,97	0,35
40°	Full DBD	100	15°	1,5°	400	4,6	0,34	3,31	74,86	0,63
40°	Full DBD	100	15°	2,75°	400	4,6	0,34	4,37	198,55	1,68

Ru+Rh (kN)	Slope	Te²	Te (m)
2,69	0,0085	1,77	1,33

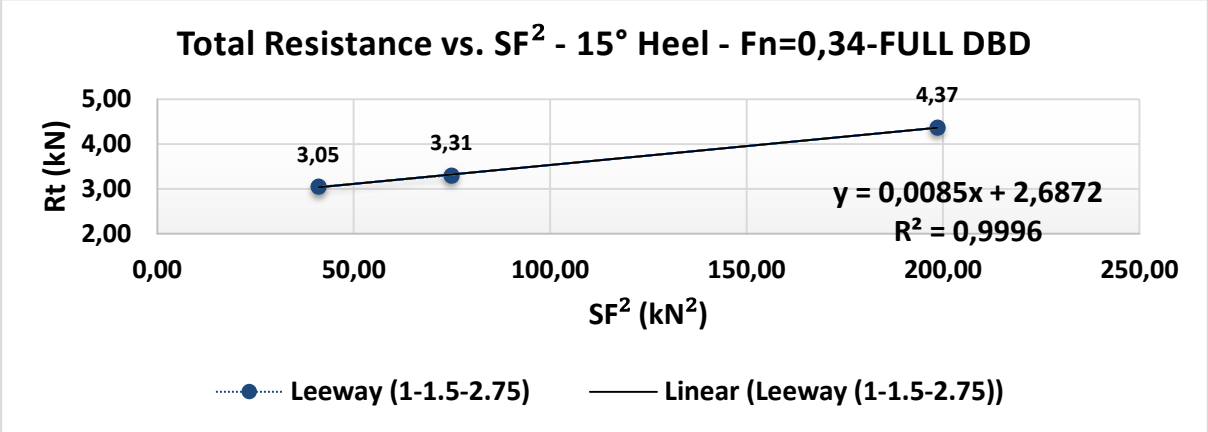

Figure- D-3: Graph of full-straight daggerboard at 15° heel angle and 0.34 Froude number

Effective Draft of Full DBD at 15° Heel Angle & 0.43 FN

Table- D-4: Effective draft table of Full DBD at 15° heel angle & 0.43 FN

Keel Position	DBD Position	% DBD	Heel	Leeway	Clock No	V-Full Size (m/s)	FN	Full Size Total-Rt (kN)	SF² (kN)	Ri (kN)
40°	Full DBD	100	15°	1°	500	5,71	0,43	5,10	184,11	1,54
40°	Full DBD	100	15°	1,5°	500	5,71	0,43	5,66	273,61	2,30
40°	Full DBD	100	15°	2,75°	500	5,71	0,43	7,91	524,51	4,40

Ru+Rh (kN)	Slope	Te²	Te (m)
3,48	0,0084	1,13	1,07

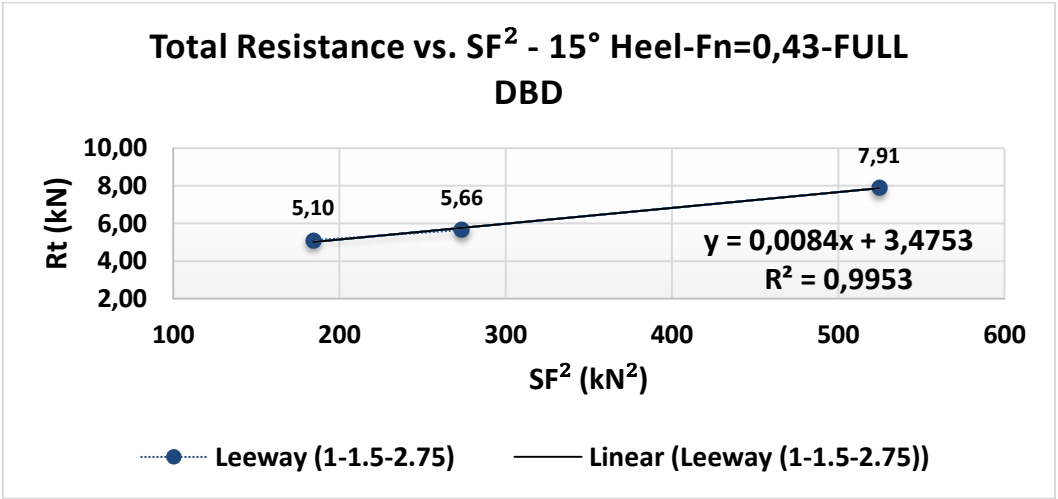

Figure- D-4: Graph of full-straight daggerboard at 15° heel angle and 0.43 Froude number

E. Appendix - Effective Draft Graphs and Tables of 1/2-Full Curved Daggerboards & 40° Canting Keel at 10° and 25° Heel Angles & 0.30 and 0.39 Froude Numbers

Effective Draft of 1/2 DSS at 10° Heel Angle & 0.30 FN

Table- E-1: Effective draft table of 1/2 DSS at 10° heel angle & 0.30 FN

Keel Position	DBD Position	% DBD	Heel	Leeway	Clock No	V-Full Size (m/s)	FN	Full Size Total-Rt (kN)	SF² (kN)	Ri (kN)
40°	1/2 DBD	35	10°	4°	350	4,0	0,30	2,74	44,28	0,43
40°	1/2 DBD	35	10°	5°	350	4,0	0,30	2,84	66,81	0,65
40°	1/2 DBD	35	10°	6°	350	4,0	0,30	3,19	91,43	0,88

Ru+Rh (kN)	Slope	Te²	Te (m)
2,27	0,0097	2,01	1,42

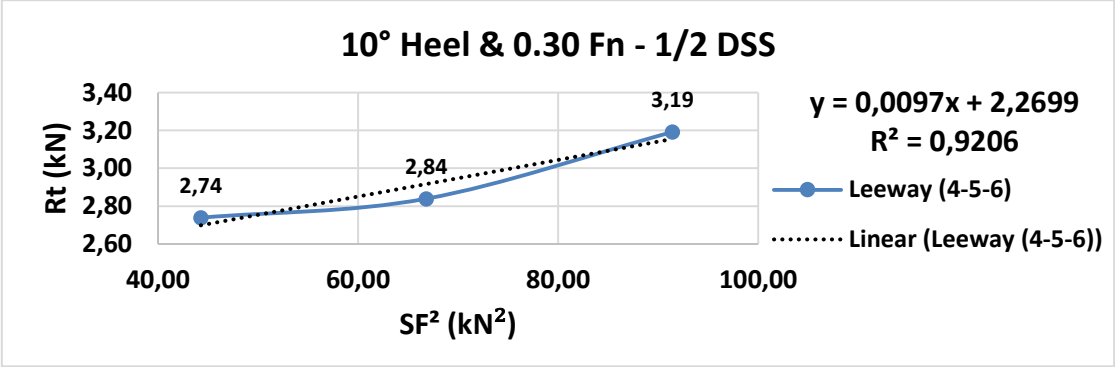

Figure- E-1: Graph of 1/2-curved daggerboard at 10° heel angle & 0.30 Froude number

Effective Draft of 1/2 DSS at 10° Heel Angle & 0.39 FN

Table- E-2: Effective draft table of 1/2 DSS at 10° heel angle & 0.39 FN

Keel Position	DBD Position	% DBD	Heel	Leeway	Clock No	V-Full Size (m/s)	FN	Full Size Total-Rt (kN)	SF² (kN)	Ri (kN)
40°	1/2 DBD	35	10°	3°	450	5,13	0,39	3,65	10,11	0,07
40°	1/2 DBD	35	10°	4°	450	5,13	0,39	3,82	37,05	0,27
40°	1/2 DBD	35	10°	5°	450	5,13	0,39	4,09	76,17	0,55
40°	1/2 DBD	35	10°	6°	450	5,13	0,39	4,44	120,10	0,86

Ru+Rh (kN)	Slope	Te²	Te (m)
3,56	0,0072	1,64	1,28

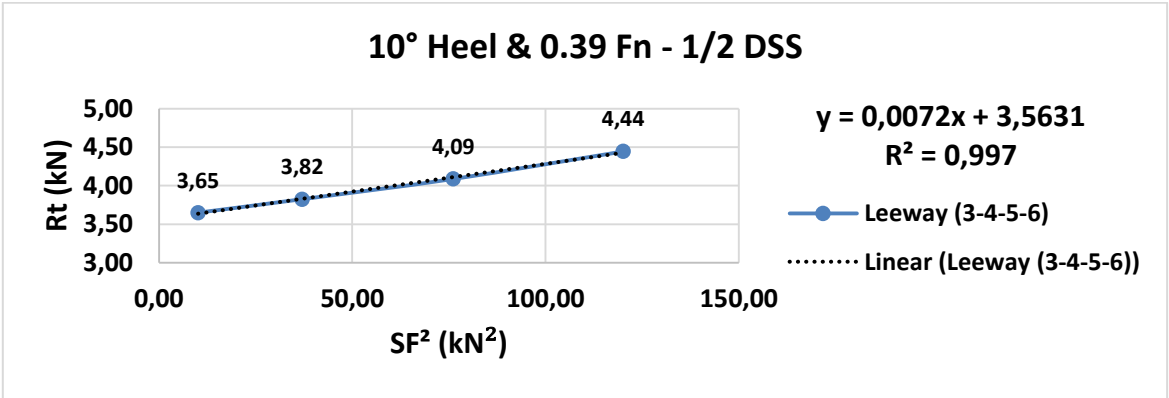

Figure- E-2: Graph of 1/2-curved daggerboard at 10° heel angle & 0.39 Froude number

Effective Draft of 1/2 DSS at 25° Heel Angle & 0.30 Fn

Table- E-3: Effective draft table of 1/2 DSS at 25° heel angle & 0.30 Fn

Keel Position	DBD Position	% DBD	Heel	Leeway	Clock No	V-Full Size (m/s)	FN	Full Size Total-Rt (kN)	SF² (kN)	Ri (kN)
40°	1/2 DBD	50	25°	4°	350	4,0	0,30	2,57	4,28	0,21
40°	1/2 DBD	50	25°	5°	350	4,0	0,30	3,03	14,21	0,68
40°	1/2 DBD	50	25°	6°	350	4,0	0,30	3,59	25,51	1,23

Ru+Rh (kN)	Slope	Te²	Te (m)
2,36	0,0482	0,40	0,64

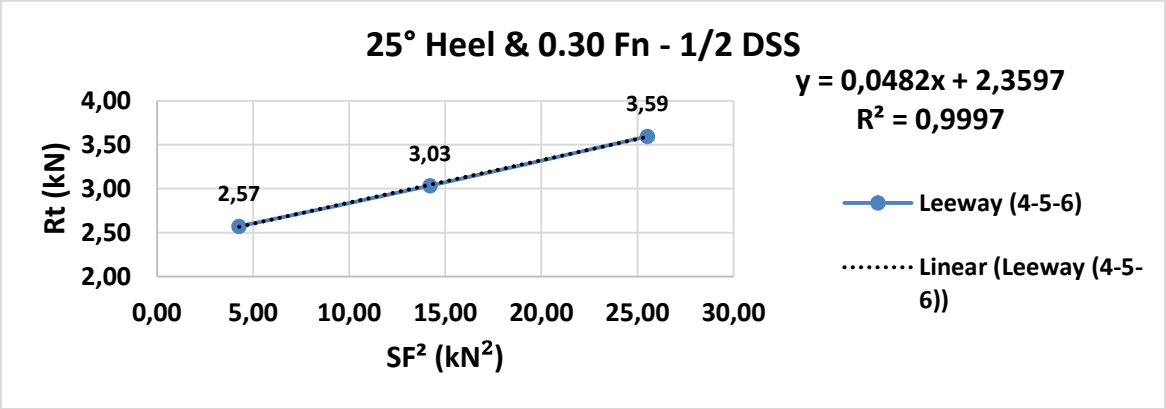

Figure- E-3: Graph of 1/2-curved daggerboard at 25° heel angle & 0.30 Froude number

Effective Draft of 1/2 DSS at 25° Heel Angle & 0.39 Fn

Table- E-4: Effective draft table of 1/2 DSS at 25° heel angle & 0.39 Fn

Keel Position	DBD Position	% DBD	Heel	Leeway	Clock No	V-Full Size (m/s)	FN	Full Size Total-Rt (kN)	SF² (kN)	Ri (kN)
40°	1/2 DBD	50	25°	3°	450	5,13	0,39	4,03	0,95	0,02
40°	1/2 DBD	50	25°	4°	450	5,13	0,39	4,18	6,18	0,13
40°	1/2 DBD	50	25°	5°	450	5,13	0,39	4,39	17,67	0,38
40°	1/2 DBD	50	25°	6°	450	5,13	0,39	4,76	34,22	0,73

Ru+Rh (kN)	Slope	Te²	Te (m)
4,02	0,0214	0,55	0,74

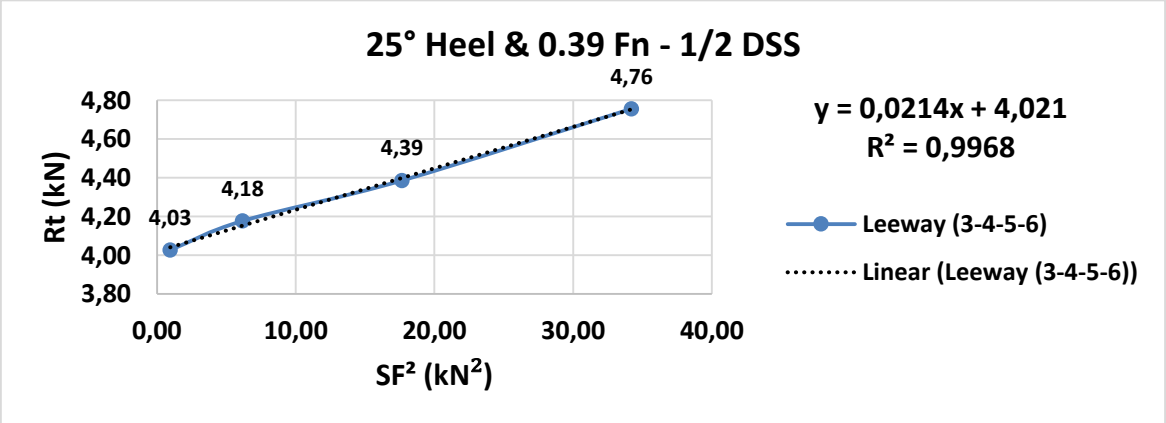

Figure- E-4: Graph of 1/2-curved daggerboard at 25° heel angle & 0.39 Froude number

Effective Draft of Full DSS at 10° Heel Angle & 0.30 FN

Table- E-5: Effective draft table of Full DSS at 10° heel angle & 0.30 FN

Keel Position	DBD Position	% DBD	Heel	Leeway	Clock No	V-Full Size (m/s)	FN	Full Size Total-Rt (kN)	SF² (kN)	Ri (kN)
40°	Full DBD	85	10°	6°	350	4,0	0,30	2,80	68,12	0,98
40°	Full DBD	85	10°	8°	350	4,0	0,30	3,17	96,31	1,38
40°	Full DBD	85	10°	10°	350	4,0	0,30	3,52	125,19	1,80
40°	Full DBD	85	10°	12°	350	4,0	0,30	4,17	162,63	2,33

Ru+Rh (kN)	Slope	Te²	Te (m)
1,79	0,0143	1,36	1,16

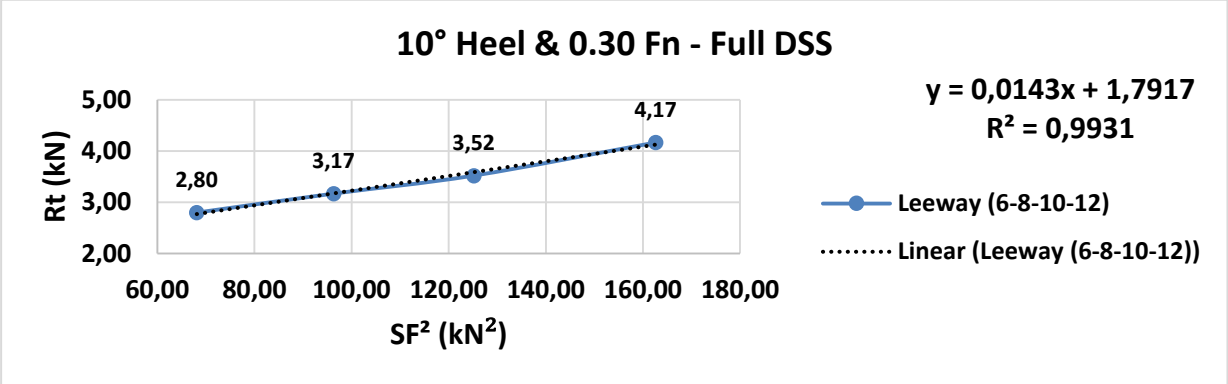

Figure- E-5: Graph of full-curved daggerboard at 10° heel angle & 0.30 Froude number

Effective Draft of Full DSS at 10° Heel Angle & 0.39 FN

Table- E-6: Effective draft table of Full DSS at 10° heel angle & 0.39 FN

Keel Position	DBD Position	% DBD	Heel	Leeway	Clock No	V-Full Size (m/s)	FN	Full Size Total-Rt (kN)	SF² (kN)	Ri (kN)
40°	Full DBD	85	10°	6°	450	5,13	0,39	5,07	198,41	1,92
40°	Full DBD	85	10°	8°	450	5,13	0,39	6,07	291,62	2,83
40°	Full DBD	85	10°	10°	450	5,13	0,39	6,94	387,61	3,76
40°	Full DBD	85	10°	12°	450	5,13	0,39	8,04	502,40	4,87

Ru+Rh (kN)	Slope	Te²	Te (m)
3,19	0,0097	1,22	1,10

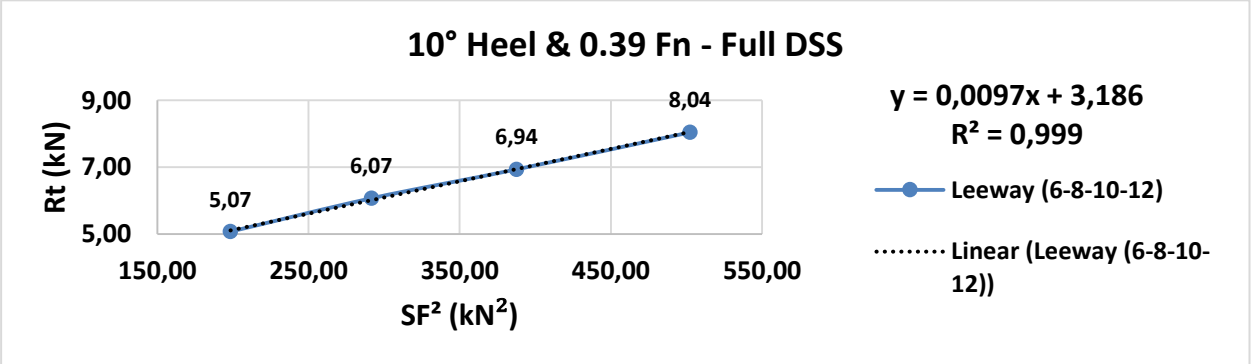

Figure- E-6: Graph of full-curved daggerboard at 10° heel angle & 0.39 Froude number

Effective Draft of Full DSS at 25° Heel Angle & 0.30 Fn

Table- E-7: Effective draft table of Full DSS at 25° heel angle & 0.30 Fn

Keel Position	DBD Position	% DBD	Heel	Leeway	Clock No	V-Full Size (m/s)	FN	Full Size Total-Rt (kN)	SF² (kN)	Ri (kN)
40°	Full DBD	100	25°	6°	350	4,0	0,30	3,46	17,71	0,37
40°	Full DBD	100	25°	8°	350	4,0	0,30	3,95	36,27	0,76
40°	Full DBD	100	25°	10°	350	4,0	0,30	4,39	59,30	1,25
40°	Full DBD	100	25°	12°	350	4,0	0,30	5,12	95,45	2,01

Ru+Rh (kN)	Slope	Te²	Te (m)
3,14	0,0210	0,93	0,96

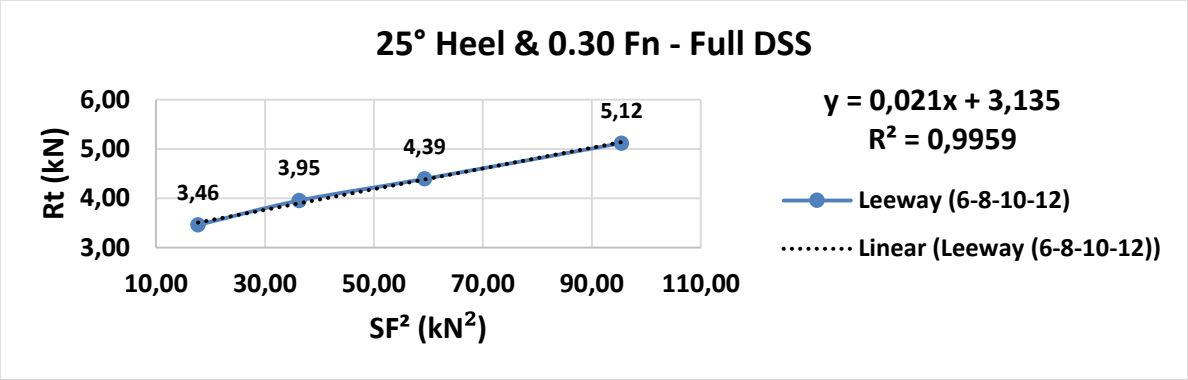

Figure- E-7: Graph of full-curved daggerboard at 25° heel angle & 0.30 Froude number

Effective Draft of Full DSS at 25° Heel Angle & 0.39 Fn

Table- E-8: Effective draft table of Full DSS at 25° heel angle & 0.39 Fn

Keel Position	DBD Position	% DBD	Heel	Leeway	Clock No	V-Full Size (m/s)	FN	Full Size Total-Rt (kN)	SF² (kN)	Ri (kN)
40°	Full DBD	100	25°	6°	450	5,13	0,39	6,22	84,80	1,21
40°	Full DBD	100	25°	8°	450	5,13	0,39	7,28	155,94	2,23
40°	Full DBD	100	25°	10°	450	5,13	0,39	8,34	231,37	3,31
40°	Full DBD	100	25°	12°	450	5,13	0,39	10,04	350,80	5,02

Ru+Rh (kN)	Slope	Te²	Te (m)
5,02	0,0143	0,83	0,91

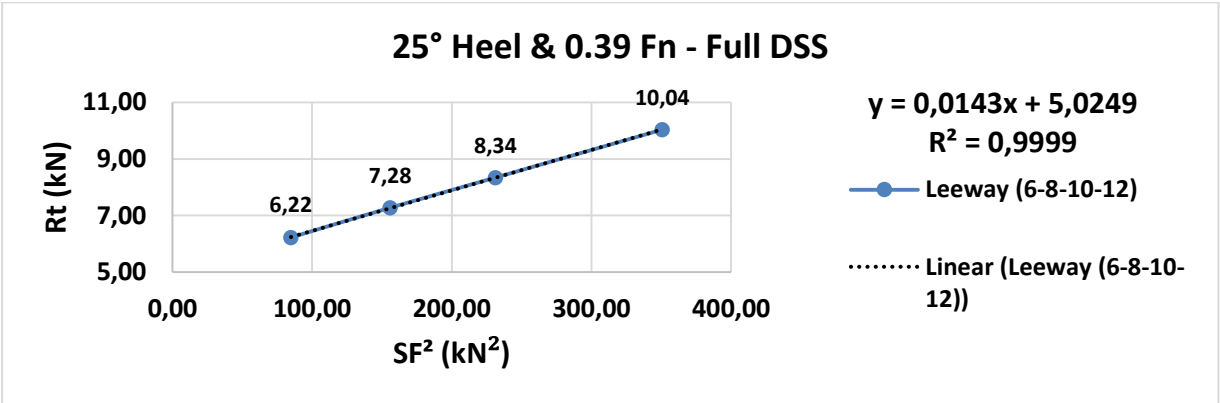

Figure- E-8: Graph of full-curved daggerboard at 25° heel angle & 0.39 Froude number

F. Appendix-Effective Draft and Resistance Calculations of Full Curved Daggerboard & 40° Canting Keel at 15° Heel Angle and 0.39 F_N

RUN No.	Keel Pos.	DBD Pos.	DBD %	Heel°	Leeway°	Clock No.	Model Speed(m/s)	V full size(m/s)
88	40 degrees	FULL DBD	90	15	6	450	1,813	5,13
89	40 degrees	FULL DBD	90	15	8	450	1,813	5,13
90	40 degrees	FULL DBD	90	15	10	450	1,813	5,13
91	40 degrees	FULL DBD	90	15	12	450	1,813	5,13

Model-DRAG (N)	Model-Side F. (N)	Model-Trim (mm)	Model-Heave (mm)	F_N
13,56	22,05	-0,33	-5,27	0,4
15,55	30,29	-0,28	-4,26	0,4
17,61	35,06	-0,16	-3,82	0,4
20,14	40,60	-0,12	-4,35	0,4

Cf_{hull}	Cf_{keel}	Cf_{rudder}	Cf_{bulb}	Cf_{DBD}
0,0021	0,0038	0,0046	0,0028	0,0040
0,0021	0,0038	0,0046	0,0028	0,0040
0,0021	0,0038	0,0046	0,0028	0,0040
0,0021	0,0038	0,0046	0,0028	0,0040

$Rv_{hull\ (N)}$	$Rv_{keel\ (N)}$	$Rv_{rudder\ (N)}$	$Rv_{bulb\ (N)}$	$Rv_{DBD\ (N)}$	$Rv_{total\ (kN)}$	$Rw_{total\ (kN)}$	Full size – Total Resistance (kN)
1481,06	295,60	0	143,75	205,73	2,13	3,33	5,45
1481,06	295,60	0	143,75	205,73	2,13	4,37	6,50
1481,06	295,60	0	143,75	205,73	2,13	5,45	7,58
1481,06	295,60	0	143,75	205,73	2,13	6,78	8,91

Full Size Side Force (kN)	Full Size SF^2 (kN)	Ri - Induced Drag (kN)
11,57	133,91	1,46
15,89	252,64	2,76
18,40	338,46	3,69
21,31	453,94	4,95

SLOPE	Te^2 - Effective Draft	Te - Effective Draft
0,01	1,08	1,04

G. Appendix- The Foil Configuration of the Le Figaro Bénéteau 3

- There is a new monohull racing sailboat design which will be launched by Bénéteau. It has been equipped with a very interesting and different foil configuration as compared with the Open 60 foil shapes. The curved part of the new foil shape is turned down unlike curved section of the Open 60 and the foil tends to move inward when the sailboat is heeled due to the wind force.
- Based on the test observations and results of the thesis, they try to keep the 3D vector directions of the foil parts (lift vertically and side force horizontally) close to the 2D force vectors of the foil theory. This situation enables to generate the total side force with less induced drag, so this enables to get the more effective draft. Also, it does not lose excessive total side force energy due to moving inward when it is heeled. Because the horizontal side force effect of the curved section turns into lift force vertically in the heeling positions, so there is always some lifting force due to the shape of the foil hence it is a very versatile configuration. Therefore, there is always some dynamic power gain effectively, and this is a critical advantage for boat speed (drive force).
- It seems that the foils are designed mainly for generating the side force (righting moment) with lift force vertically. This design approach is similar to the new generation foil configuration of the Open 60s. It can be said that the lifting advantage is a very critical factor for the competitions based on the ranking list [27] of the Vendée Globe 2016-2017.

Figure- G-1: A view of the Le Figaro Bénéteau 3 [28]